DEVELOPMENT OF LOCAL ACTIVE NOISE CONTROL SYSTEM FOR VEHICLE CABIN

NUR BIDAYATUL HIDAYAH BINTI ABDUL KADER

2013180

DEPARTMENT OF MECHATRONICS ENGINEERING

KULLIYAH OF ENGINEEERING

INTERNATIONAL ISLAMIC UNIVERSITY MALAYSIA

JUNE 2024

DEVELOPMENT OF LOCAL ACTIVE NOISE CONTROL SYSTEM FOR VEHICLE CABIN

NUR BIDAYATUL HIDAYAH BINTI ABDUL KADER

Project Supervisor: Dr. Khairul Affendy Bin Md Nor

A REPORT SUBMITTED IN PARTIAL FULFILMENT OF THE REQUIREMENT FOR A DEGREE OF BACHELOR OF ENGINEERING (MECHATRONICS) (HONOURS)

APPROVAL

I certify that I have supervised and read this study and that in my opinion, it conforms to acceptable standards of scholarly presentation and is fully adequate, in scope and quality, as Final Year Project report as partial fulfilment for a degree of Bachelor of Engineering (Mechatronics)(Honors).

.....

Dr. Khairul Affendy Md Nor

Supervisor

ABSTRACT

This study focuses on designing and implementing an active noise cancellation (ANC) system to reduce unwanted noise in vehicle cabins, ensuring a quieter and more comfortable environment for passengers. By precisely tuning this anti-noise signal to match the frequency and amplitude of the engine noise, the ANC system effectively cancels out the unwanted sound using the principle of superposition. In real-life situations, signal variations can cause the system to become unstable if the error signal is not perfectly time-aligned with the input signal. Therefore, an adaptive controller is necessary to ensure that the inverted and real signals remain synchronized. This research aims to model sound wave propagation using MATLAB and COMSOL Multiphysics, develop a local active noise control system with a feedforward controller, and experimentally verify the system's performance, focusing on adaptive local active noise cancellation within vehicle cabins. Simulations were performed using MATLAB Simulink and COMSOL Multiphysics to model sound wave behaviors and optimize the controller settings for various noise scenarios. The implementation involved a combination of real-time digital signal processing with adaptive algorithms to adjust the noise cancellation effects dynamically using LabVIEW and compact RIO controller. The controller was tested in controlled environment to reduce noise at 200 Hz and 63.47 Hz from a car engine sound, achieving noise attenuation of approximately 6.02 dB and 3.52 dB, respectively. Future research will explore the integration of more complex adaptive algorithms, such as Recursive Least Squares (RLS) and Neural Network-based approaches, to further enhance the system's adaptability.

Keywords: *Active Noise Cancellation, Feedforward Control, Adaptive Algorithms, MATLAB Simulink, COMSOL Multiphysics, LabVIEW, Compact RIO*

ACKNOWLEDGEMENTS

Praise be to Allah S.W.T for His Mercy that give strength and blessings for me to complete this Final Year Project. Alhamdulillah.

First and foremost, my appreciation and absolute gratitude are extended to my supervisor, Dr. Khairul Affendy Bin Md Nor for all of his support and encouragement during my research, experiment and report writing, as well as for his enthusiasm, patience, and wise inquiries. I appreciate him taking the time to help me, to answer my questions, to revise and improve the ideas in my research paper and while conducting the experiment.

In addition, I would like to thank my coordinator for this subject, Dr. Hasmawati Bt. Antong and Dr. Aimi Shazwani Bt. Ghazali for leading me since early of the semester.

My next gratitude is forwarded to my parents and family for their unwavering support and sacrifices for me throughout the semester. Their prayers have kept me thus far. Not forgetting, a great thanks also to all my friends that help directly or indirectly while completing this research.

TABLE OF CONTENTS

APPROVAL **1**

ABSTRACT **2**

ACKNOWLEDGEMENTS **3**

LIST OF TABLES **8**

LIST OF FIGURES **9**

LIST OF ABBREVIATIONS **13**

CHAPTER 1 ..... **15**

INTRODUCTION **15**

1.1 INTRODUCTION 15

1.2 PROBLEM STATEMENT 16

1.3 OBJECTIVE 17

1.4 RESEARCH SCOPE 17

1.5 RESEARCH METHODOLOGY 18

1.6 REPORT OUTLINE 19

CHAPTER 2 ..... **20**

LITERATURE REVIEW **20**

2.1 OVERVIEW 20

2.2 INTRODUCTION TO SOUND AND NOISE 20

2.2.1 Sound *20*

2.2.2 Noise *22*

2.3 NOISE SOURCES AND CHARCTERISTIC IN VEHICLE CABINS 23

2.3.1 Engine Noise *23*

2.3.2 Road and Tire Noise *23*

2.3.3 Wind and Aerodynamic Noise *23*

2.3.4 Interior Noise Reflection and Resonance *24*

2.4 NOISE CONTROL 24

2.4.1 Passive Noise Control *24*

2.4.2 Active Noise Control *26*

2.4.3 Combine ANC and PNC method. *27*

2.5 ACTIVE NOISE CANCELLATION 28

2.5.1 Acoustic Wave Superposition *28*

2.5.2 Effectiveness and Limitations of ANC *29*

2.6 ACTIVE NOISE CONTROL STRATEGY 29

2.6.1 Feedforward Control System *29*

2.6.2 Feedback Control System *31*

2.6.3 Hybrid Feedforward-Feedback Active Control (HANC) *33*

2.7 ADAPTIVE CONTROL 34

2.7.1 Adaptive Filters *34*

2.7.2 Normalize Least Mean Square (NLMS) *35*

2.7.3 Filtered-x least mean square (FXLMS) *35*

2.7.4 Adaptive Step Size with FxLMS (ASSFxLMS) Algorithms *36*

2.8 ANC APPLICATION ON VEHICLE CABIN 36

2.9 SUMMARY 37

CHAPTER 3 39

RESEARCH METHODOLOGY 39

3.1 OVERVIEW 39

3.2 MATHEMATICAL MODEL 39

3.2.1 Sound Wave Equation *39*

3.2.2 Helmholtz Equation *42*

3.3 THEORY OF ACTIVE NOISE CANCELLATION 44

3.3.1 Feedforward Active Control *45*

3.4 MATLAB-SIMULINK SIMULATION 47

3.4.1 Propagation of sound wave signal 49

3.4.2 Superposition with Secondary speaker 50

3.4.3 Feedforward Active Noise Cancellation 51

3.5 COMSOL MULTIPHYSICS SIMULATIONS 52

3.5.1 Propagations of Sound Waves in FEA 52

3.5.2 Superposition with Secondary Speaker in FEA 54

3.5.3 Feedforward Active Noise Cancellation in FEA 55

3.6 EXPERIMENT 56

3.6.1 Components 56

3.6.2 Propagation of Sound Wave 67

3.6.3 Superposition with Secondary Speaker 70

3.6.4 Feedforward Active Noise Control using Adaptive Filter 72

3.7 SUMMARY 78

CHAPTER 4 79

RESULTS AND DISCUSSIONS 79

4.1 OVERVIEW 79

4.2 MATHLAB SIMULINK SIMULATION 80

4.2.1 Propagation of Sound Wave Signal Result Analysis 80

4.2.2 Superposition with Secondary speaker Result Analysis 82

4.2.3 Feedforward Active Noise Cancellation Result Analysis 83

4.3 COMSOL MULTIPHYSICS 84

4.3.1 Propagations of Sound Waves in FEA 84

4.4 EXPERIMENT 88

4.4.1 Components 88

4.4.2 Propagation of Sound Wave 90

4.4.3 Superposition with Secondary Speaker 95

4.4.4 Active Noise Cancellation using Adaptive Filter 99

4.5 SUMMARY 106

CHAPTER 5 107

CONCLUSION AND RECOMMENDATION 107

5.1 CONCLUSION 107

5.2 RECOMMENDATION 108

REFERENCES 110

APPENDIX A 112

APPENDIX B 113

APPENDIX C 115

LIST OF TABLES

TABLE 3-1 SPEED SOUND IN VARIOUS MEDIUM IN ROOM TEMPERATURE 42

TABLE 3-2 SPECIFICATION OF COMPACTRIO 9004 57

TABLE 3-3 COMPARISON TABLE BETWEEN 3 SOUND INPUT 63

TABLE 3-4 CALIBER MID BASS SPEAKER SPECIFICATIONS 64

TABLE 3-5 SPECIFICATION OF WPA-425T AUDIO POWER AMPLIFIER 66

LIST OF FIGURES

FIGURE 1-1 CANCELLATION OF SOUNDS (MAREKICH, 2012) 16

FIGURE 1-2 RESEARCH METHODOLOGY 18

FIGURE 2-1 SOUND WAVE IN FREQUENCY AND TIME DOMAIN (FOREMAN, 1990). 22

FIGURE 2-2 SCHEMATIC DIAGRAM OF USING ACTIVE AND PASSIVE CONTROL AT THE SAME TIME (WU ET AL., 2022). 27

FIGURE 2-3 THE CONCEPT OF ANC (MOAZZAM & RABBANI, 2013). 29

FIGURE 2-4 FEEDFORWARD ANC SYSTEM WITH SINGLE CHANNEL (PADHI ET AL., 2017). 30

FIGURE 2-5 FEEDBACK ANC SYSTEM WITH SINGLE CHANNEL (PADHI ET AL., 2017). 32

FIGURE 2-6 HYBRID ANC SYSTEM (PADHI ET AL., 2017). 34

FIGURE 2-7 BASIC ADAPTIVE FILTER STRUCTURE (PARK ET AL., 2020) 35

FIGURE 2-8 FEED-FORWARD FXLMS SCHEMATIC DIAGRAM (JIANG ET AL., 2023). 36

FIGURE 3-1 NOISE CANCELLATION MECHANISM 44

FIGURE 3-2 ANC SYSTEM 45

FIGURE 3-3 FEEDFORWARD ANC SYSTEM BLOCK DIAGRAM 45

FIGURE 3-4 VARIABLE VALUE FROM MATLAB WORKSPACE 48

FIGURE 3-5 GP 49

FIGURE 3-6 GS 49

FIGURE 3-7 HC 49

FIGURE 3-8 SOUND PRESSURE EQUATION USING PRIMARY SPEAKER 50

FIGURE 3-9 SUPERPOSITION USING TWO SPEAKERS. 50

FIGURE 3-10 FEEDFORWARD ACTIVE NOISE CANCELLING 51

FIGURE 3-11 DOMAIN FOR THE INPUT SOUND PRESSURE FROM BIG BOUNDARY. 53

FIGURE 3-12 DOMAIN FOR THE INPUT SOUND PRESSURE FROM SMALL BOUNDARY 54

FIGURE 3-13 DOMAIN FOR THE TWO INPUT CONDITIONS. 55

FIGURE 3-14 SIMULATION ANC SETUP. 55

FIGURE 3-15 COMPACTDAQ 56

FIGURE 3-16 COMPACTRIO 9004 57

FIGURE 3-17 RCA FEMALE TO BNC MALE 59

FIGURE 3-18 MALE RCA TO XML 59

FIGURE 3-19 CRIO SETUP CONFIGURATIONS 60

FIGURE 3-20 LABVIEW 2014 61

FIGURE 3-21 MICROPHONE BEHRINGER ECM 8000 62

FIGURE 3-22 CALIBER MID BASS SPEAKER 64

FIGURE 3-23 BLUETOOTH SPEAKER 65

FIGURE 3-24 WPA-425T AUDIO AMPLIFIER 65

FIGURE 3-25 FUNCTION GENERATOR 66

FIGURE 3-26 ONLINE SOUND GENERATOR (ONLINETONEGENERATOR.COM) 67

FIGURE 3-27 EXPERIMENTAL SETUP FOR CLOSED ENVIRONMENT USING PVC PIPE 68

FIGURE 3-28 EXPERIMENT SETUP IN OPEN SPACE ENVIRONMENT 69

FIGURE 3-29 EXPERIMENT SETUP 73

FIGURE 3-30 ACTIVE NOISE CANCELLATION (WANG & THOMAS, 2017) 76

FIGURE 3-31 SECONDARY PATH AND FEEDBACK PATH MODELLING (NI LEARNING CENTRE) 76

FIGURE 4-1 PROPAGATION OF SOUND IN 1 M IN THE AIR 80

FIGURE 4-2 PROPAGATION OF SOUND IN 10 M IN THE AIR 80

FIGURE 4-3 PROPAGATION OF SOUND IN 1 M THROUGH IRON 81

FIGURE 4-4 SUPERPOSITION OF SOUND WAVE SIGNAL 82

FIGURE 4-5 FEEDFORWARD ANC 83

FIGURE 4-6 ACOUSTIC PRESSURE 84

FIGURE 4-7 TOTAL ACOUSTIC PRESSURE IN TIME DOMAIN. 85

FIGURE 4-8 TOTAL ACOUSTIC PRESSURE IN FREQUENCY DOMAIN 86

FIGURE 4-9 TOTAL ACOUSTIC PRESSURE IN TIME DOMAIN 87

FIGURE 4-10 TOTAL ACOUSTIC PRESSURE IN FREQUENCY DOMAIN 87

FIGURE 4-11 SOUND SIGNAL CAPTURE USING ACCELEROMETER SENSOR 88

FIGURE 4-12 SOUND SIGNAL CAPTURE USING BEHRINGER C-1 CONDENSER MICROPHONE 88

FIGURE 4-13 SOUND SIGNAL CAPTURE USING BEHRINGER ECM 8000 MEASUREMENT MICROPHONE 89

FIGURE 4-14 MICROPHONE 1 FOR 200 HZ SOUND SIGNAL CLOSE ENVIROMENT 90

FIGURE 4-15 MICROPHONE 2 FOR 200 HZ SOUND SIGNAL CLOSE ENVIRONMENT 90

FIGURE 4-16 MICROPHONE 1 FOR 1000HZ SOUND SIGNAL CLOSE ENVIRONMENT 91

FIGURE 4-17 MICROPHONE 2 FOR 1000HZ SOUND SIGNAL CLOSE ENVIRONMENT 91

FIGURE 4-18 MICROPHONE 1 FOR 50HZ SOUND SIGNAL CLOSE ENVIRONMENT 92

FIGURE 4-19 MICROPHONE 2 FOR 50HZ SOUND SIGNAL IN CLOSE ENVIRONMENT 92

FIGURE 4-20 MICROPHONE 1 FOR 200HZ SOUND SIGNAL IN OPEN SPACE 93

FIGURE 4-21 MICROPHONE 2 FOR 200HZ SOUND SIGNAL IN OPEN SPACE 93

FIGURE 4-22 MICROPHONE 1 FOR 50HZ SOUND SIGNAL IN OPEN SPACE 94

FIGURE 4-23 MICROPHONE 2 FOR 50HZ SOUND SIGNAL IN OPEN SPACE 94

FIGURE 4-24 MICROPHONE 1 FOR SUMMATION OF 50 HZ SOUND SIGNAL IN CLOSED ENVIRONMENT 95

FIGURE 4-25 MICROPHONE 2 FOR SUMMATION OF 50 HZ SOUND SIGNAL IN CLOSED ENVIRONMENT 96

FIGURE 4-26 MICROPHONE 1 FOR SUMMATION OF 50 HZ SOUND SIGNAL IN OPEN SPACE 97

FIGURE 4-27 MICROPHONE 2 FOR SUMMATION OF 50 HZ SOUND SIGNAL IN OPEN SPACE 97

FIGURE 4-28 TIME DOMAIN ON ALFA ROMEO V6 CAR ENGINE 99

FIGURE 4-29 FREQUENCY DOMAIN ON ALFA ROMEO V6 CAR ENGINE 99

FIGURE 4-30 TIME DOMAIN ON FERRARI MONDIAL T CAR ENGINE 100

FIGURE 4-31 FREQUENCY DOMAIN ON FERRARI MONDIAL T CAR ENGINE 101

FIGURE 4-32 SECONDARY AND FEEDBACK PATH COEFFICIENT FOR 200 HZ SOUND 102

FIGURE 4-33 RESIDUAL NOISE FOR 200 HZ WENT CONTROL OFF 103

FIGURE 4-34 RESIDUAL NOISE FOR 200 HZ WENT CONTROL ON 103

FIGURE 4-35 SECONDARY AND FEEDBACK PATH COEFFICIENT FOR FERRARI MONDIAL T SOUND 104

FIGURE 4-36 RESIDUAL NOISE FOR FERRARI MONDIAL T ENGINE CAR WENT CONTROL OFF 105

FIGURE 4-37 RESIDUAL NOISE FOR FERRARI MONDIAL T ENGINE CAR WENT CONTROL ON 105

LIST OF ABBREVIATIONS

ANC - Active Noise Control

PNC - Passive Noise Control

COMSOL - COMSOL Multiphysics Software

MATLAB - Matrix Laboratory Software

RPM - Revolutions Per Minute

FxLMS - Filtered-x Least Mean Square

RLS - Recursive Least Squares

FPGA - Field Programmable Gate Array

RT - Real-Time

cRIO - CompactRIO (Compact Reconfigurable Input/Output)

LMS - Least Mean Square

IDC - Insulation-Displacement Connector

BNC - Bayonet Neill-Concelman Connector

RCA - Radio Corporation of America Connector

XML - Extensible Markup Language

DAQ - Data Acquisition

IEPE - Integrated Electronics Piezo-Electric

NLMS - Normalized Least Mean Square

ASSFxLMS - Adaptive Step Size Filtered-x Least Mean Square

FFT - Fast Fourier Transform

DSP - Digital Signal Processing

AI - Analog Input

AO - Analog Output

Hz - Hertz

dB - Decibel

ZoQ - Zone of Quiet

m - Meter

s - Second

Pa - Pascal

V - Volt

c - Speed of Sound

CHAPTER 1

INTRODUCTION

1.1 INTRODUCTION

Unwanted noise and sound while driving always becomes a problem to the driver. It can be stressful and make it hard for the driver to focus. This topic has been one of the main types of research in automobile industry for the last 20 years (Samarasinghe et al., 2016). Before Active Noise Cancellation (ANC) technology became known and widely used, this problem was solved by using Passive Noise Cancellation (PNC) approach. PNC technique provides solution by using absorption and damping method. Specific materials embedded in the vehicles based on the noise that wanted to be reduced.

PNC technique is good at reducing high frequency noise, but low frequency noise can pass through the insulation easily. However, ANC has good attenuation ability to remove unwanted low-frequency noise (Jiang et al., 2023). In the case of engine noise, ANC technique can completely remove the unwanted noise.

ANC technique works with the superposition principle. The waves will be summed together and create the resulting noise where the inverted noise will cancel the noise source. Figure 1-1 shows how the cancellation of sounds works. For the ANC to work, a small speaker needs to be installed at the driver headrest. The speaker will propagate the inverted sound produced by a controller. In real life situation where the signal is not always be the same and synchronous perfectly,

system will become unstable because the error signal will not be correctly time-aligned with the input signal. Hence, an adaptive controller needs to be used to make sure inverted and real signal will be aligned at the same time.

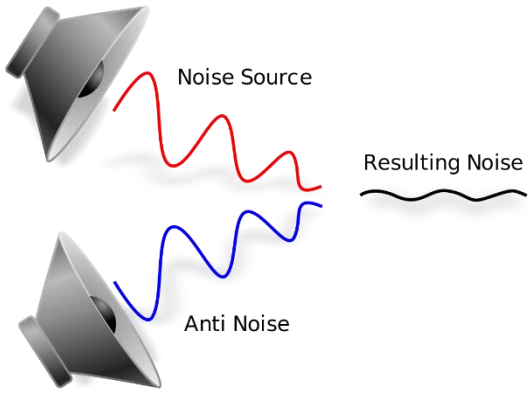

Figure 1-1 Cancellation of sounds (Marekich, 2012)

1.2 PROBLEM STATEMENT

Noise sources and cabin acoustics change depending on vehicle speed, road surface, and passenger position. The system needs to adapt to these dynamic conditions in real-time for optimal noise cancellation. This involves addressing issues such as optimal sensor placement, designing an effective controller, and optimizing the overall system to ensure practical and efficient noise control. The difficulty lies in balancing the need for noise suppression with the constraints of the confined space, while also considering factors like real-time adaptability and user comfort. Furthermore, the system's performance needs to be rigorously verified to validate its efficiency and reliability in real-world scenarios.

1.3 OBJECTIVE

There are 3 objective of this project which are:

1. To model the propagation of sound wave generated from a sound source to the error sensor location using MATLAB and COMSOL Multiphysics software.
2. To develop a local active noise control system using the feedforward controller method.
3. To verify the performance of the system experimentally

1.4 RESEARCH SCOPE

The purpose of this research is to create an adaptive local active noise cancellation system that can eliminate unwanted noise in a vehicle cabin by generating inverted noise waves using a controller. Simulations are performed using MATLAB Simulink and COMSOL Multiphysics. The experimental verification setup consists of a reference microphone, an error microphone, a noise speaker, a control speaker, and a National Instruments real-time controller. The experiment takes place in a controlled environment within the laboratory. A noise speaker is used to create a tonal noise that resembles engine noise..

1.5 RESEARCH METHODOLOGY

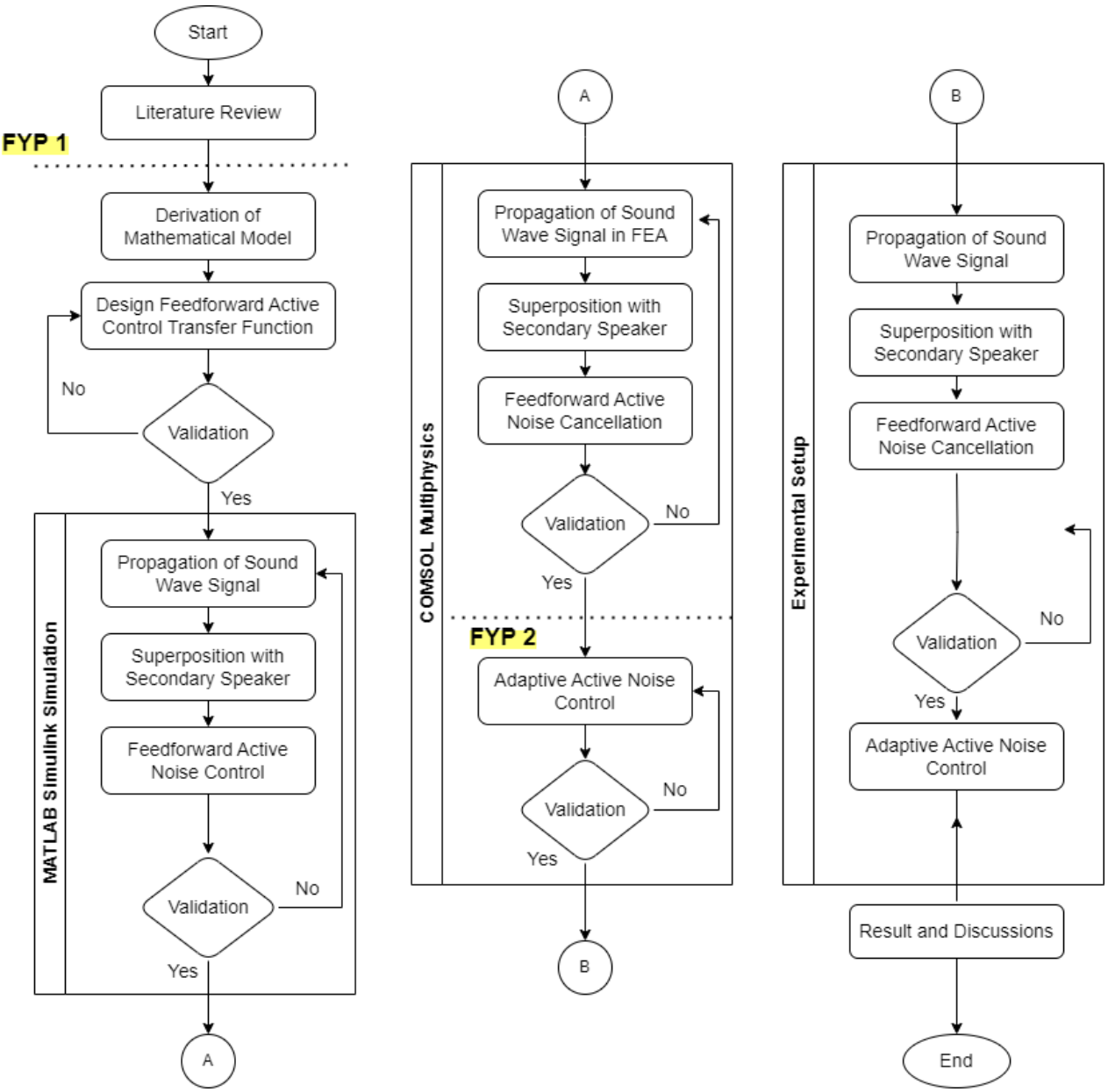

Figure 1-2 Research Methodology

.

1.6 REPORT OUTLINE

Chapter 1: Introduction

This chapter gives the introduction, problem statement and objective of the project. The research will be conducted based on these objectives.

Chapter 2: Literature Review

This chapter is about literature review from other research papers, articles, and journals that have been previously conducted to identify the best method for this research. All topics and subtopics related to this research has been identified and reviewed to gain better understanding about this research.

Chapter 3: Research Methodology

This chapter focuses on methodology that has been used in this research. All methodology and every step have been explained in detail in this chapter.

Chapter 4: Result and Discussions

This chapter contains result and analysis of the simulation conducted. The results obtained have been described in detail.

Chapter 5: Conclusions

This chapter concludes research overall with an explanation about the limitation and future planning about this project.

CHAPTER 2

LITERATURE REVIEW

2.1 OVERVIEW

This chapter is dedicated to the collection of data from previous research papers and journals that are relevant to the project's title. Every existing method and research have been studied and reviewed to get the best method to achieve all the objective of this project. At the end of this chapter, the method to be used in this project will be decided to produce the best outcomes.

2.2 INTRODUCTION TO SOUND AND NOISE

2.2.1 Sound

Sound is a type of energy that appears as vibrations, usually transmitted through a medium like air, water, or solids. The vibrations generate pressure waves that are detectable by the human ear, which then convert them into auditory perceptions. Sound is defined by its fundamental attributes, such as frequency, which determines the pitch, and amplitude, which affects the volume. The velocity of sound is not constant and is dependent upon the medium through which it propagates. Notably, sound waves propagate at a higher rate in solids compared to gases.

Various fundamental elements characterize the essence of sound. First and foremost, frequency is of utmost importance as it encompasses the entire range of

frequencies that can be heard by humans, which typically extends from 20 Hz to 20,000 Hz. Frequency refers to the rate at which a sound wave repeats, which determines the pitch of the sound that is heard. Concurrently, the amplitude, measured in decibels, represents the intensity of a sound. This characteristic affects the strength of the sound, ultimately influencing the impact of its volume. Moreover, the velocity of sound fluctuates depending on the medium it travels. Within the atmosphere, specifically in the air, the velocity of sound is approximately 340 meters per second. Comprehending the speed of sound is essential for understanding how it travels through various substances such as air, water, and solid materials. The propagation of sound waves in different media is influenced by various factors, including the distinct properties of the medium and the possible existence of obstacles. Furthermore, our auditory perception is intricately interconnected with various factors. The human auditory system is highly sensitive in detecting sounds within a specific frequency range referred to as the audible range, which typically spans from 20 Hz to 20,000 Hz. The perception is influenced by not only the frequency but also the amplitude and the context of background noise. (Helmholtz, 1878). Sound waves move in 3-dimensional domain which are in time domain and frequency domain. Figure 2-1 show the sound waves in frequency and time domain.

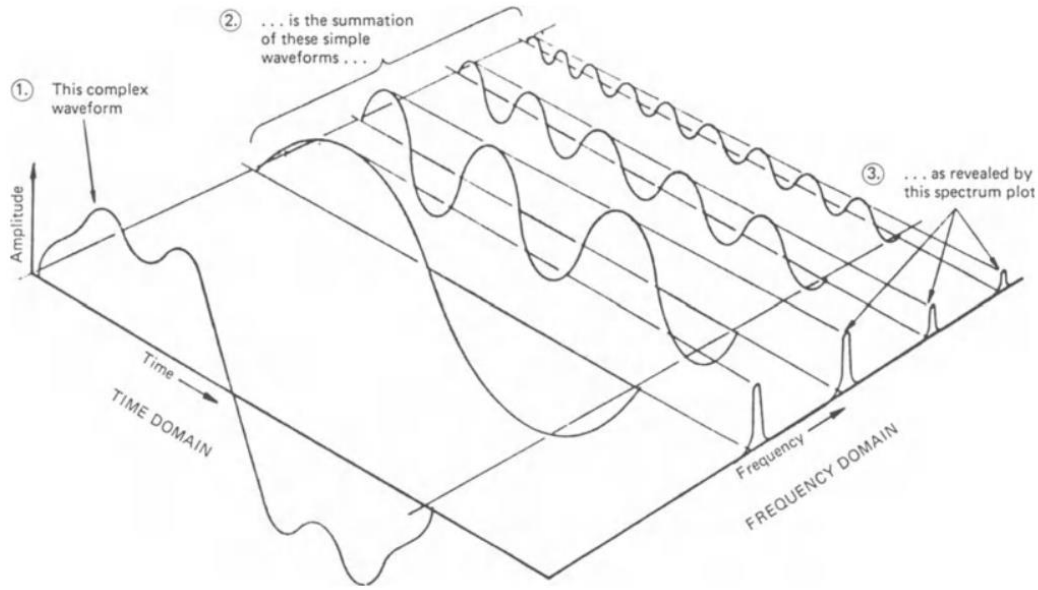

Figure 2-1 Sound wave in frequency and time domain (Foreman, 1990).

2.2.2 Noise

Noise, in its most general sense, refers to unwanted sound that has diverse negative impacts on individuals. It can impede optimal performance, reduce the enjoyment of leisure activities, disturb sleep, cause increased nervous tension, and lead to psychological consequences. Of particular significance is its ability to cause damage to the auditory system, potentially leading to early hearing loss. Similar to the contamination of air and water, noise is gaining more recognition and causing increased attention at the community, industrial, and governmental levels. This acknowledgment highlights the increasing recognition of noise as a type of "air pollution," emphasizing its diverse effects on both health and the environment (Foreman, 1990). According to Song (2022), noise can be defined as unintentional sound waves that are present in all aspects of our daily life.

2.3 NOISE SOURCES AND CHARCTERISTIC IN VEHICLE CABINS

2.3.1 Engine Noise

Most road vehicles with four or more wheels utilize a reciprocating, four-stroke, internal combustion engine. The noise is primarily caused by two processes: the piston crank mechanism and the combustion process. The predictive nature of combustion noise processes makes ANC highly effective to use (Samarasinghe et al., 2016).

2.3.2 Road and Tire Noise

Road-tire noise arises from the interaction between the road surface and the tire. It can be categorized into two main types: air pumping noise and vibration-induced noise, also known as road booming noise. The noise is primarily characterized by high frequencies and its intensity is influenced by factors such as road size, tire cavity size, tire load, and tire pressure. This noise is difficult to reduce using the ANC technique (Samarasinghe et al., 2016).

2.3.3 Wind and Aerodynamic Noise

The vehicle produces a low-frequency broadband noise when moving at mid to high speeds through the air. Additionally, there is a narrowband beating noise caused by the airflow over open windows, and an impulsive noise above 300 Hz resulting from the varying external wind conditions. The primary source of noise in the vehicle occurs within the interior when travelling at speeds exceeding 100 km/h (Samarasinghe et al., 2016).

2.3.4 Interior Noise Reflection and Resonance

The vehicle cabin is commonly regarded as a compact space with unique acoustic characteristics. Comparable to room resonance, at lower frequencies, the sound field is primarily influenced by a small amount of acoustic modes (Samarasinghe et al., 2016).

2.4 NOISE CONTROL

Noise control, or noise mitigation, comprises a range of strategies and techniques designed to diminish noise pollution and mitigate its effects, both in outdoor and indoor environments. This involves strategies such as implementing transportation noise control, employing effective architectural design, utilizing urban planning techniques through zoning codes, and implementing measures to control occupational noise (Elizabeth González, 2023). The main objective of noise control is to attain tolerable noise levels within a specified setting.

2.4.1 Passive Noise Control

Passive noise control involves a wide variety of techniques designed to reduce the amount of noise to a level that is acceptable to the users (Elizabeth González, 2023). In the research by Song (2022), explained that Passive Noise Control (PNC), also referred to as Passive Noise Isolation technology, involves using physical objects such as earbuds, headphones, or any other materials that can obstruct unintended sound waves to isolate your ears. Additionally, Zahir et al. (2019), mentioned that PNC is a technique that relies on sound-absorbing materials to effectively eliminate undesired noise.

According to Zahir et al. (2019) and Shi et al. (2020), PNC are most suitable to cancel or reduce high frequency noise. Shi et al. (2020) also mentioned that the efficiency of PNC decreases when the frequency of the noise becomes comparatively low, mainly due to the substantial size, excessive cost, and complicated deployment process. High frequency noise is sound waves that have a frequency exceeding 2000 Hz. These sound waves exhibit short cycles and are commonly noted for a "hissing" attribute. High-frequency noise has poor long-distance propagation and can rapidly dissipate due to its elevated energy levels. It is frequently associated with car horns door creaking and fans humming (Foreman, 1990).

2.4.1.1 **Existing Technology**

PNC is a type of passive system. It can acting either through their geometrical features or the incorporation of noise-absorbent materials (Elizabeth González, 2023). Similarly, Zahir et al. (2019) also mentioned that PNC used acoustic materials to attenuate undesired sound.

One of the application PNC is on the engine noise control using heat recovery boilers. According to Elizabeth González (2023) this method is highly effective for controlling noise in large engines. The heat recovery boiler will not only act as the passive silencer but also can decrease the viscosity of fuel.

2.4.1.2 *Effectiveness and Limitations of PNC*

According to Song (2022), the advantages of PNC are it have cost-effective power consumption and a broad operational frequency range. However, PNC technologies require large size and have limited flexibility for use in compact devices. On the contrary, Shi et al. (2020) argues that the efficiency of PNC diminishes when the noise frequency is comparatively low, as a result of the large size, expensive cost, and complex complexity of its implementation.

Additionally Park et al. (2020) mentioned that PNC offers the benefit of effectively attenuating all forms of noise across the entire frequency spectrum but this method lacks the ability to selectively eliminate a particular noise and incurs a higher cost relative to the size of the system.

2.4.2 Active Noise Control

According to Li et al. (2021), Shi et al. (2020), Zahir et al. (2019) and Jiang et al. (2023), ANC usually used to control low frequency noise. Moazzam & Rabbani (2013) also support this by stating that active noise control gives low-frequency noise reduction at a low cost, with minimal volume and weight, depending on the specific application. Low frequency noise is lower than 300 Hz.

According to Wu et al. (2015), the ANC technology has been implemented in various practical applications, including communication headsets, helmets, and ventilation ducts. Furthermore, ANC has been applied to reduce attenuating noise in a duct (Moazzam & Rabbani, 2013), inside vehicles cabin (Jiang et al., 2023; Kim & Altinsoy, 2022; Samarasinghe et al., 2016; Yin et al., 2023) and inside rail vehicles (Li et al., 2021).

2.4.3 Combine ANC and PNC method.

Zahir et al. (2019) presumed that installing ANC and PNC at the same time will produce better results. Shi et al. (2020) mentioned that ANC is an alternative complement for PNC as ANC can control the low-frequency noise while PNC can control the high-frequency noise

Supporting this, Wu et al. (2022) in their research, cancelling noise in the ventilation duct system by combining both active and passive techniques. The passive silencer is specifically designed to reduce high-frequency noise, while the feedforward ANC system is built into the passive damper in order to further reduce noise.

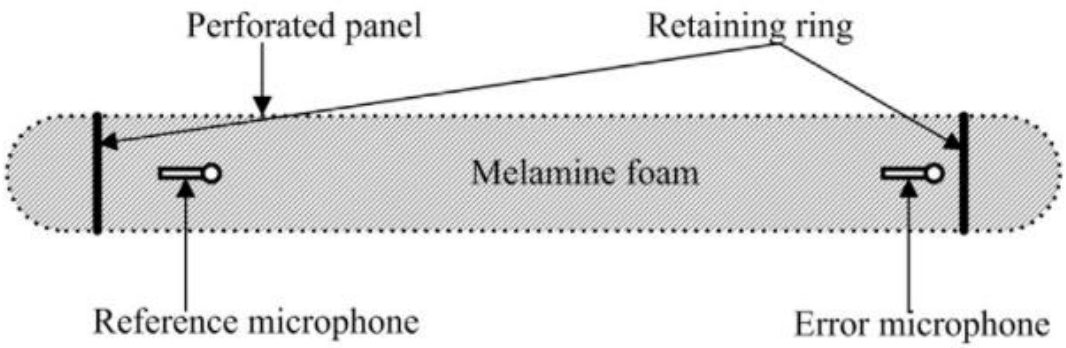

Figure 2-2 Schematic diagram of using active and passive control at the same time (Wu et al., 2022).

2.5 ACTIVE NOISE CANCELLATION

2.5.1 Acoustic Wave Superposition

Active noise control is a system that effectively eliminates the primary (undesirable) noise by applying the principle of superposition (Samarasinghe et al., 2016; Zahir et al., 2019). Similarly, Song (2022) explained that ANC employs an electro-acoustic technology to effectively eliminate the original noise. It accomplishes this by introducing a noise-canceling signal that has the same opposite phase and amplitude. Scientists employed ANC in the embedded device and successfully attenuated 25 decibels of the 60Hz periodic noise frequency.

In ANC, normally microphones serve to capture sound, while loudspeakers serve for transmitting counteracting sound within the same environment. In additional, according to the principle of interference, the original noise wave can be lowered or even eliminated by the anti-noise wave. The anti-noise wave is produced in a phase opposite to that of the noise. Hence, by superimposing an anti-noise wave that has exactly the same amplitude and opposite phase as the unwanted noise wave, the sound pressure level in a zone of quiet (ZoQ) can be reduced (Padhi et al., 2017; Shi et al., 2020; Zahir et al., 2019). Figure below visualize on how the ANC works.

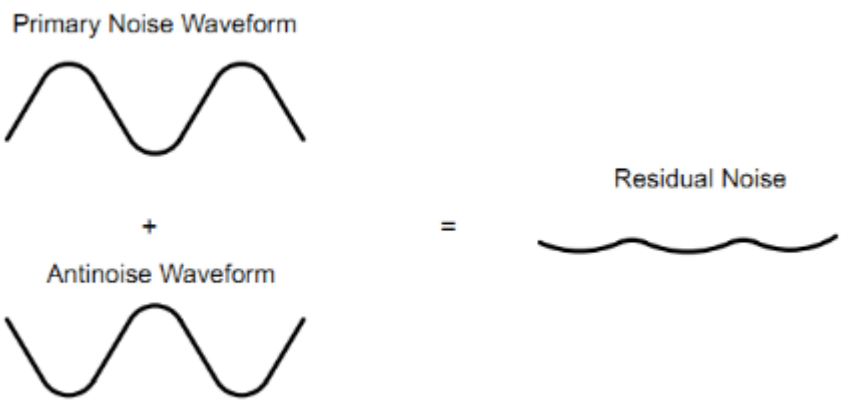

Figure 2-3 The concept of ANC (Moazzam & Rabbani, 2013).

2.5.2 Effectiveness and Limitations of ANC

The effectiveness of is ANC maintains a consistent cost regardless of the system size, and it allows for selective elimination of specific noise as mentioned by Park et al. (2020).

2.6 ACTIVE NOISE CONTROL STRATEGY

2.6.1 Feedforward Control System

According to Samarasinghe et al. (2016) feed-forward systems rely on a time-advanced "reference signal(s)" that corresponds with the signal from noise in order to reduce the intensity of the main noise field. Control with feedforward structure the reference signal must fulfil the causality requirement by providing time-advanced data and meet the correlation requirement by being highly correlated with the source noise. However, in the lack of a suitable location for the reference sensor, it is possible that these two requirements may not be met in certain

frequency ranges, resulting in the inability to control the noise components in those frequency bands through the feedforward structure (Wu et al., 2015).

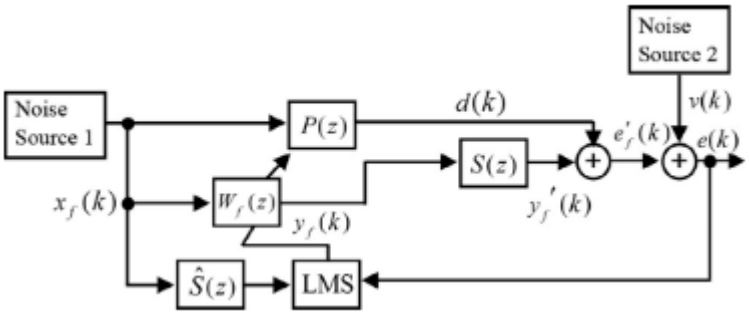

Figure 2-4 Feedforward ANC system with single channel (Padhi et al., 2017).

2.6.1.1 **Reference Sensors**

There are two type of reference sensors usually used which are microphones and accelerometers. Kim & Altinsoy (2022) stated that while microphones are affordable, accelerometers are often preferred for the practical application of feedforward control systems to mitigate issues like music interference or external noise.

Previous method used by Oh et al. (2014) and Sutton et al. (1994) are by minimize the noise levels inside the car cabin by utilizing reference signals acquired through direct measurement of the vibrations caused by road excitation. Research conducted by Cheer & Elliott (2015) utilizes inexpensive microphone error sensors, car audio loudspeakers as control sources, and the car audio DSP capabilities to function. However, to achieve reasonable levels of control, it is important to utilize a minimum of six accelerometers that are mounted on both the suspension and bodywork of the vehicle. These accelerometers will provide

reference signals that have a high degree of coherence with the error signals. This technique is a bit expensive. The cost can be overcome by putting a microphone on the floor in the car cabin.

2.6.2 Feedback Control System

Feedback structures are different than feedforward structures in that they do not necessitate the use of reference sensors to provide a reference signal that is advanced in time for the primary noise (Wu et al., 2015). This feedback system provides details about the noise level at a specified location to the control unit. The system require a microphone to record the sample noise that will be eliminated, controller to perform the analysis of the sample noise and generate the corresponding anti-noise and speaker to produce the anti-noise (Zahir et al., 2019).

According to Cheer & Elliott (2015), feedback control system can solve the cost problem when using the feedforward control by using the SISO controller that has been integrated in mass-production car. This method can only substantial reduction in noise level is accomplished within a limited frequency range of acoustic resonance, specifically around 40 Hz, in the front seats.

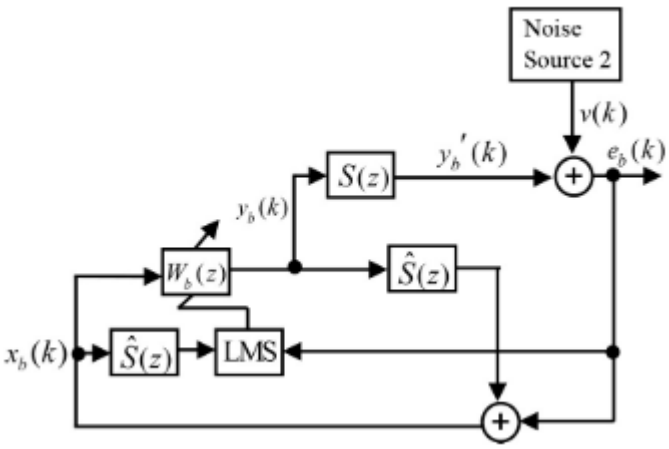

Figure 2-5 Feedback ANC system with single channel (Padhi et al., 2017).

2.6.2.1 **Reduce Car Horns in an Enclosed Cavity**

Based on the research by Zahir et al. (2019), a feedback controller was used to reduce car horn sound on the enclosed cavity. The ability of a feedback control system is efficient for any periodic signal as it can accurately anticipate the signal's behavior without the need for a reference microphone. Car horn are continuous so using feedback control should be efficient.

2.6.2.2 **Multi -channel and Single Channel feedback control**

Multi-channel feedback control use many error microphone. Thus, it will increasing complexity while simultaneously enhancing accuracy. It produces a larger zone of quiet. However, this configuration is also more expensive. On the other hand, single channel feedback control only need a microphone. The quiet zone created a just a limited area around the microphone (Zahir et al., 2019).

2.6.3 Hybrid Feedforward-Feedback Active Control (HANC)

The research conducted by Wu et al. (2015), shows that order to achieve efficient active control, the reference signal must meet two requirements: it should provide information that is ahead of time (known as the causality requirement) and it should have a strong correlation with the primary noise (known as the correlation requirement). However, according to Duan et al. (2014) and Wu et al. (2015), these problem can occur only using the feedforward ANC system. It can be solve by combined the feedforward system with feedback system that also known as hybrid control system.

A hybrid structure utilises the feedforward component to reduce the main noise that is related to the reference signal, while utilising the feedback component to eliminate narrowband components that are not detected by the reference sensor. This structure is capable of effectively managing both noise and unrelated narrowband disturbances. Hybrid control shows excellent performance in both narrowband and broadband noise reduction, and provides great flexibility in the design of active noise control systems (Wu et al., 2015).

Besides, the study demonstrated by Akhtar & Mitsuhashi (2011) also shows that the hybrid structure control effectively reduced both correlated and uncorrelated noise detected by the error sensor. This improvement was achieved by incorporating a third adaptive filter, which generated suitable signals for the feedforward and feedback structures. Notably, the noise reduction achieved by the hybrid structure control surpassed that of either the feedforward or feedback structure alone.

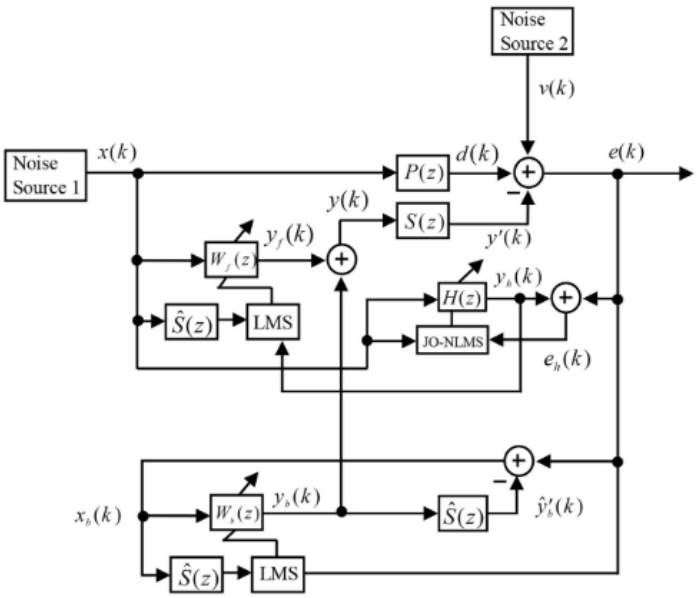

Figure 2-6 Hybrid ANC system (Padhi et al., 2017).

2.7 ADAPTIVE CONTROL

2.7.1 Adaptive Filters

According to Park et al. (2020), an adaptive filter algorithm has been used to perform inverse estimation of a channel. A commonly used algorithm for adaptive filtering is the least-mean-square (LMS) algorithm. The adaptive filter algorithm utilizes the input signal and error signal to estimate the system and adjust the filter coefficients. However, in the ANC setting, as the signal is received via the microphone, there is a significant likelihood of introducing different types of noises. Specifically, when Gaussian noise is introduced into the input stage, it results in a decrease in the accuracy of the system.

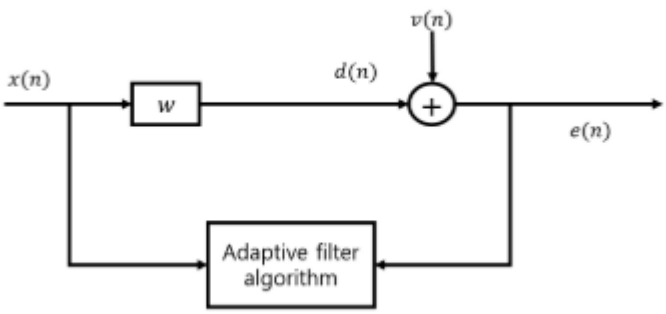

Figure 2-7 Basic adaptive filter structure (Park et al., 2020).

Least mean Square (LMS) algorithm is simple to execure. However, in real-world application scenarios, it is challenging to prevent the occurrence of secondary channel acoustic feedback problem, and the accuracy of convergence is relatively low. Besides, there are still limitations in effectively controlling nonlinear noise (Li et al., 2021).

2.7.2 Normalize Least Mean Square (NLMS)

Based on Park et al. (2020), the normalized-least-mean-square (NLMS) algorithm is recognised as the most popular adaptive filter algorithm. It can be applied to approximate the inverse channel of ANC based on information from the error signal.

2.7.3 Filtered-x least mean square (FXLMS)

In this ANC circumstances, the output of the filter is not directly compared with the desired signal, which is different from the general adaptive filter. Obtaining precise estimates is challenging due to the distortion of the adaptive filter's output caused by the secondary path. Hence, the secondary path, which is

estimated offline, filters out the primary noise. This becomes FxNLMS when the gaussioan noise is introduced (Park et al., 2020).

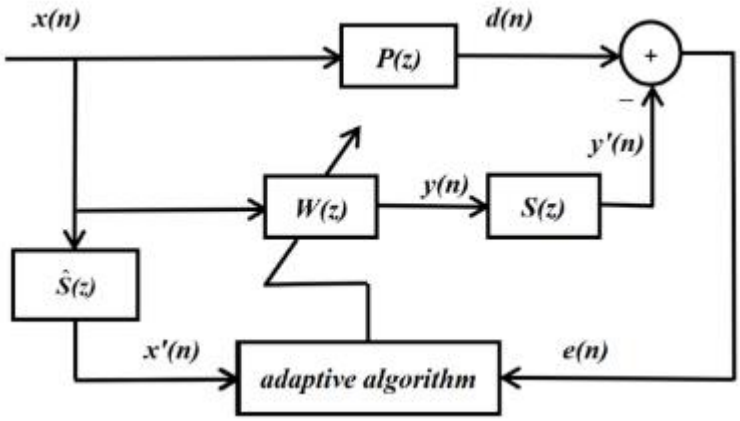

Figure 2-8 Feed-forward FxLMS schematic diagram (Jiang et al., 2023).

2.7.4 Adaptive Step Size with FxLMS (ASSFxLMS) Algorithms

Based on the research from (Jiang et al., 2023) it mentioned about adjust step size parameters based on the reference signal to create an adaptive step size algorithm. The FxLMS algorithm experiences instability when there is a sudden and significant increase in noise, causing the filter weight coefficient to undergo excessive amplitude changes due to a sudden increase in the reference signal. By using a small step factor intentionally to avoid instability will result in a notably sluggish convergence of the adaptive process. In order to address those problems, it is imperative to modify the step factor in order to enable the adaptive algorithm to effectively adjust to the abrupt surge in the noise signal.

2.8 ANC APPLICATION ON VEHICLE CABIN

An affordable feedforward engine noise control system can be established by utilizing an engine speed reference sensor, inexpensive microphone error sensors,

car audio loudspeakers and their amplifiers as control sources, and the car audio digital signal processing (DSP) capabilities. Several manufacturers have implemented active engine noise control systems (Cheer & Elliott, 2015).

According to Samarasinghe et al. (2016), as vehicle manufacturers aim to create more efficient and lightweight designs, the car interiors inevitably become louder due to the amplified structural vibrations. These noise are in low-frequency. Thus, ANC are more effective to use in order to reduce the noise. ANC techniques were devised to mitigate the noise within the cabin by utilizing secondary sources. Modern in-car entertainment systems typically come equipped with 4 to 6 built-in loudspeakers. Adding an ANC system to these systems incurs a relatively affordable extra expense.

2.9 SUMMARY

This literature review chapter systematically explores various aspects of noise control, particularly focusing on active noise cancellation (ANC) techniques within vehicle cabins. It begins by defining sound and noise, detailing their properties and the environmental factors affecting their propagation. The review then categorizes noise sources within vehicles, such as engine, road, and aerodynamic noise, and discusses their characteristics and the challenges they present for noise cancellation. Different noise control methods, including both passive and active techniques, are evaluated for their effectiveness and application suitability. The chapter highlights the advantages of combining ANC and passive noise control (PNC) to enhance noise reduction across different frequency ranges. It extensively covers various ANC strategies, including

feedforward and feedback systems, and discusses the use of adaptive filters like LMS and FXLMS to improve the precision of noise cancellation efforts. The review concludes with insights into practical ANC applications in vehicle cabins, suggesting that integrating ANC systems with existing vehicle audio systems can be a cost-effective method to significantly reduce in-cabin noise, thereby enhancing passenger comfort and vehicle appeal.

To summarize, based on the literature review, active noise cancellation (ANC) is the best option compared to using passive noise cancellation (PNC) to control the engine noise in the vehicle cabin because the engine produces a low frequency noise. A feedforward control system will be used along with adaptive filters. Based on the founding, all the research, equations, simulations and experimental setup will be elaborated in detail in Chapter 3.

CHAPTER 3

RESEARCH METHODOLOGY

3.1 OVERVIEW

This chapter discusses research methodology done to achieve this project objectives. Theory and equation involve also discussed and explained throughout the chapter. Firstly, derivation of the equation of sound was done to determine the mathematical model. Then, a simulation with MATLAB Simulink and COMSOL Multiphysics is done to study the sound wave and controller design.

3.2 MATHEMATICAL MODEL

3.2.1 Sound Wave Equation

Sound will propagate though medium such as air, water and any solid materials by transmitting its acoustic waves. The acoustic pressure from the propagation of sound are from particles that oscillate in the medium. Hence, sound will be produced when a vibrating object interferes with the nearby air particles. Sound waves can reflect off surfaces, changing in direction, absorb by some materials, diffraction and attenuate when travels through a medium.

Sound can be represented in both time domain and frequency domain. In the time domain the sound waves is represented as a function of time. While in frequency domain, it represents different frequency components that make the

acoustic signal. Whereas the frequency domain shows the signal's each frequency component, the time domain shows how a signal changes over time.

Time domain representation is commonly used in research and simulation because time domain representation provides detailed information on how sound waves change over time. Moreover, it captures more details about transients and variations of sound waves to make it possible to fully comprehend the temporal features of sound pressure. This project simulation will be done in the time domain, but the results will also show frequency domain.

Sound pressure as a function of time can be represented as

$$p(t) = p_A \sin(\omega t + \phi) \tag{3-1}$$

Where p_A is the amplitude of the pressure fluctuation which is the maximum displacement from the equilibrium position. ϕ is the phase angle of sound signal. ω is the angular frequency. Angular frequency can also be represented as

$$\omega = 2\pi f \tag{3-2}$$

Where f is the frequency of the wave measures in Hertz, Hz. Wave frequency, f can also represent as the number of cycles per unit of time.

$$f = \frac{1}{T} \tag{3-3}$$

T is a period which is time for one complete cycle. Thus, angular frequency, ω can be represented as

$$\omega = \frac{2\pi}{T} \tag{3-4}$$

Above equation is a derivation from general simple harmonic motion equation which is:

$$x(t) = A\cos(\omega t + \phi) \tag{3-5}$$

The use of cosine and sine are based on the initial conditions and based angle.

Simple harmonic sound waves are used to comprehend the basic ideas behind waves behavior more easily. Sound in the real world is more complicated and comprises a range of frequencies. Hence, comprehending basic harmonic waves in simulation will help on the experimental setup using real world sound. Simple harmonic sound wave can be known as sinusoidal wave that shows in simple harmonic motion. It can be represented by sine or cosine functions.

The simple harmonic sound wave equation below will derive general wave equation as function of time and spatial coordinates (x, t).

$$\frac{\partial^2 p}{\partial t^2} = c^2 \frac{\partial^2 p}{\partial x^2} \tag{3-6}$$

Where c is the velocity of propagation of sound or sound speed. Sound travel in different speed of sound based on the medium it is going through and the surrounding temperature, T. According to (Foreman, 1990), in his book sound speed in the air at sea level with temperature around 15℃ is approximately 335 meter per seconds and in the room temperature which is 20℃, the sound speed is $343\ \mathrm{m/s}$. Sound travel slow in gases, faster in liquid and fastest in solid. Table 3-1 shows the speed sound in various mediums in room temperature.

Table 3-1 Speed sound in various medium in room temperature

Medium	Sound Speed
Iron	5120 m/s
Polyethylene	19950 m/s
Water (liquid)	1481 m/s

Sound waves in 3-dimention can be represented in rectangular cartesian coordinates, x,y and z. The sound wave equations in x,y,z coordinates equation is:

$$\frac{\partial^2 p}{\partial x^2} + \frac{\partial^2 p}{\partial y^2} + \frac{\partial^2 p}{\partial z^2} = \frac{1}{c^2}\frac{\partial^2 p}{\partial t^2} \qquad (3\text{-}7)$$

3.2.2 Helmholtz Equation

The one-dimensional Helmholtz equation can be derived from general one-dimensional wave equation:

$$\frac{\partial^2 p(x,t)}{\partial x^2} = \frac{1}{c^2}\frac{\partial^2 p(x,t)}{\partial t^2} \qquad (3\text{-}8)$$

By using this sinusoidal wave equation form which is a derivation from Equation (3-1):

$$p_{(x,t)} = P\cos(kx - wt) \qquad (3\text{-}9)$$

Where P is the amplitude. k is the wave number from the equation:

$$k = \frac{2\pi}{\lambda} \qquad (3\text{-}10)$$

Where λ is the wavelength. The Equation (3-8) will be substituted into the equation (3-9) by taking the second partial derivatives as

$$\frac{\partial^2}{\partial t^2}(P\cos(kx - wt)) = c^2 \frac{\partial^2}{\partial x^7}(P\cos(kx - wt)) \qquad (3\text{-}11)$$

After simplifying the second partial derivatives solution and solve for k:

$$k = \frac{\omega}{c} \qquad (3\text{-}12)$$

The k is substituted back to the sinusoidal equation to get the one-dimensional Helmholtz equation:

$$\frac{d^2p}{dx^2} + k^2 p = 0 \qquad (3\text{-}13)$$

The pressure of sound can also be represented as $p(x,t)$ in terms of time domain and spatial domain:

$$p(x,t) = \tilde{p}\, e^{(-jkx)}\, e^{jwt} \qquad (3\text{-}14)$$

Where the $e^{(-jkx)}$ is the spatial domain and $e^{j\omega t}$ is for time domain. In 3-dimensional, the Equation (3-14) can be written as

$$p(x,y,z,t) = \tilde{p} e^{(-jk_x x - jk_y y - jk_z z)}\, e^{j\omega t} \qquad (3\text{-}15)$$

Where the $e^{(-jk_x x - jk_y y - jk_z z)}$ are for 3-dimensional spatial domain.

3.3 THEORY OF ACTIVE NOISE CANCELLATION

Active noise cancellation is done by cancelling unwanted noise using another inverted noise produced by a controller using superposition principle. Superposition principle is when two waves overlap at the same time it will be sum of the waves. The feedforward controller used in this project is a stable and can surely produce the desired output even though by using basic controller.

The noise cancellation simulation will be simulated with simple harmonic sound wave equation. In the simulation, 2 speakers and 1 microphone will be used. The primary speaker will represent the source of the sound which is noise of engine car. In the simulation it will be represented as sinusoidal wave. The secondary speaker will act as the anti-noise wave to eliminate the noise with a feedforward controller. The microphone will act as input to detect error after the cancellation. Figure 3-2 shows the direction of the noise and the inverted noise waves.

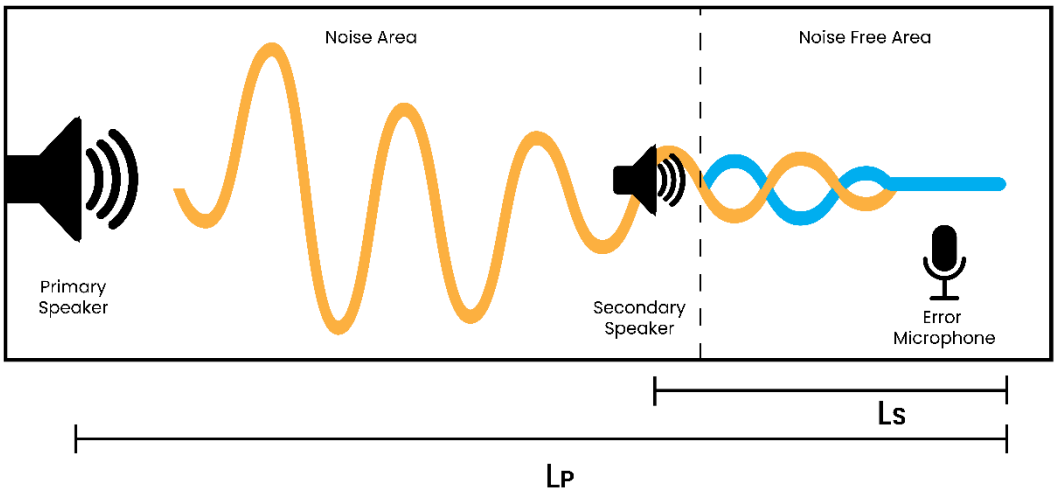

Figure 3-1 Noise Cancellation Mechanism

3.3.1 Feedforward Active Control

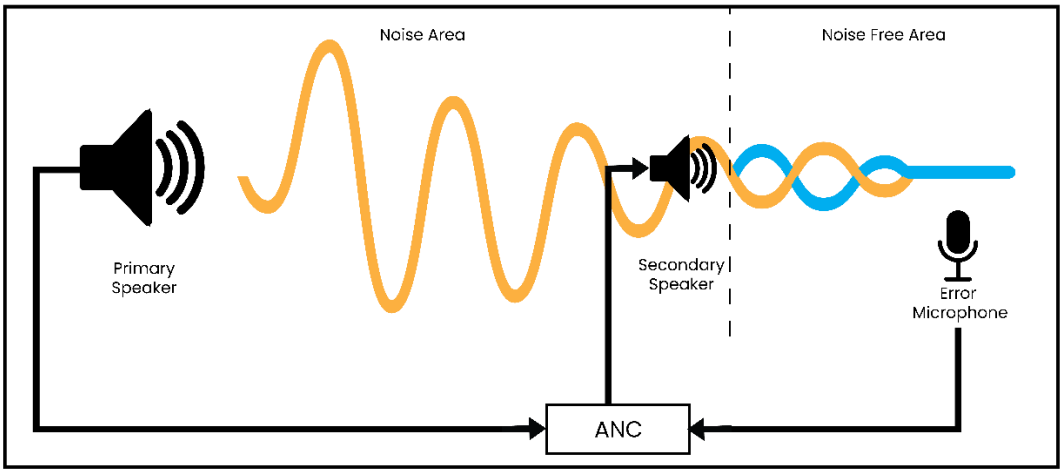

Figure 3-2 ANC System

Figure 3-2 shows the block diagram of feedforward active control mechanism that used in this ANC system.

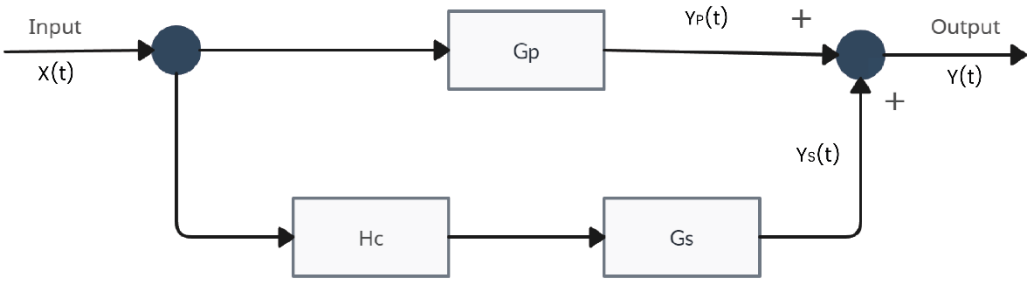

Figure 3-3 Feedforward ANC system block diagram

The unwanted noise, $X(t)$ is the input into the primary $Y_P(t)$ and secondary $Y_S(t)$ paths. The primary path, $Y_P(t)$ is the noise from the reference microphone (input) to the error microphone (output). The secondary path, $Y_S(t)$ is the noise from the reference microphone that has been inverted using controller, H_C.

The feedforward transfer function of the system can be derive based on the block diagram in Figure 3-2. The primary and secondary path can be defined as

$$Y_P = G_P X(t) \tag{3-16}$$

$$Y_s = H_C\, G_s X(t) \tag{3-17}$$

The output, $Y(t)$ can be derived from the summation of Y_P and Y_s. Hence, the output is:

$$Y(t) = Y_P + Y_S \tag{3-18}$$

From Equation (3-16) and (3-17), Y(t) is:

$$Y(t) = H_C\, G_S X(t) + G_P X(t) \tag{3-19}$$

The output of the system should be zero as the objective for this is system is to eliminate the unwanted noise.

$$Y(t) = 0 \tag{3-20}$$

By substitute the Equation (3-20) into (3-19),

$$0 = H_C\, G_S X(t) + G_P X(t) \tag{3-21}$$

From Equation (3-21), the transfer function for this feedforward system is:

$$Hc = -\frac{G_p}{G_S} \tag{3-22}$$

3.4 MATLAB-SIMULINK SIMULATION

Simulink is a MATLAB based graphical programming environment for modelling, designing, simulating, and analyzing design a system. Simulink is a suitable simulation environment for this project due to its ability to create graphical block diagrams and produce results needed. All the simulations are run on the MATLAB version R2023b with academic license.

There are 3 equations involved in the simulations for the primary speaker, secondary speaker, and controller. The equation is a derivation from equation (14) but only the spatial domain part.

$$P = e^{-jkx} \tag{3-23}$$

Where x will be substituted with L which is the length between the speaker and the error microphone.

$$P = e^{-jkL} \tag{3-24}$$

As shown in figure 3-1, the L used in the simulation were Lp and Ls which are length from primary speaker to the error microphone and length from secondary speaker to the error microphone respectively.

$$\lambda = \frac{c}{f} \tag{3-25}$$

Then, by substituting the Equation (3-25) into (3-10),

$$k = \frac{2\pi f}{c} \tag{3-26}$$

The new pressure equation can be derived by substitute equation (26) into (24)

$$p = e^{-j2\pi f \frac{L}{c}} \quad (3\text{-}27)$$

$$G_P = e^{-j2\pi f \frac{L_P}{c}} \quad (3\text{-}28)$$

$$G_S = e^{-j2\pi f \frac{L_S}{c}} \quad (3\text{-}29)$$

The variables used in the simulation are declared in the command window and stored in the model workspace. For this simulation the sampling frequency, f was set at 10 Hz with sample time,Ts, 0.001s. The amplitude is set at 10 m. Sound speed,c used is 343 m/s at room temperature. Length from primary speaker to error microphone, Lp is 1m and length from secondary speaker to error microphone, Ls is 0.1m.

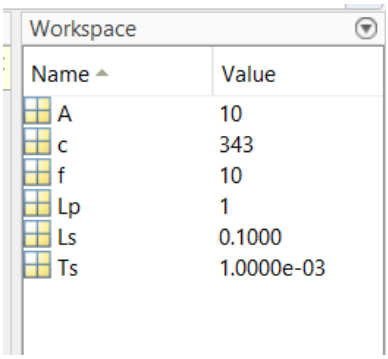

Workspace

Name	Value
A	10
c	343
f	10
Lp	1
Ls	0.1000
Ts	1.0000e-03

Figure 3-4 Variable value from Matlab workspace

Input signal for the simulation is sinusoidal wave from the Simulink sine wave generator function. The output signal will be shown in the graph using scope. If there is more than one output, it will be shown with mux block. Block diagrams involved in the simulation are Primary speaker, Gp, Secondary speaker, Gs and Controller, Hc as shown in the figure 3-, 3- , and 3- respectively.

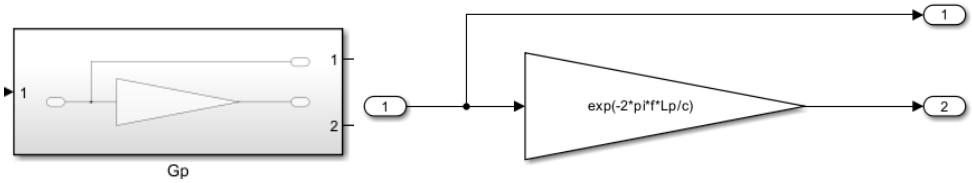

Figure 3-5 Gp

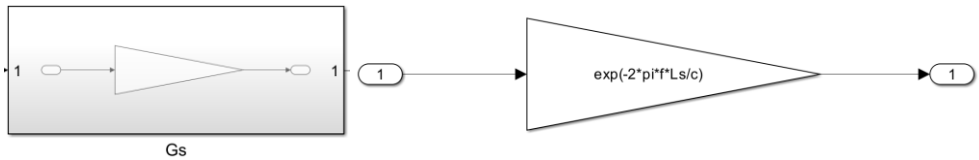

Figure 3-6 Gs

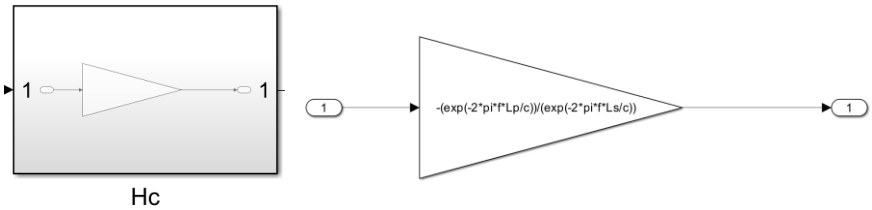

Figure 3-7 Hc

3.4.1 Propagation of sound wave signal

3.4.1.1 **Same medium different length**

This simulation is simulating the sinusoidal wave going through the sound pressure equation for different lengths in the same medium. It is to shows that the sound wave will be reduced as it propagates through the air based on the length between source and the reference point. Increase in length will further reduce the sound waves. For this simulation only the *Lp* value will be changed from the block diagram in Figure 3-8.

3.4.1.2 **Same length different medium**

This simulation is simulating the same signal going through a different medium but with same length. The signal will go through air and iron. The sound speed for iron is 5120 *m/s* in the room temperature.

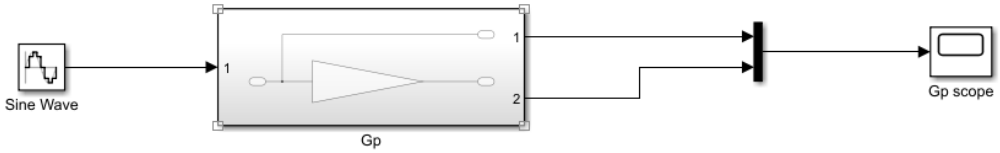

Figure 3-8 Sound Pressure Equation using Primary Speaker

3.4.2 Superposition with Secondary speaker

This simulation is to show the superposition principle. When the two-sound waves travel together it will sum together.

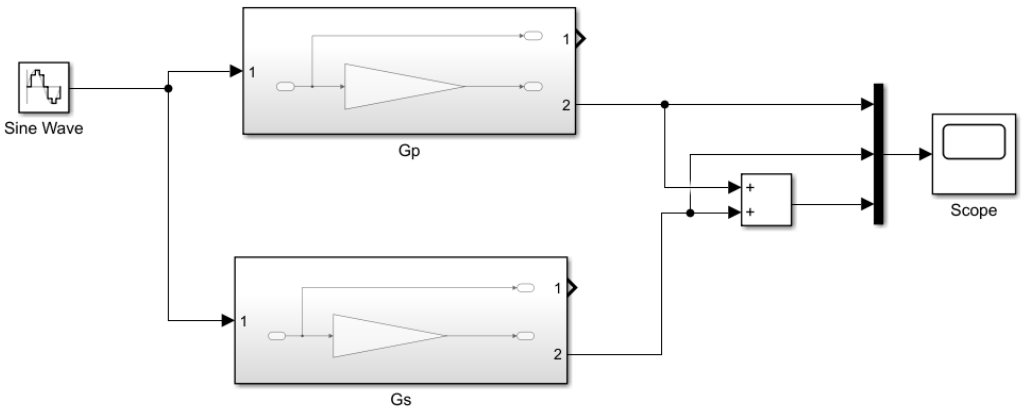

Figure 3-9 Superposition using two speakers.

3.4.3 Feedforward Active Noise Cancellation

This simulation is to cancel the sound wave in the primary speaker by using the controller, *Hc*. The controller will invert the sound waves in the secondary speaker to cancel the sound after the summing point. The step signal with the step time 0.3s is to include delay in the cancellation. It will show the difference between before and after the cancellation.

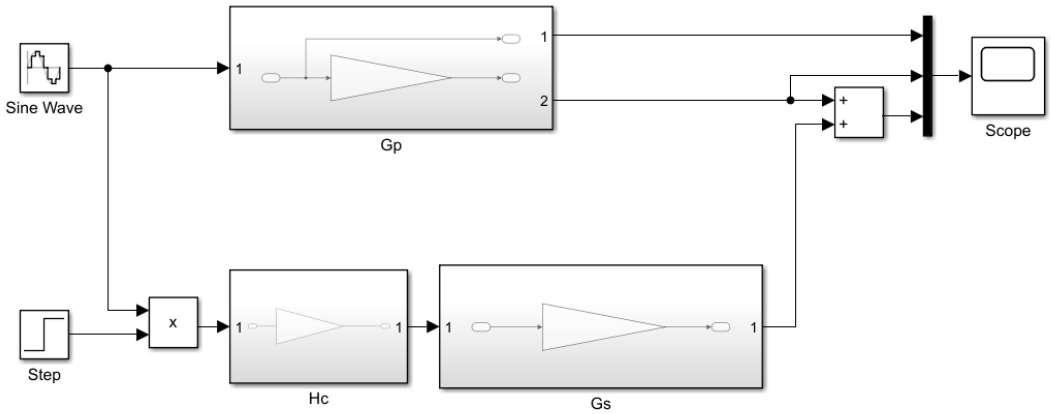

Figure 3-10 Feedforward Active Noise Cancelling

3.5 COMSOL MULTIPHYSICS SIMULATIONS

COMSOL Multiphysics is software that is capable of simulating Multiphysics and single-physics modeling. In this study, COMSOL Multiphysics version 5.5 has been used to do all the related simulations.

Finite Element Analysis (FEA) with COMSOL involves creating a virtual model of a space, breaking it into small elements (mesh), and simulating the propagation of sound waves. The model considers the physical properties of materials, acoustic characteristics of air, and boundary conditions. COMSOL's solver processes equations to calculate sound wave behavior, and the results reveal details like pressure and velocity distributions. This approach aids in understanding and optimizing sound interactions within a given environment, offering insights for effective noise control or sound enhancement in applications such as vehicle cabins.

3.5.1 Propagations of Sound Waves in FEA

3.5.1.1 **Input Sound Pressure from Big Boundary**

This simulation is simulating the propagation of sound wave in the close boundary conditions as in Figure 3-11. The size of the domain is 100 cm width, 50 cm depth and 50 cm height. The material in the domain is air with pressure acoustics time explicit and hard boundary wall.

The input acoustic pressure is defined by the equation,

$$P_0(t) = A\sin(2\pi f t) \qquad (3\text{-}30)$$

Where the amplitude, A is 1 m and the frequency, f is 10 Hz. The simulation is done in time dependent with range 0s to 1s, step time of 0.01s and physics-controlled tolerance. The input is from the purple-colored boundary as shown in Figure 3-11.

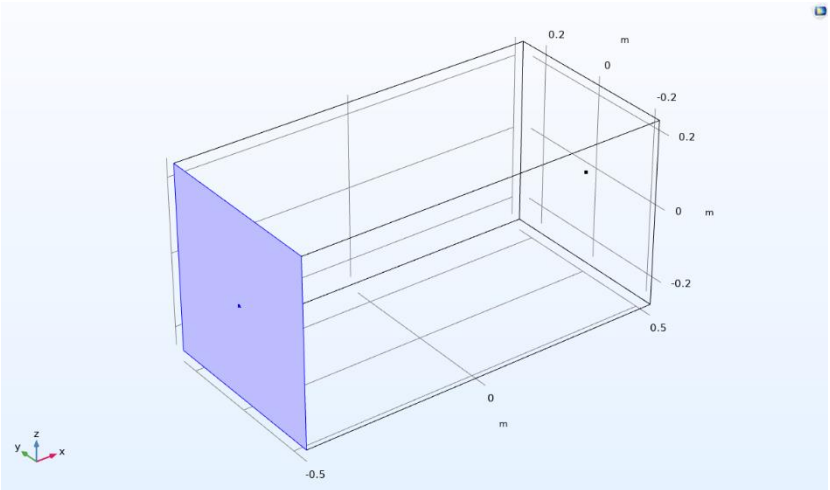

Figure 3-11 Domain for the input sound pressure from big boundary.

3.5.1.2 **Input Sound Pressure from Small Surface**

This simulation simulates the propagation of sound waves in the close boundary as in Figure 3-12. This simulation uses the same parameter as the simulation in the 3.5.1.1 except for the input pressure and the amplitude, A. The amplitude is 5. For this simulation the input wave is from the purple-colored boundary as in Figure 3-12.

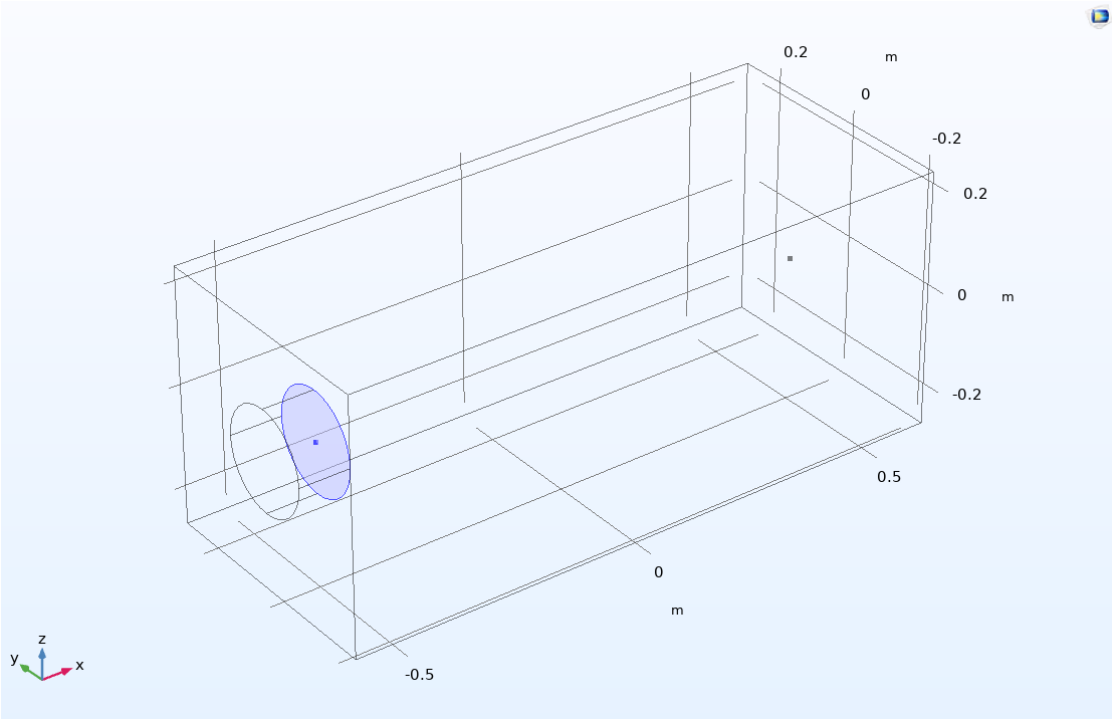

Figure 3-12 Domain for the input sound pressure from small boundary.

3.5.2 Superposition with Secondary Speaker in FEA

This simulation is simulating the propagation of sound wave in the close boundary conditions as in Figure 3-11. The size of the domain is 110 cm width, 50 cm depth and 50 cm height. The material in the domain is air with pressure acoustics time explicit and soft boundary wall.

The input acoustic pressure is defined by the equation,

$$P_0(t) = A\sin(2\pi f t) \qquad (3\text{-}31)$$

The input is from the purple-colored boundaries as shown in Figure 3-13.

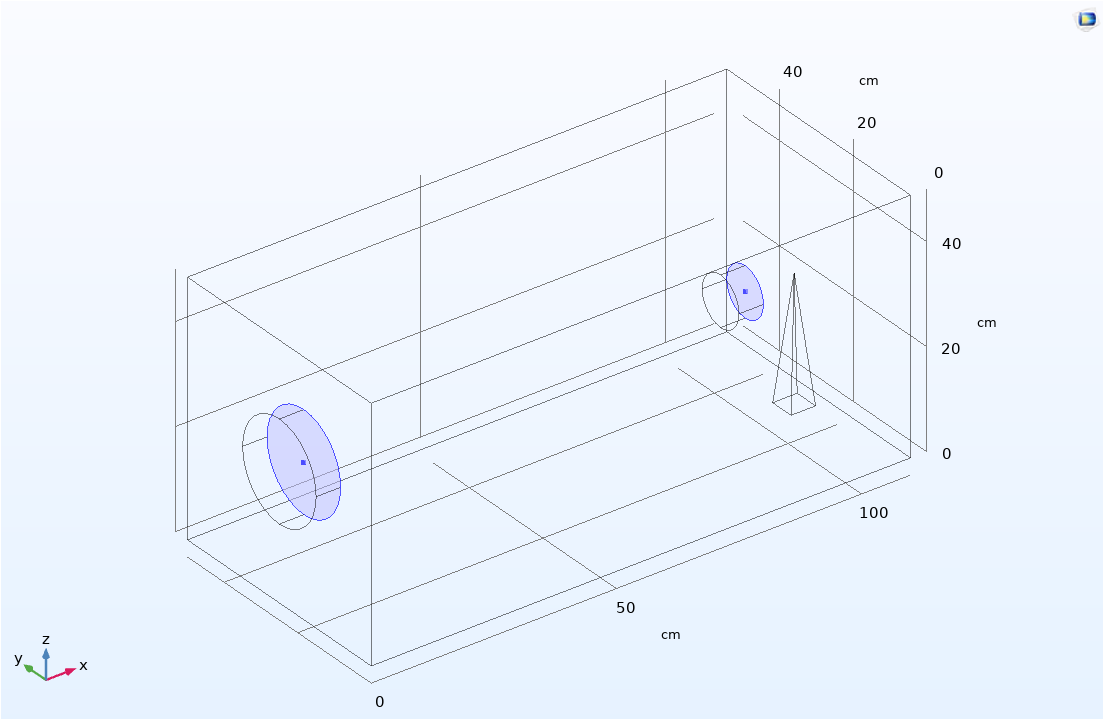

Figure 3-13 Domain for the two input conditions.

3.5.3 Feedforward Active Noise Cancellation in FEA

Figure 3-14 shows the setup for simulation of feedforward ANC in COMSOL.

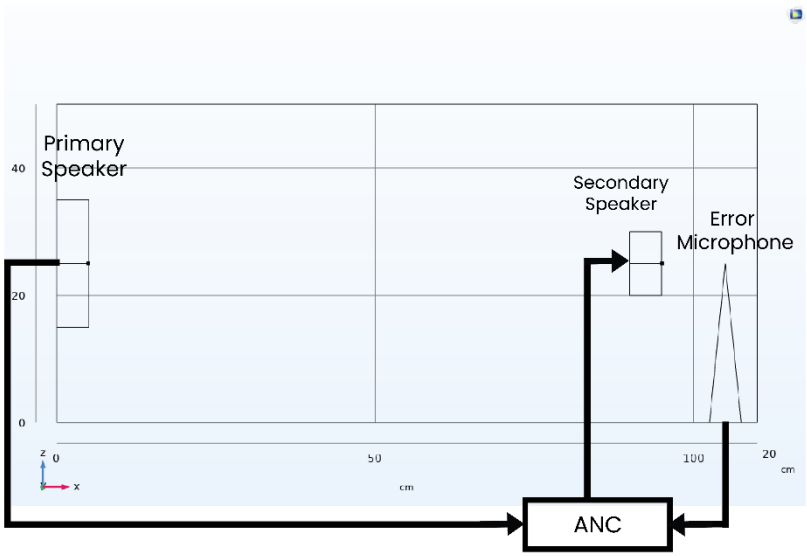

Figure 3-14 Simulation ANC setup.

3.6 EXPERIMENT

3.6.1 Components

3.6.1.1 ***Controller***

3.6.1.1.1 *Compact DAQ*

Figure 3-15 CompactDAQ

The Compact DAQ is used for data acquisition and input verification in the project. Microphone testing is conducted using the Compact DAQ prior to selecting the appropriate microphone for the experiment with the Compact RIO. This decision is based on the ease and straightforwardness of using the Compact DAQ compared to the DAQ in terms of graphical programming before learning the complex programming using the compact RIO. The Compact DAQ, used which is offers a simpler setup and configuration process through NI LabVIEW, making it easier to quickly interface with and test various microphones. This allows for efficient evaluation of microphone performance and characteristics before

integration into the more complex Compact RIO setup for the active noise cancellation project.

3.6.1.1.2 *Compact Rio*

Figure 3-16 CompactRIO 9004

Table 3-2 Specification of CompactRIO 9004

Memory	64 MB of DRAM for real-time processing
FPGA	Xiilinx Spartan-3 FPGA for custom, high-speed processing tasks
I/O Modules	Support for up to eight swappable C series I/O modules for a wides range of signa types and sensors
Communication Ports	Ethernet port
OS	Runs NI Real-Time OS (RTOS)

The CompactRIO 9004 (cRIO-9004) by National Instruments is an advanced control and acquisition system, perfect for applications that require real-time

performance and FPGA capabilities. Equipped with a real-time processor and reconfigurable FPGA, it is ideal for complex control systems. This includes tasks like active noise cancellation using adaptive filters, which need precise timing and detailed signal processing. The cRIO-9004 ensures consistent performance with its real-time processor and supports quick data handling and parallel processing with its FPGA. This setup allows for the direct implementation of complex algorithms in hardware. NI's LabVIEW software provides a graphical interface for developing both real-time and FPGA-based applications, making system design simpler. While offering exact real-time processing and a customizable FPGA for better flexibility and performance, the cRIO-9004's advanced features may add complexity and increase power consumption. Additionally, dependence on NI’s proprietary LabVIEW software can limit flexibility. Nevertheless, the cRIO-9004 remains a strong choice for projects that need high precision and advanced processing capabilities.

In the early stages of our project, the Single-Board RIO (sbRIO) controller was initially selected. However, due to limitations with the available sbRIO models, specifically the use of IDC connectors incompatible with microphone inputs and the absence of BNC connectors, it was decided to switch to the CompactRIO (cRIO) instead. The cRIO offers more flexible I/O options, including modules with suitable connectors for microphones, which are crucial for this active noise cancellation project. Additionally, the cRIO's customizable FPGA provides the capability to implement complex algorithms like adaptive filters in real-time. This makes it a more suitable choice for the project's needs compared to the sbRIO.

To effectively use the CompactRIO 9004 (cRIO-9004) for data acquisition, it needs to be paired with its C Series universal analog input module and current output module. Figures 3-xx show the cRIO 9215 input module and cRIO 9263 output module used in the experiment. The input module needs to be use with RCA female to BNC male connector and RCA male to XML cable to connect it with the microphone.

Figure 3-17 RCA Female to BNC Male

Figure 3-18 Male RCA to XML

These modules are essential for connecting to various sensors and actuators. For example, the input module includes an IEPE power supply, which can power microphones without the need for a phantom power supply. This setup is especially useful for tasks such as active noise cancellation, as it ensures accurate data

collection. By integrating these modules, the cRIO-9004 can manage the necessary data inputs and outputs for control and monitoring applications.

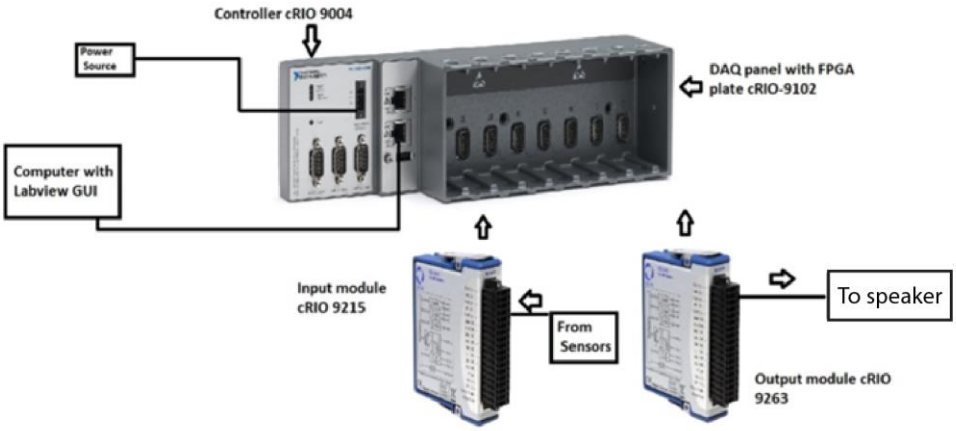

Figure 3-19 cRIO setup Configurations

Figure xx show cRIO-9004 controller serves as the central component, connected to a DAQ module equipped with an FPGA for customized processing. A computer running LabVIEW software interacts with the controller to configure and monitor its operations. Sensor data from microphone is collected via the input module (CRIO-9215) and transmitted to the controller for processing. Based on these calculations, the controller sends the generated control sound signal to the output module (CRIO-9263), which then cancels the input sound. This configuration shows the real-time capabilities of the Compact RIO system for both data acquisition and control purposes which is the target of this experiment.

3.6.1.2 ***Software***

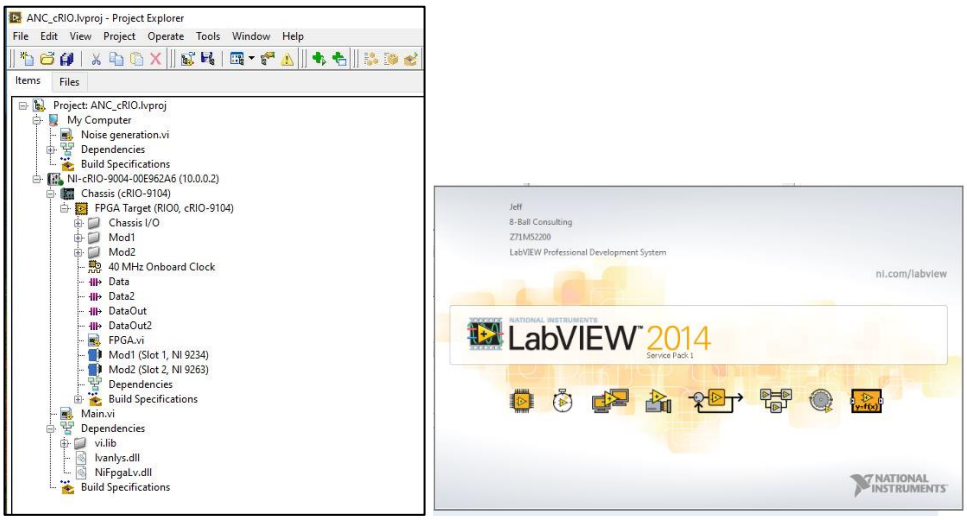

Figure 3-20 LabVIEW 2014

The controller includes its proprietary software, LabVIEW also from National Instrument. LabVIEW 2014 used in this project due to its robust features and extensive compatibility. LabVIEW provides a graphical programming environment that simplifies the development of complex control and data acquisition systems, making it particularly suitable for real-time applications. Its extensive library of functions and toolkits enables efficient implementation of signal processing algorithms, which is essential for the active noise cancellation project.

LabVIEW 2014 also features a user-friendly interface that supports three key development phases. The first phase involves the FPGA target, where custom logic is designed and compiled using the FPGA compilation tool. The second phase focuses on the real-time (RT) target, where deterministic operations are executed by the real-time processor on the local chassis. The third phase entails the host computer, which interfaces with the RT system for configuration, monitoring, and data analysis.

The FPGA was compiled using the Xilinx 10.1 compilation tool, compatible with the FPGA controller. This tool ensures that custom FPGA code is efficiently translated into hardware, allowing for high-speed data handling and parallel processing capabilities required for real-time performance.

3.6.1.3 ***Microphone***

Figure 3-21 Microphone Behringer ECM 8000

The microphone being used is the Behringer ECM8000 measurement microphone like shown in the Figure 3-21. 2 microphones been used in this experiment as reference microphone and error microphone. It is specifically designed for audio measurement applications, providing high precision and accuracy. The ECM8000 features a condenser capsule with a wide frequency response range and low distortion, making it suitable for capturing detailed acoustic measurements. Its omnidirectional polar pattern ensures consistent sound pickup from all directions, which is beneficial for tasks such as room acoustic analysis and calibration. The microphone is also recognized for its flat frequency response, ensuring that recorded signals accurately reflect the original sound source without altering it. The ECM8000 is suitably used with measurement systems like the

Compact RIO 9004 for where precise and reliable acoustic data is critical for effective noise reduction algorithms.

Before deciding the best microphone to use, testing was performed to identify the most suitable microphone for the experiment. The testing has been done between Behringer ECM 8000, Behringer C-1 and Accelerometer. Different microphones produce different outputs due to their varying specifications. The testing involved using the Compact DAQ to record the input sound signals from each microphone. This method allowed for a comprehensive comparison of performance characteristics such as frequency response, sensitivity, and signal-to-noise ratio. The collected data was crucial for determining which microphone provides the most accurate and reliable acoustic measurements needed for the experiment.

Table 3-3 Comparison table between 3 sound input

Feature/Specification	*Behringer ECM8000*	*Behringer C-1*	*Accelerometer*
Type	Measurement Microphone	Studio Condenser Microphone	Vibration Sensor
Frequency Response	15 Hz to 20 kHz	40 Hz to 20 kHz	Typically, DC to thousands of Hz
Sensitivity	-37 dBV/Pa (14.1 mV/Pa)	-33 dBV/Pa (22.4 mV/Pa)	Varies by model
Applications	Acoustic measurement for room calibration	Vocal and instrument recording	Vibration and shock measurement
Power Requirements	Phantom power (15-48V)	Phantom power (36-52V)	Varies (often DC powered)

3.6.1.4 ***Speaker***

Figure 3-22 Caliber Mid Bass Speaker

Figure 3-22 shows the speaker that been use in the experiment are caliber midbass speaker. This Caliber 4" Mid Bass Speaker is particularly suitable for an active noise cancellation study due to its wide frequency response of 55-20kHz. This range allows it to handle a broad spectrum of sounds, necessary for both generating and canceling diverse noise frequencies. Its high sensitivity of 91 dB/W/M ensures it can produce significant volume at lower power levels, crucial for precise control in experimental setups. Additionally, the speaker's ability to manage up to 200 watts maximizes performance without distortion. Its 4-ohm impedance facilitates compatibility with various audio systems, making the speaker an effective choice for detailed and rigorous noise cancellation research.

Table 3-4 Caliber Mid Bass Speaker Specifications

Frequency response	55-20kHz
Materials	High Temperature 1 Inch Aluminum Voice Coil with 100 Oz Magnet
Sensitivity	91 dB
Impedance	4 Ohm
Power	200 W Maximum

Figure 3-23 Bluetooth Speaker

Another speaker that has been used is a Bluetooth speaker in the Figure 3-23 to play the sound from online sound generator.

3.6.1.5 ***WPA-425T Audio Power Amplifier***

Figure 3-24 WPA-425T Audio Amplifier

The sound signal amplifier used in this experiment is WPA-425 2 Channel Bridgeable Mosfet Power Amplifier shown in Figure 3-24. It offers a robust power output of 95W per channel RMS and up to 200W per channel at maximum, allowing for clear sound reproduction without distortion. The amplifier supports an adjustable speaker impedance range from 40 Hz to 250 Hz, making it versatile for

use with different speakers. Its frequency response from 10 Hz to 50 Hz is ideal for focusing on low-frequency sounds, crucial in noise cancellation. Additionally, the high and low input sensitivity options cater to varied signal levels, facilitating seamless integration with other system components. This combination of features ensures that the amplifier can effectively handle demanding audio tasks and provide precise control necessary.

Table 3-5 Specification of WPA-425T Audio Power Amplifier

Channels and Power Output	95W/Channel RMS Continuous Output 200W x 2 Channel Maximum Power Output
Speaker Impedance	Adjustable 40 Hz – 250 Hz
Frequency Response	10 Hz - 50 Hz
Input Sensitivity	High: 1.0 V – 6.0 (Impedance 20K Ohm) Low: 100mV – 2 V (Impedance10 Ohm)

3.6.1.6 ***Function Generator***

Figure 3-25 Function Generator

A function generator was used in the experiment to generate sinusoidal inputs at desired frequencies. This allows control over the frequency and amplitude of the signals. Figure 3-25 show the function generator that has been use in this

experiment. Besides using function generator, some of the experiments also conducted using online sound generator.

Figure 3-26 Online Sound Generator (onlinetonegenerator.com)

3.6.2 Propagation of Sound Wave

The propagation of sound wave experiment was conducted to demonstrate that sound dissipates over distance and through air. This phenomenon occurs because as sound waves travel, they spread out and their energy is absorbed by the medium through which they pass, which in this case is air. The experiment aimed to measure how the intensity and clarity of sound decrease as the distance from the sound source increases. Understanding this behavior can better predict and manage how sound behaves in different environments, crucial for applications such as acoustic design, noise control, and audio technology development.

3.6.2.1 **Propagation of Sound in Closed Environment**

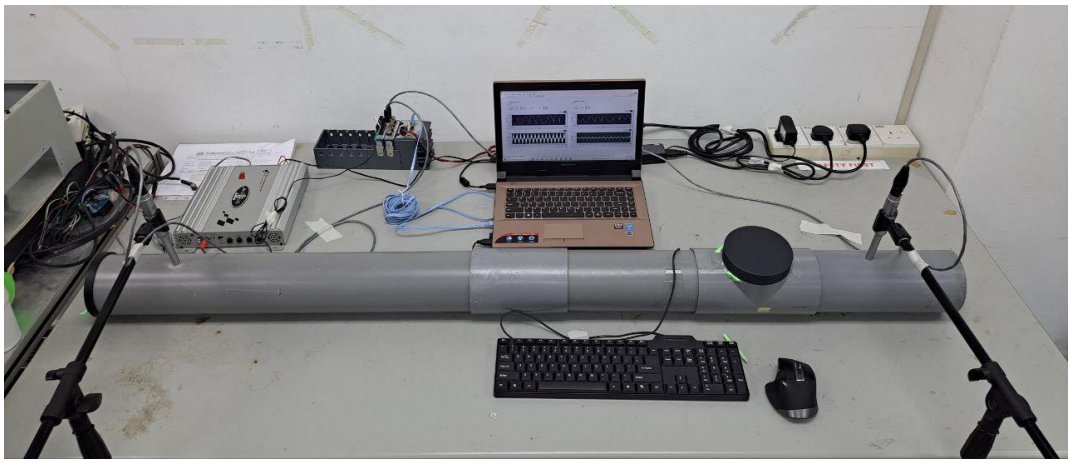

Figure 3-27 Experimental Setup for Closed Environment using PVC pipe

The experimental setup for studying sound propagation in a closed environment is shown in the Figure 3-27. The setup comprises a speaker as the signal source and two Behringer ECM8000 microphones to capture the sound at two distinct locations. The speaker is affixed to the left end of a polyvinyl chloride (PVC) pipe, facilitating sound propagation from left to right. The first microphone is positioned 15 cm to the right of the speaker, while the second microphone is located 141.5 cm from the speaker. Both microphones capture the sound signals, demonstrating the effect of sound propagation in a closed environment.

The microphones are connected to the Compact RIO input module, with the sound signal readings acquired via the Compact RIO controller. The captured sound signals are initially processed into time-domain graphs. These time-domain graphs are then converted into frequency-domain graphs using Fast Fourier Transform (FFT) in MATLAB to verify the frequency signal. The results of these analyses are explained in detail in Chapter 4.4. This process ensures a thorough

understanding of sound behaviour in a confined space and validates the experimental setup and data processing methodology.

3.6.2.2 **Propagation of Sound in Open Space Environment**

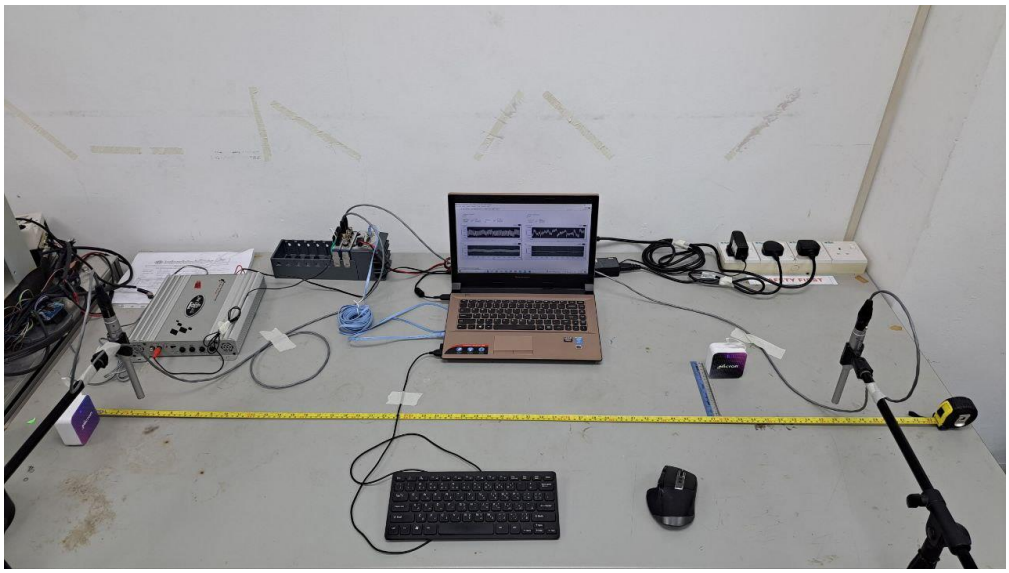

Figure 3-28 Experiment Setup in Open Space Environment

The experiment setup for analysing sound propagation in an open space environment is depicted in the Figure 3-28. This setup also includes a speaker serving as the signal source and two Behringer ECM8000 microphones positioned to capture sound at two different locations. The speaker is placed at one end of the experimental area (Point A), and sound propagates outward. The first microphone is positioned at 15 cm from the speaker, while the second microphone is placed 141.5 meters from the speaker. The distance between the microphone and the speaker are the same with the previous setup. Both microphones are strategically positioned to capture the sound signals as they travel through the open space, allowing for a detailed analysis of sound propagation in an unobstructed environment.

3.6.3 Superposition with Secondary Speaker

To validate the superposition principle in both closed and open environments, an experimental setup was modified by introducing a secondary speaker, located 121 cm from the primary speaker. This setup enabled the examination of sound wave interactions from two sources in both environments. In the closed environment, such as within a PVC tube, the sound waves from the two speakers are expected to demonstrate constructive interference, enhancing the amplitude where the waves are in phase. In contrast, in an open environment, although the superposition principle still holds where the resultant sound wave is the sum of the individual waves the effects of constructive interference may be less noticeable due to the greater dissipation of sound energy. The experiment captures these interactions through strategically placed microphones, analyzing the resultant waveforms to assess how effectively the superposition principle manifests under varying environmental conditions.

3.6.3.1 **Summation in Closed Environment**

In the closed experiment setup, as illustrated in Figure 3-xx, an additional speaker referred to as Speaker 2 has been added. This speaker emits an identical sound signal to that of Speaker 1, facilitating the observation of sound wave interactions based on the superposition principle. The setup is configured such that the sound waves emitted from both speakers converge and overlap, ideally demonstrating constructive interference where the sound signals enhance each other due to their in-phase relationship. The distances in the experimental setup are meticulously maintained to ensure consistency and accuracy in data collection. The

distance between Speaker 1 and Microphone 1 is kept constant at 15 cm. Same with the distance between Speaker 1 and Microphone 2 is set at 141.5 cm. Speaker 2 is strategically positioned 121 cm away from Speaker 1, with an additional 10 cm setback. This precise arrangement of speakers and microphones is crucial for investigating the effects of sound wave superposition in the controlled environment.

3.6.3.2 **Open Space**

To study the superposition effect under different conditions, a similar experimental setup was created in an open area, the same with the configuration shown in Figure 3-xx used in the closed environment. This setup not only replicates the arrangement of speakers and microphones but also includes an additional speaker, referred to as Speaker 2, which is positioned 121 cm distance with Speaker 1 with a 10 cm setback. This arrangement allows for a direct comparison of how sound behaves in both environments.

The reason for conducting a similar experiment in an open area is to demonstrate the superposition principle without the influence of boundaries or reflective surfaces that are present in the closed setup. By removing the PVC pipe and other barriers, the sound waves can travel freely. This configuration is crucial for observing the natural behavior and fundamental properties of sound waves, providing insights into how environmental factors affect sound. This consistent approach helps to clearly show the different impacts that enviroment conditions have on wave behavior and interactions.

Both the experiment of propagation of sound and the superposition principle are using compact RIO 9004 and LabVIEW 2014. The programming code for the FPGA target is shown in Appendix C, while the code for the real-time (RT) level is detailed in Appendix E. The front panel interface for the FPGA and RT are in Appendix B and Appendix D respectively.

3.6.4 Feedforward Active Noise Control using Adaptive Filter

The theory and simulation about feedforward active noise control can be proof by this experiment that using LabVIEW graphical programming. An algorithm has been create in LabVIEW to generate new control signal based on input from reference microphone and error microphone.

3.6.4.1 **Analyze engine sound signal**

Engine sound has been analyzed before the experiment to know the engine sound frequency. The frequency of an engine's sound is intricately linked to its RPM (revolutions per minute), as described by the equation:

$$f = \frac{n\ x\ RPM}{60} \qquad (3\text{-}32)$$

In this equation, f signifies the frequency in hertz (Hz), n represents the number of sound cycles produced per revolution of the engine, and RPM denotes the engine's speed. This relationship reveals that each full revolution of the engine, driven by mechanisms such as pistons and valves, produces a sound cycle. Consequently, the fundamental frequency of the sound is directly proportional to the RPM, increasing as the engine accelerates and decreasing as it decelerates.

Regarding the parameter n in the frequency formula, it is determined by specific engine configurations. Components like pistons and valves operate in systematic sequences, generating vibrations that manifest as sound. In a four-stroke engine, for example, a full operational cycle which are encompassing intake, compression, power, and exhaust that occurs over two crankshaft revolutions, thus affecting the value of n. Moreover, engine sounds comprise not only the fundamental frequency but also harmonics, which are integral multiples of this base frequency, adding complexity to the acoustic output. These dynamics are essential for analyzing engine sounds and employing them in diagnostic evaluations.

To determine the engine frequency to be use in the experiment, a recorded sound of a Ferrari Mondial t and Alfa Romeo V6 car engine with constant RPM has been use to be plot in MATLAB using Fast Fourier Transform (FFT).

3.6.4.2 **Experiment Setup**

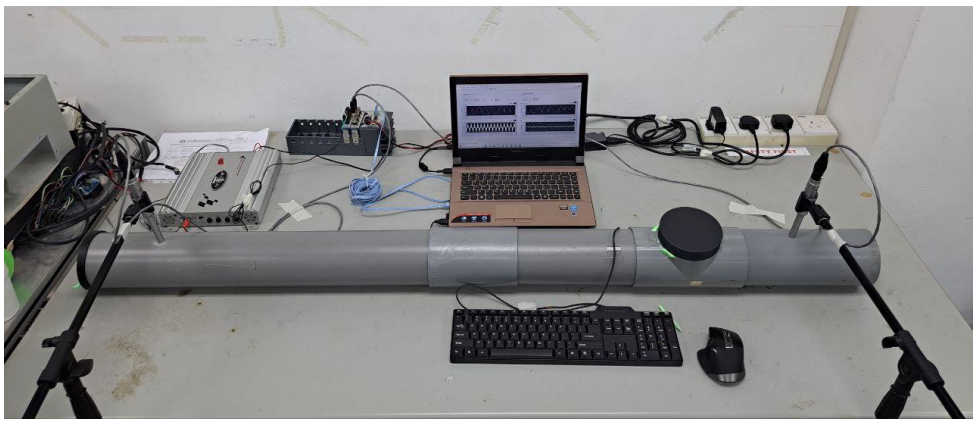

Figure 3-29 Experiment setup

The described experimental setup is designed for a feedforward adaptive active noise cancellation (ANC) system. It consists of two speakers positioned within a

Polyvinyl chloride (PVC) pipe, which is 150 cm long and 12 cm in diameter, facilitating a controlled environment for simulating one-dimensional sound propagation.

At one end of the PVC pipe, the primary speaker is mounted vertically and acts as the noise source. This Bluetooth speaker is wirelessly connected to a computer that emits sound frequencies to mimic the noise produced by a car engine operating at a constant RPM. The secondary speaker, known as the control speaker, is placed horizontally 121 cm away from the primary speaker. It plays a crucial role in emitting a counteractive sound wave intended to negate the noise from the primary speaker. The output from this speaker is enhanced by an amplifier connected to a Caliber mid-bass speaker system before being routed to the Compact Rio's AO0 module.

To monitor and adjust the sound cancellation effectiveness, two microphones are strategically integrated into the system. Positioned 15 cm from the primary speaker, the reference microphone captures the original noise for analysis. Meanwhile, the error microphone is set 141.5 cm from the primary speaker and 20.5 cm from the secondary speaker, capturing the combined sounds for assessing the noise cancellation achieved. These microphones are connected to the Compact RIO, with the reference microphone on channel AI1 and the error microphone on channel AO0. Prior to the experiments, both microphones undergo functionality tests to confirm their operational accuracy. Functionality tests are also conducted on the secondary speaker using signals from a function generator to verify its performance within the setup.

The noise reduction will be observed from the reduction of its amplitude response. Then, based on the amplitude response, the attenuation in dB can be calculated using the equation:

$$Amplitude\ (dB) = 20\log_{10}\left(\frac{Amplitude\ 1}{Amplitude\ 2}\right) \qquad (3\text{-}33)$$

3.6.4.3 **Software and Controller Configuration**

The experiment utilizes Compact RIO as the control hardware and LabVIEW 2014 for software execution. The code designed for the FPGA target can be found in Appendix C, and the code for the real-time (RT) level is detailed in Appendix E. Interfaces for the FPGA and RT operations are provided in Appendix B and Appendix D, respectively. The compilation of the code, carried out using Xilinx 10.1 tools compatible with LabVIEW 2014, requires approximately about 10 minutes to complete. The details information about the controller and software has been describe in Section 3.6.1.

3.6.4.4 **Block diagram**

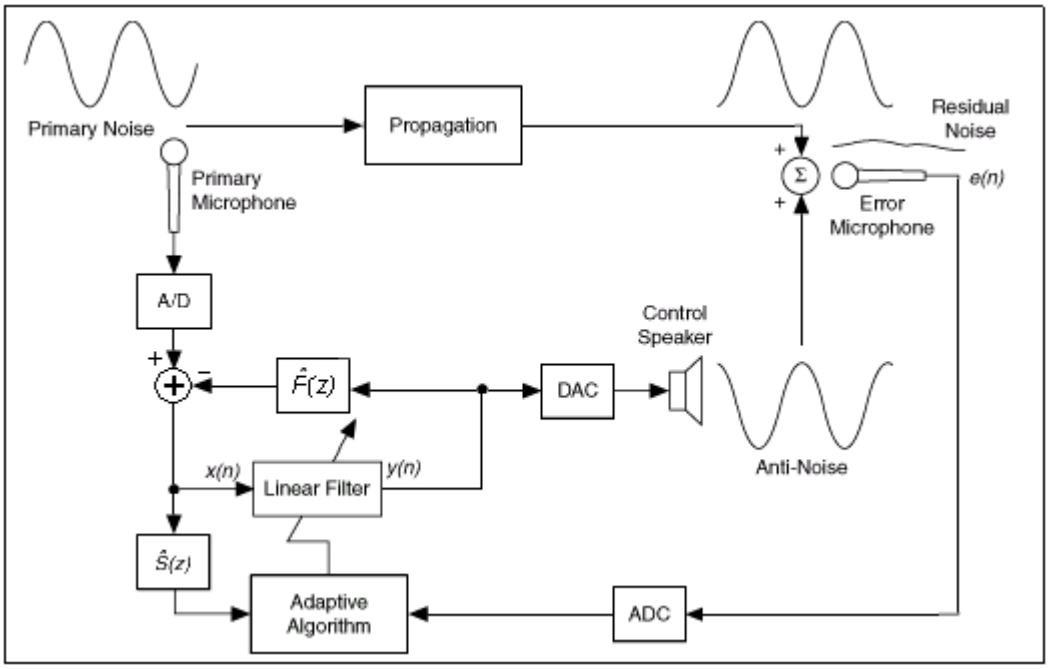

Figure 3-30 Active Noise Cancellation (Wang & Thomas, 2017)

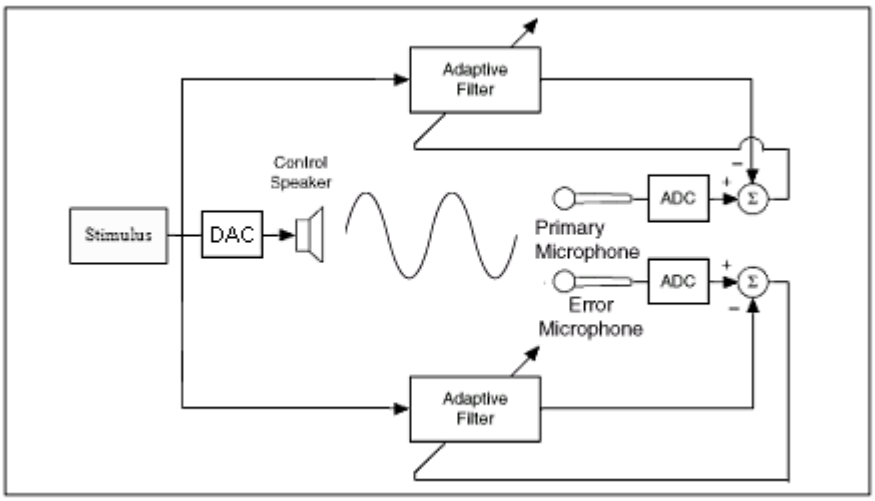

Figure 3-31 Secondary path and Feedback Path Modelling (NI learning centre)

This block diagram illustrates the function of the LabVIEW program, which is segmented into two main sequences at both the main RT and FPGA levels. The first sequence, as depicted in Figure 3-30, involves determining the coefficients for

the Secondary Path and the Feedback Path. The coefficients are determined using an LMS filter, which is key for predicting how noise travels and is detected, and for calculating the propagation delay and attenuation of the sound. The Secondary Path coefficient is crucial for estimating the distance between the control speaker and the error microphone. This coefficient helps in predicting how the noise will travel in the environment before it is picked up by the error microphone, allowing for precise adjustments in the noise cancellation process.

On the other hand, the Feedback Path coefficient is used to determine the distance between the reference microphone and the control speaker. This path calculates the propagation delay and attenuation of the sound from the speaker back to the microphone, which is critical for correctly aligning the anti-noise signal to effectively cancel the original noise.

The second sequence, shown in Figure 3-31, executes the adaptive noise cancellation using the coefficients obtained from the first sequence. It utilizes the Filtered-x Least Mean Squares (FxLMS) algorithm, a method effective in reducing noise in environments where the noise characteristics are not static and can change over time. The FxLMS algorithm in this setup adapts the control signal continuously based on the incoming noise signal captured by the reference microphone and the error feedback from the error microphone. By adjusting the anti-noise output in real-time, the control speaker can emit a sound wave that effectively negates the primary noise.

The use of the FxLMS algorithm is particularly relevant in this LabVIEW-based setup due to its ability to dynamically adjust to changes in noise

characteristics, ensuring effective noise cancellation across varied conditions. The real-time processing capabilities of LabVIEW, combined with the computational power of the FPGA, enable rapid updates to the noise cancellation signals. Thus, it will be maintaining the system's efficiency even in fluctuating acoustic environments.

3.7 SUMMARY

This chapter has described the research methodology used in the study in details ways. To summarize the methodology used in the study consists of four parts which are derivation of mathematical models, MATLAB simulation, COMSOL Multiphysics simulation and experiment setup using LabVIEW and compact RIO. This integration facilitated real-time data acquisition and control, which enhanced the accuracy and reliability of the simulation results. Results and discussions related to the study are presented in Chapter 4.

CHAPTER 4

RESULTS AND DISCUSSIONS

4.1 OVERVIEW

This chapter will discuss the result for active noise control system which is propagation of sound wave under a few conditions. The simulation is done in MATLAB Simulink and COMSOL Multiphysics software. The study parameters of the sound wave are done in the time domain for the Simulink. In COMSOL the results will show both time and frequency domain. The experiment is done using compact RIO controller with LabVIEW software using graphical programming language.

4.2 MATHLAB SIMULINK SIMULATION

4.2.1 Propagation of Sound Wave Signal Result Analysis

4.2.1.1 **Same medium different length**

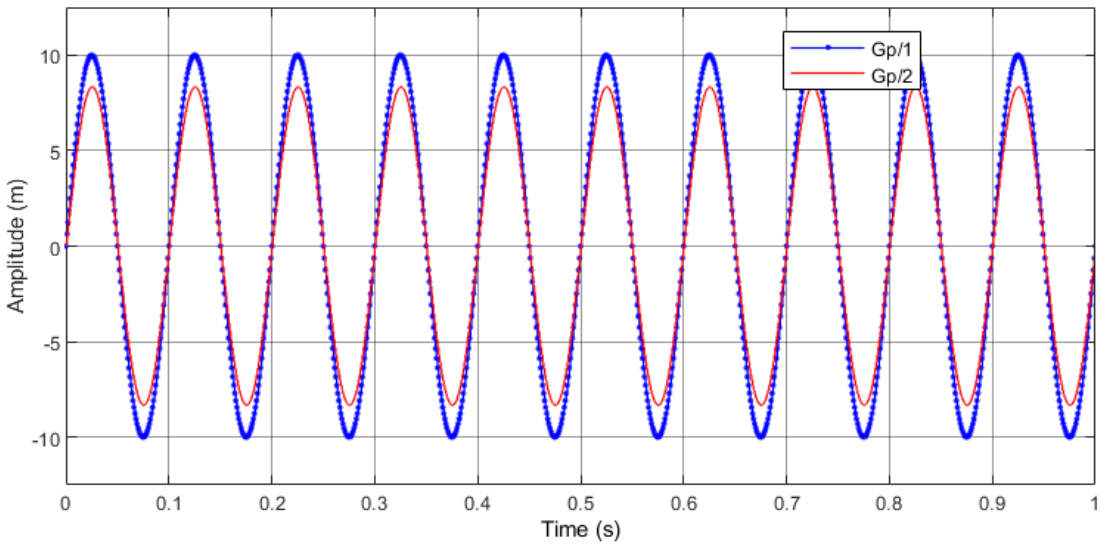

Figure 4-1 Propagation of Sound in 1 m in the air

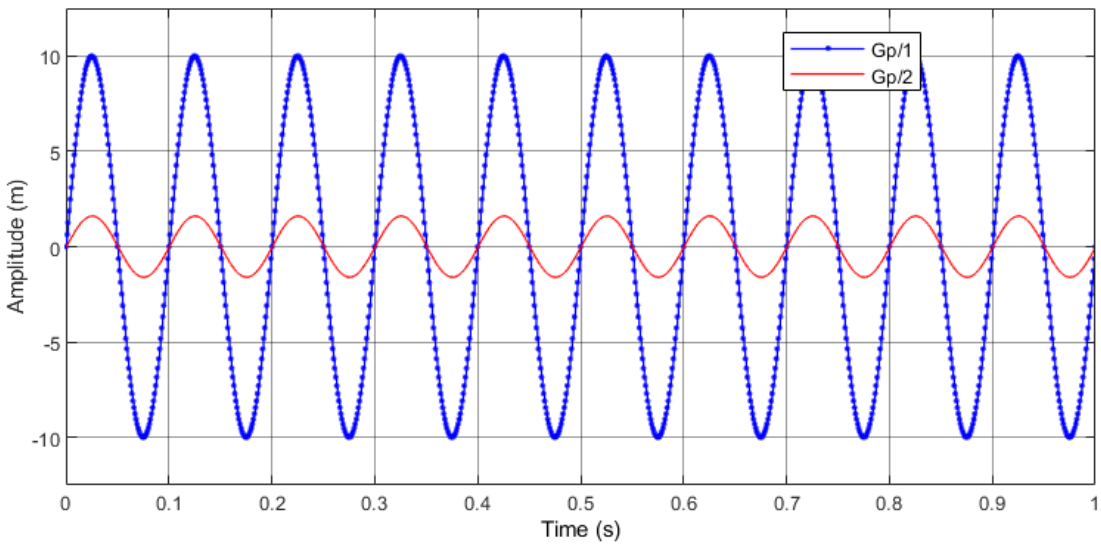

Figure 4-2 Propagation of sound in 10 m in the air

For the simulation the sound wave is going through air as the medium. Figure 4-1 shows 2 wave signals. The signal with blue color is the initial input signal while the red color is the signal after moving in Lp = 1 meter. Lp is the length from primary speaker until error microphone. The initial amplitude is 10 m then it reduces to 8.326 m, so 16.74% of the sound has been dissipated. If the length increases, then the output amplitude will decrease. Figure 4-2 shows the signal moving in 10 m in the air. The amplitude of signal reduces from 10 m to 1.601 m which is 83.99% of the sound has been dissipated.

4.2.1.2 **Same medium different length**

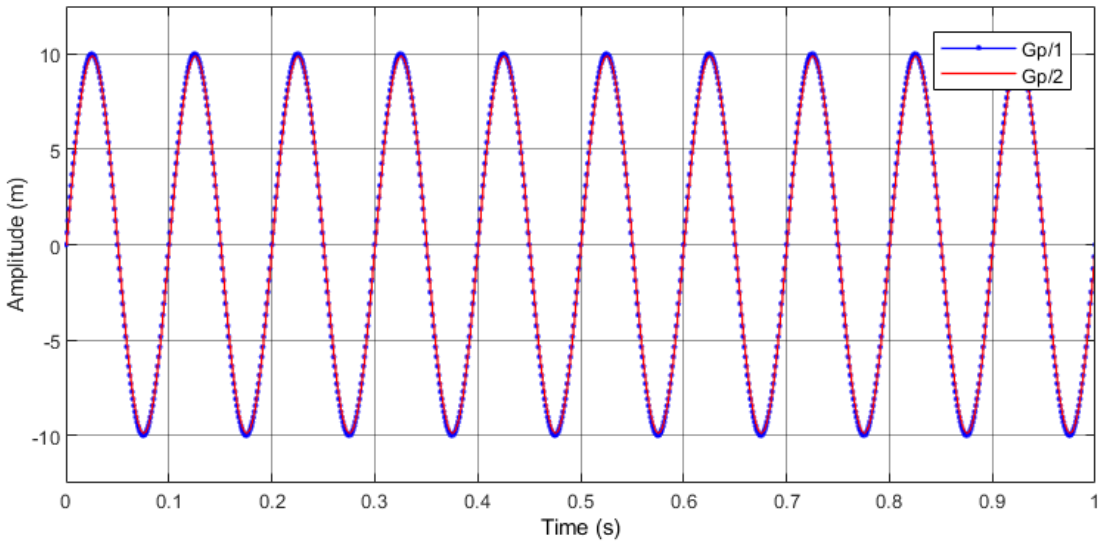

Figure 4-3 Propagation of sound in 1 m through iron

Figure 4-3 shows the sound wave signal going through iron. Iron sound speed is around 15 times faster than sound speed in the air so there is only a significant change of amplitude between initial value and the output. The amplitude of the output signal is 9.878 m.

4.2.2 Superposition with Secondary speaker Result Analysis

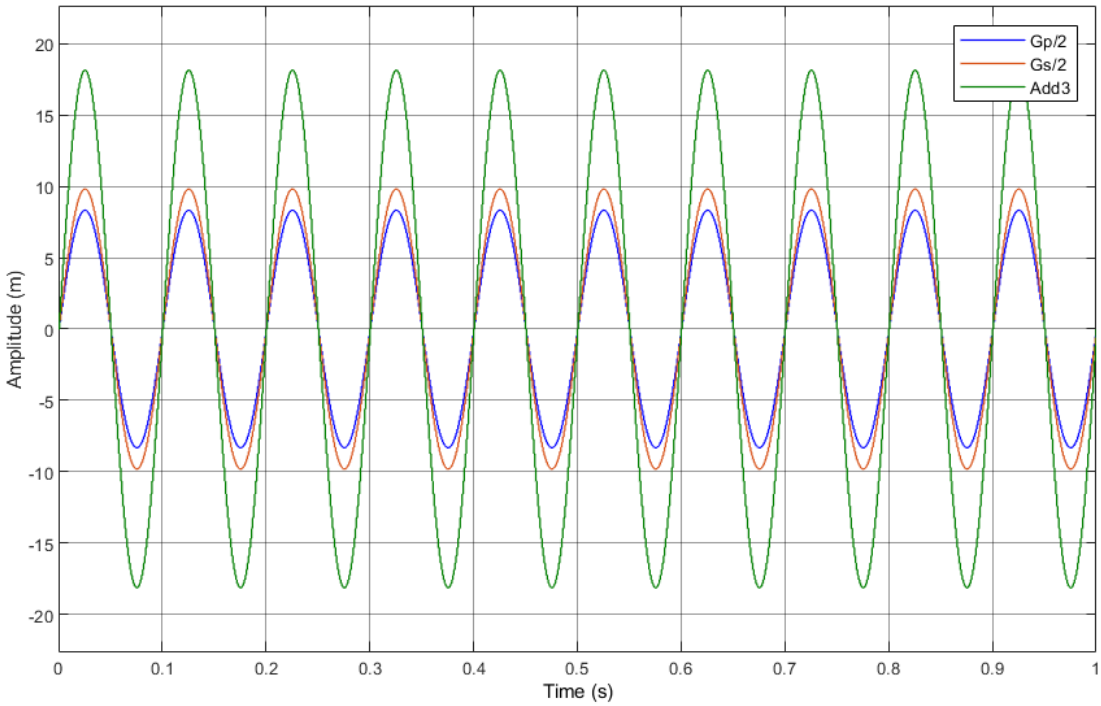

Figure 4-4 Superposition of sound wave signal

Figure 4-4 shows 3 sound wave signals in phase. The blue color is signal from primary speaker, Yp, the orange color is signal from secondary signal, Ys and the green color is the summation of signal after the summing point, Y. The amplitude value for each peak are 8.326 m, 9.818 m and 18.14 m respectively. The amplitude for Yp and Ys is different due to the difference in length. As mentioned in the chapter 3 before the Lp is 1 m and Ls is 0.1 m. Amplitude will be higher if the displacement between source and reference point is shorter.

4.2.3 Feedforward Active Noise Cancellation Result Analysis

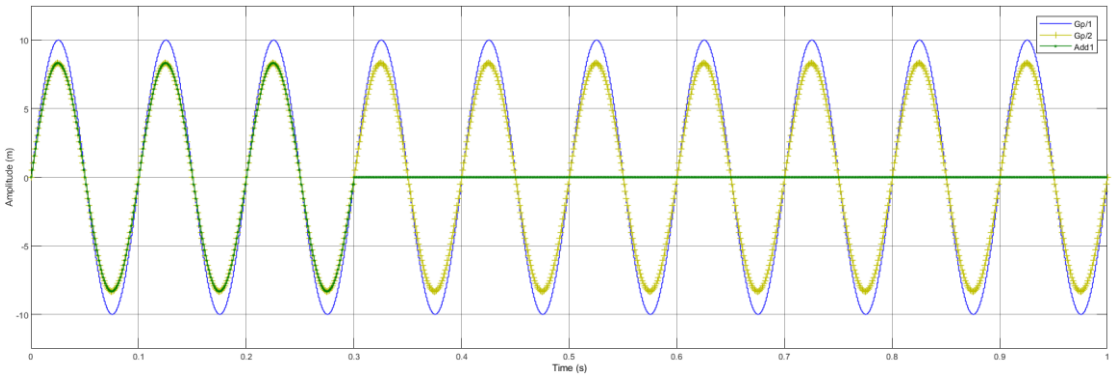

Figure 4-5 Feedforward ANC

Figure 4-5 is the wave signal after adding controller, *Hc* into the system. The controller will invert the signal. Hence, the signal from the secondary speaker is 180∘ out phase that will cancel each other. A step signal with step time 0.2 s has been added into the system to show the signal changes before and after the controller is turned on. After 0.3 s, the signal becomes zero indicate that the unwanted noise from the primary speaker has been cancelled by the secondary speaker. The blue color signal is the initial signal with the amplitude 8.326 m, the yellow signal is sound wave from primary speaker with amplitude 8.326 m and the green signal is the signal from secondary speaker with approximately zero amplitude after the step. Hence, the error from the simulation is almost 0%.

It's due to idealized simulation environment, precise modeling parameters, or a highly effective feedforward controller design that successfully predicts and cancels out the unwanted noise with no residual error in the simulation scenario. However, real-world applications will introduce additional complexities, and the

simulation results may not necessarily translate exactly to physical implementations.

4.3 COMSOL MULTIPHYSICS

4.3.1 Propagations of Sound Waves in FEA

4.3.1.1 **Input Sound Pressure from Big Boundary**

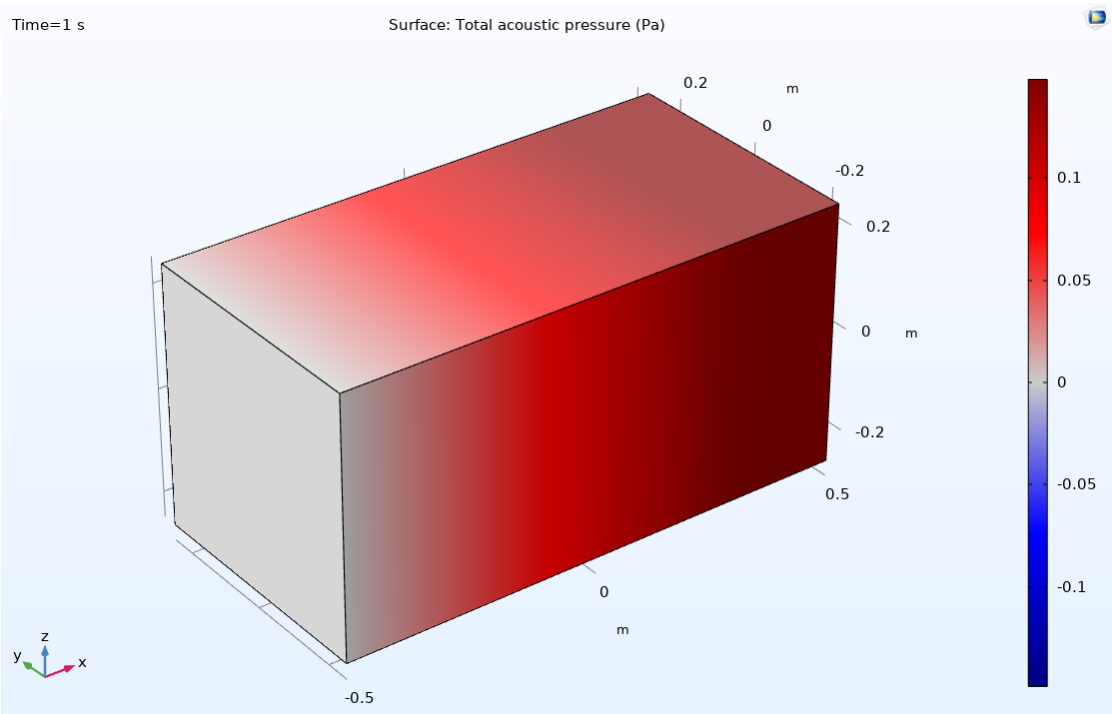

Figure 4-6 Acoustic Pressure

The graph is plot at the point probe 1 at x = - 0.5, y = 0, z = 0 as the input and point probe 2 at x = 0.5, y = 0, z = 0 as the output. Figure 4-6 show initial movement of the sound pressure.

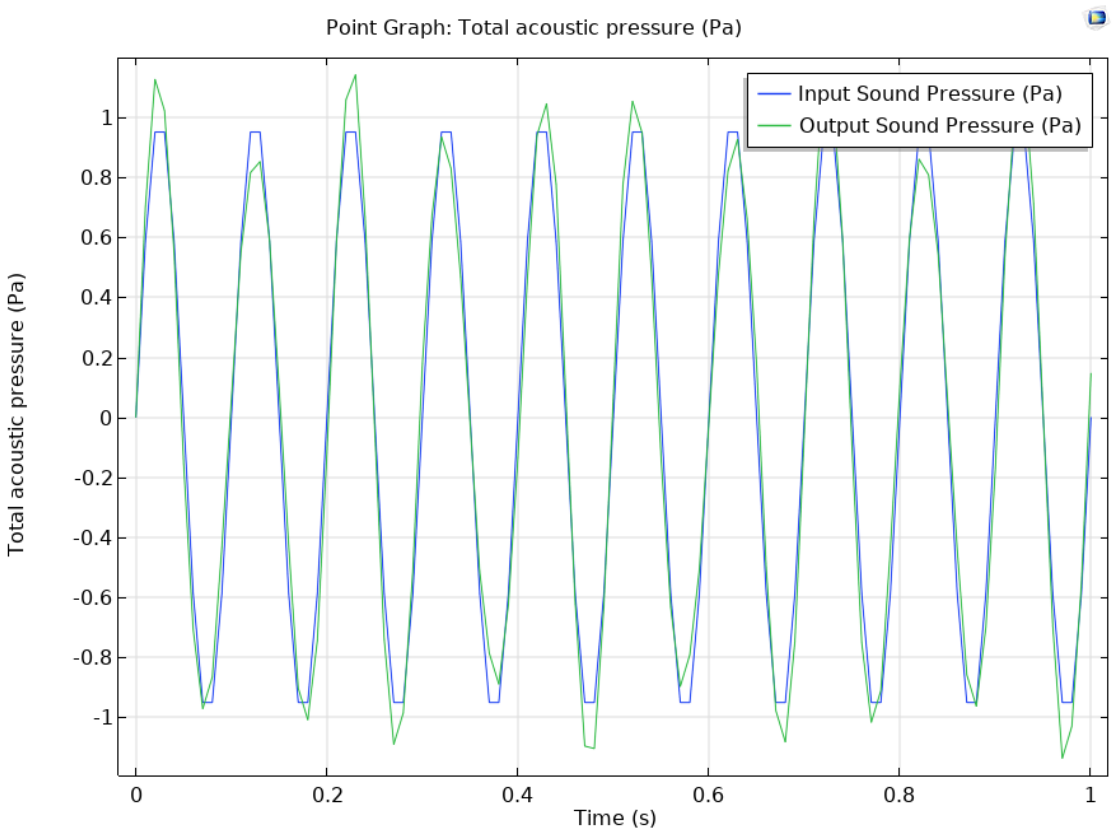

Figure 4-7 Total Acoustic Pressure in Time Domain.

In Figure 4-7, shows the total acoustic pressure in time domain. The blue color indicates the input sound pressure while the green colour indicates the output sound pressure. The amplitude response is around 0.95 Pa and 1.2 Pa for the input and output respectively. The percentage different for the results is 20.83%.

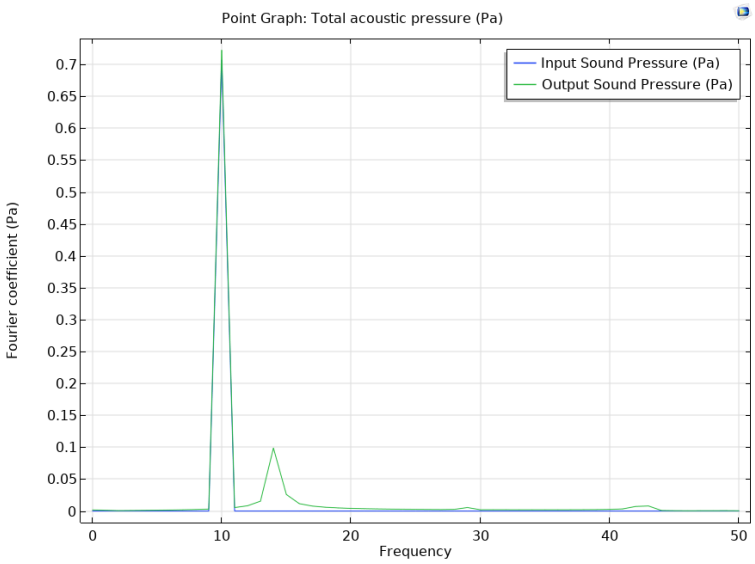

Figure 4-8 Total Acoustic Pressure in Frequency Domain

In Figure 4-8, shows the total acoustic pressure in frequency domain. The frequency for both input and output is at 10 Hz.

4.3.1.2 **Input Sound Pressure from Small Boundary**

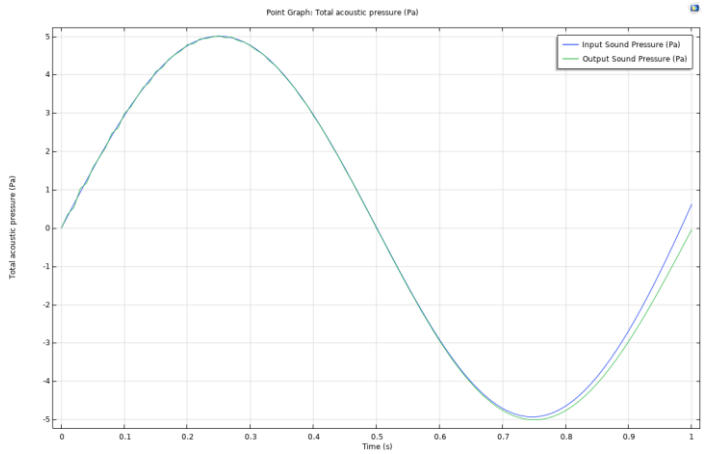

Figure 4-9 Total Acoustic Pressure in Time Domain

In Figure 4-9, shows the total acoustic pressure in time domain. The blue colour indicates the input sound pressure while the green colour indicates the output sound pressure. The amplitude response is around 5.0 Pa and 4.95 Pa for the input and output respectively. The percentage different for the results is 1.0%. The difference between the input and the output is due to the propagation of sound through the air.

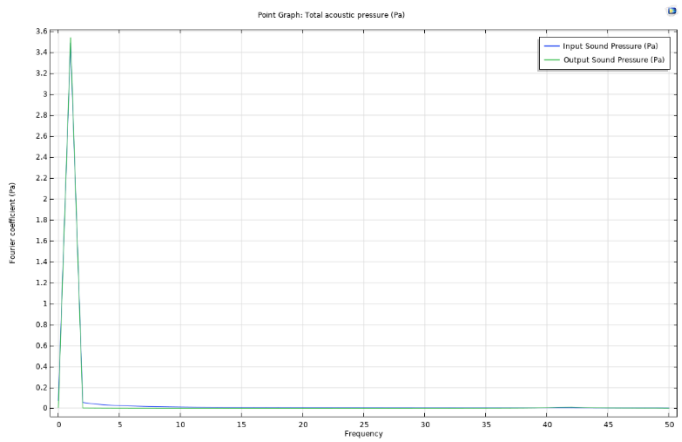

Figure 4-10 Total Acoustic Pressure in Frequency Domain

In Figure 4-10, shows the total acoustic pressure in frequency domain. The frequency for both input and output is approximately 3.55 Hz.

4.4 EXPERIMENT

4.4.1 Components

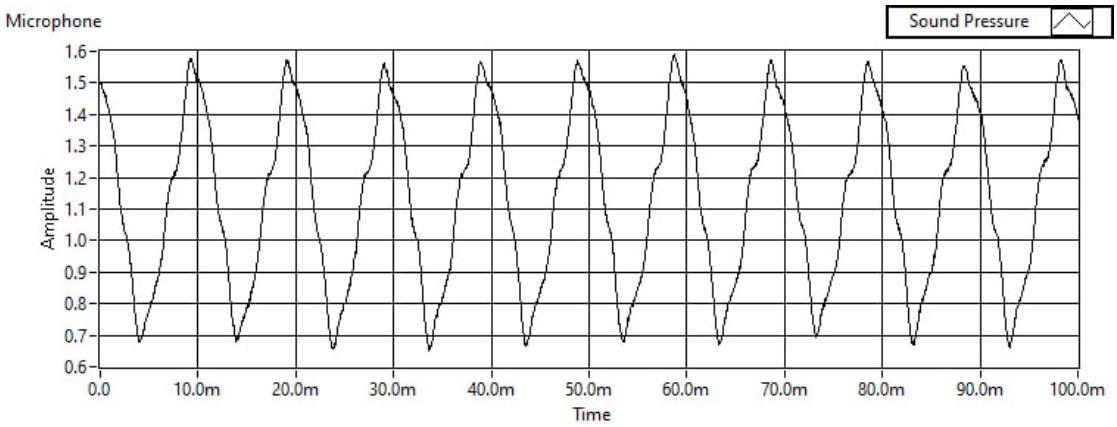

Figure 4-11 Sound signal capture using Accelerometer sensor

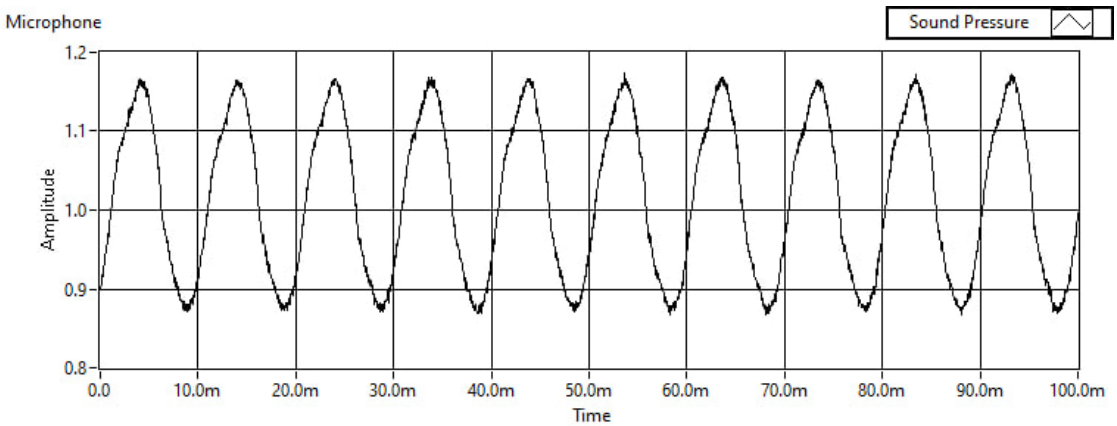

Figure 4-12 Sound signal capture using Behringer C-1 condenser microphone

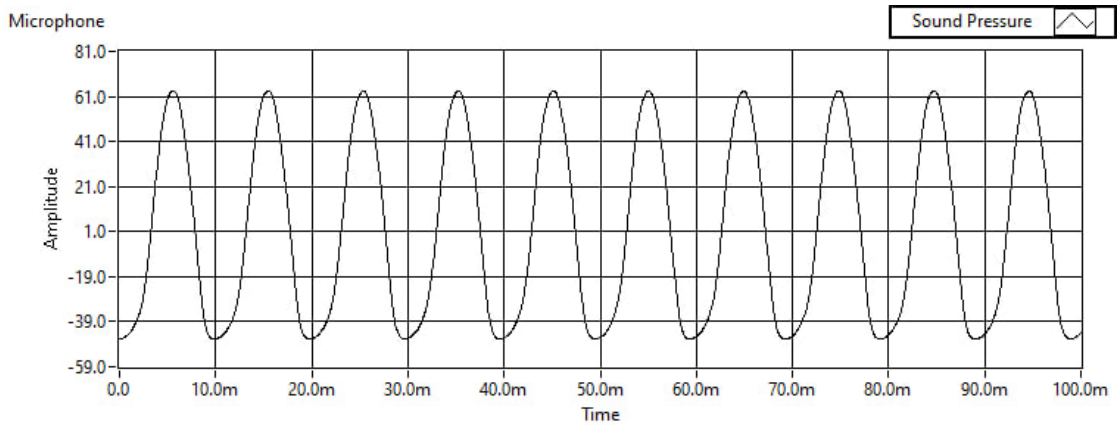

Figure 4-13 Sound signal capture using Behringer ECM 8000 measurement microphone

The analysis of sound signals captured by various devices, as presented in Figures 4-1, Figure 4-2, and Figure 4-3, suggests that the Behringer ECM8000 microphone is the most effective for precise acoustic measurements in the experimental setup. Figure 4-1 illustrates the accelerometer sensor's output, which exhibits significant amplitude fluctuations, indicative of its susceptibility to mechanical vibrations and noise interference, thereby limiting its suitability for precise sound measurement tasks. Conversely, Figure 4-2, depicting the output from the Behringer C1 microphone, shows a more stable waveform with limited amplitude variations, suggesting stability, albeit with a restricted dynamic range.

Figure 4-3 highlights the output from the Behringer ECM8000 microphone, which is able to capture a broad spectrum of amplitudes, ranging from about -59 to +81 units. This capability demonstrates high fidelity and sensitivity, crucial for detailed acoustic analysis. The waveform's smoothness reflects the microphone’s accuracy in recording both low and high-frequency sounds, offering substantial resistance to ambient noise. These characteristics make the ECM8000

exceptionally suitable for capturing precise and accurate sound data, a critical requirement in studies like noise cancellation, where detailed sound analysis is paramount.

4.4.2 Propagation of Sound Wave

4.4.2.1 **Propagation of Sound in Closed Environment**

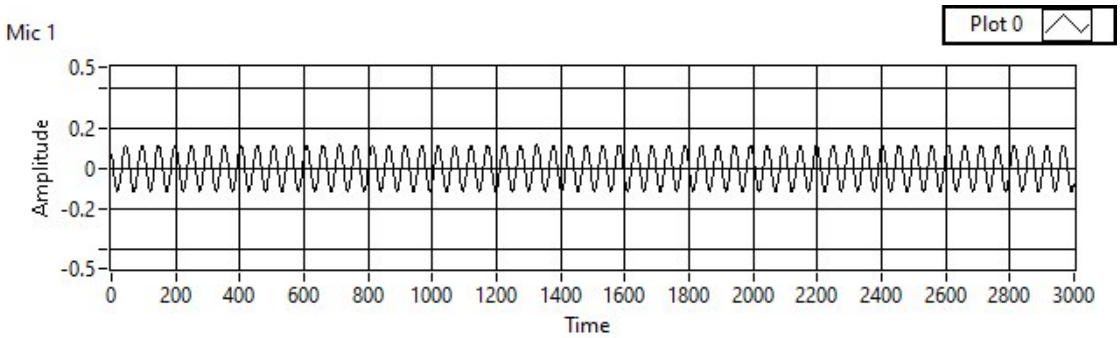

Figure 4-14 Microphone 1 for 200 Hz sound signal close enviroment

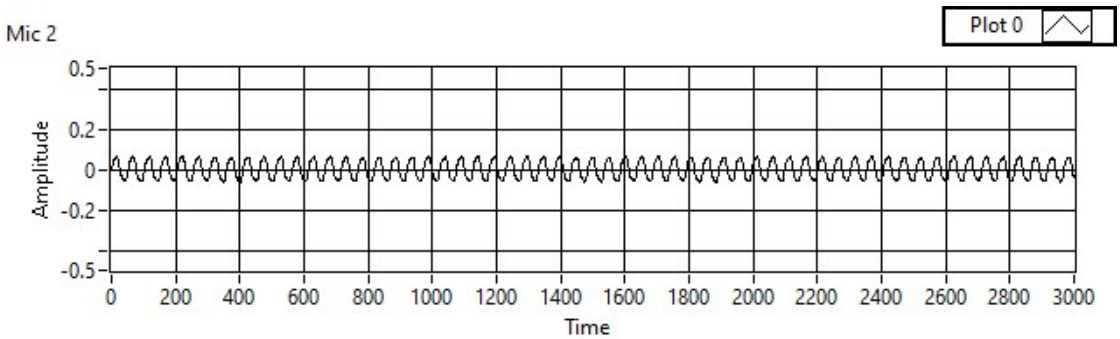

Figure 4-15 Microphone 2 for 200 Hz sound signal close environment

Figures 4-14 and 4-15 illustrate the propagation of a 200 Hz sound wave within a PVC tube in a controlled environment. Observed at 15 cm from the source speaker, the waveform in Figure 4-14 exhibits pronounced oscillations and consistent amplitude. Conversely, the waveform in Figure 4-15, recorded 141.5 cm from the source, shows a significant reduction in amplitude and a less defined

oscillatory pattern. This observed attenuation and alteration of the waveform with increased distance from the source highlight the effects of sound energy dissipation and the influence of environmental interactions, such as sound reflections and material absorption, within the enclosed space.

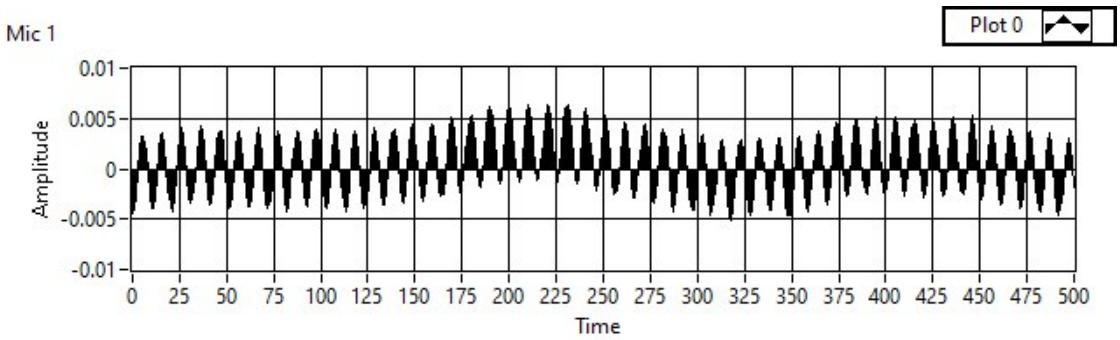

Figure 4-16 Microphone 1 for 1000Hz sound signal close environment

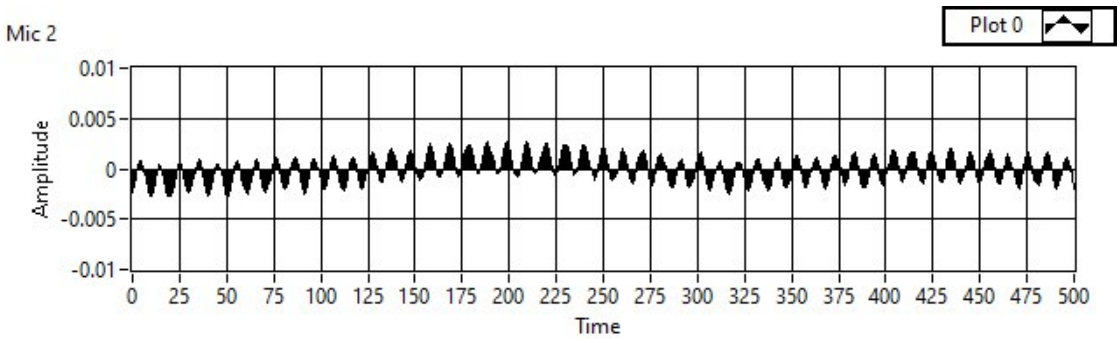

Figure 4-17 Microphone 2 for 1000Hz sound signal close environment

Figures 4-16 and 4-17 illustrate the propagation of a 1000 Hz frequency sound within a PVC tube, recorded at varying distances from the source speaker. At a proximity of 15 cm (Figure 4-16), the waveform is characterized by closely packed oscillations typical of high-frequency sounds. When the distance is extended to 141.5 cm (Figure 4-17), although the high-frequency characteristics of the waveform are preserved, there is a noticeable decrease in amplitude. This reduction

reflects energy loss as the sound travels through the tube, influenced by the absorptive properties of the medium and boundary reflections.

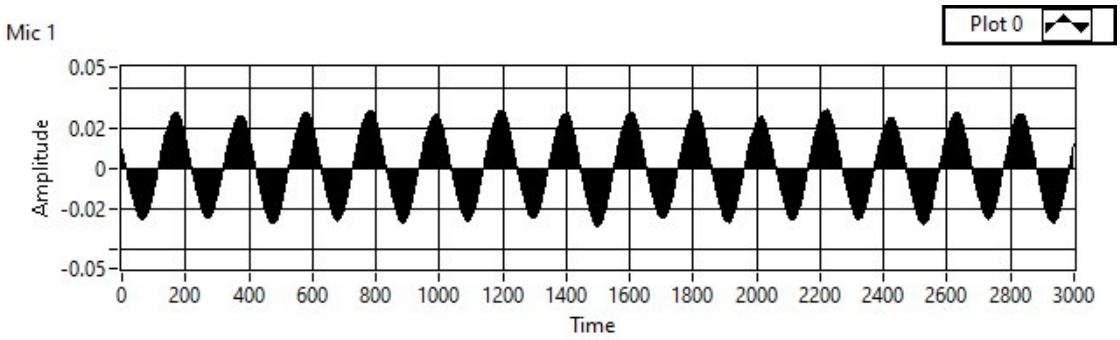

Figure 4-18 Microphone 1 for 50Hz sound signal close environment

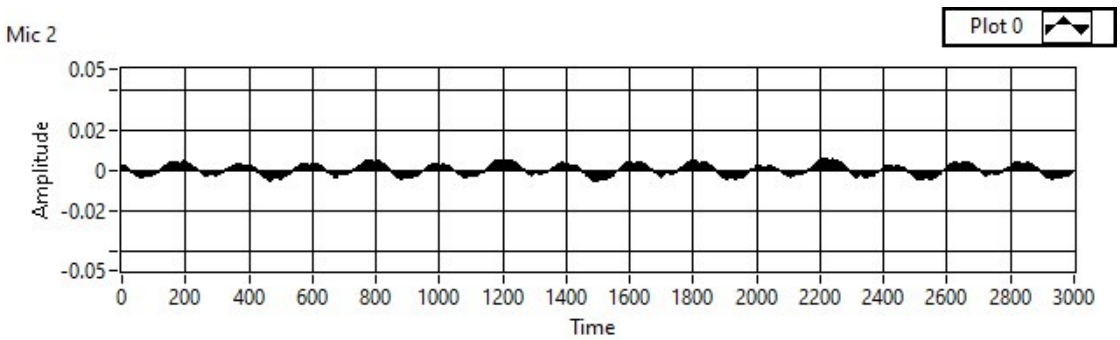

Figure 4-19 Microphone 2 for 50Hz sound signal in close environment

Figures 4-18 and 4-19 illustrate the propagation of a 50 Hz sound frequency captured at distances of 15 cm and 141.5 cm, respectively, from the source within a PVC tube. At the closer distance (Figure 4-18), the waveform is characterized by robust oscillations, demonstrating the preservation of amplitude and waveform integrity over shorter distances. Conversely, at 141.5 cm (Figure 4-19), the waveform exhibits significant attenuation, with both reduced amplitude and less defined oscillations. This indicates that even low-frequency sounds, known for

their ability to travel longer distances, experience energy losses due to absorptive properties of the medium and boundary effects, which are critical considerations in enclosed or complex acoustic environments.

4.4.2.2 **Propagation of Sound in Open Environment**

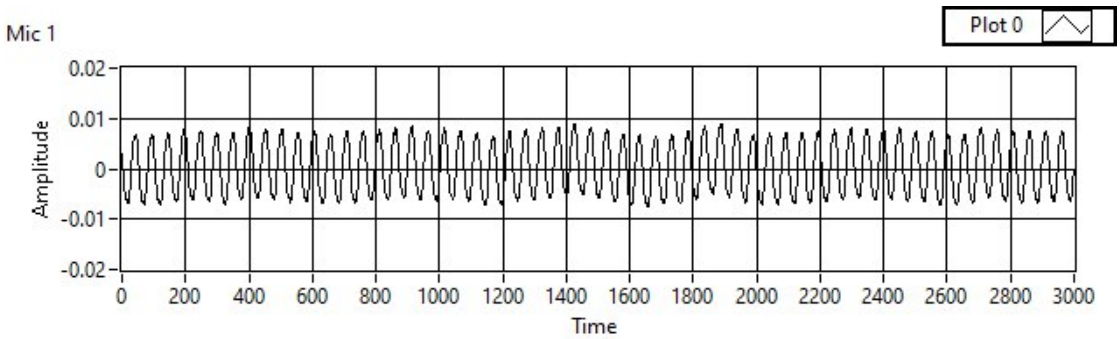

Figure 4-20 Microphone 1 for 200Hz sound signal in open space

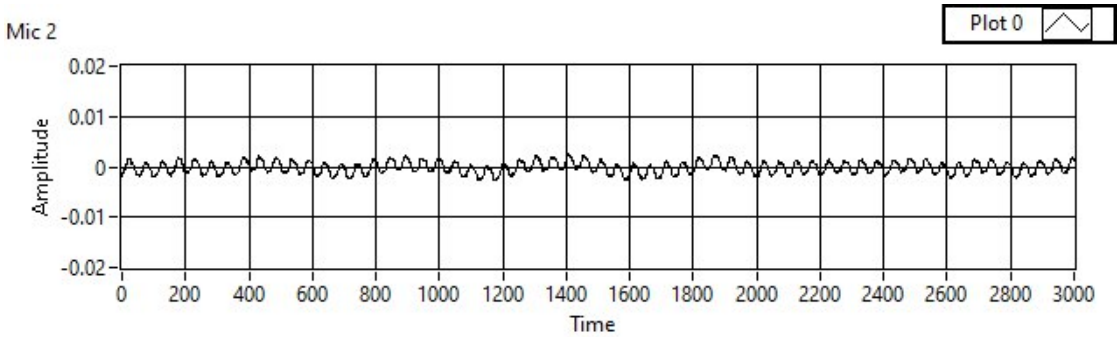

Figure 4-21 Microphone 2 for 200Hz sound signal in open space

Figures 4-20 and 4-21 illustrate the propagation of a 200 Hz sound frequency in open space, recorded at distances of 15 cm and 141.5 cm from the source, respectively. Compared to similar experiments conducted in a closed PVC tube, the waveforms in open space exhibit less amplitude stability and more pronounced attenuation. Specifically, the waveform at 15 cm shows clear oscillations, but with less amplitude consistency than observed in a confined environment. At 141.5 cm,

the waveform is significantly subdued, highlighting a greater loss of sound integrity than seen within the confined space. These findings emphasize how open spaces allow sound waves to disperse more freely, resulting in faster amplitude reduction and greater waveform degradation over distance, which underscores the impact of environmental conditions on acoustic propagation.

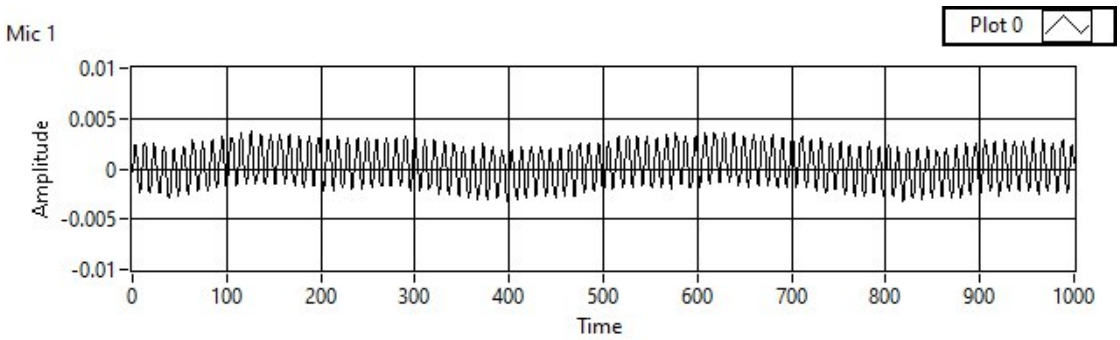

Figure 4-22 Microphone 1 for 50Hz sound signal in open space

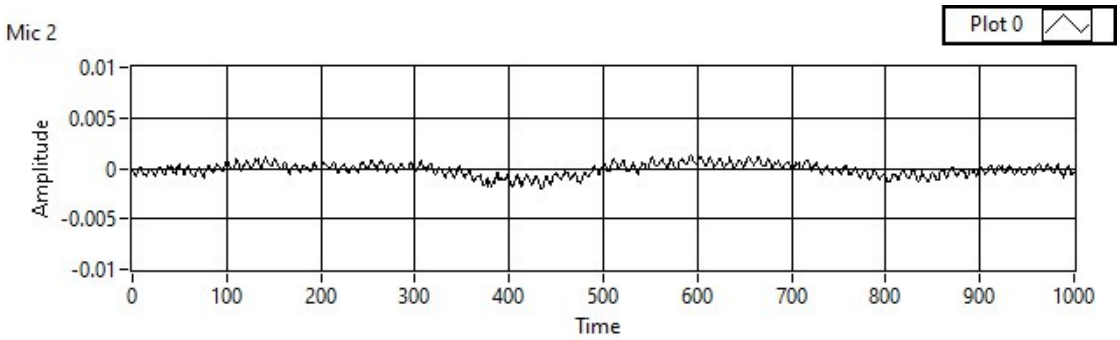

Figure 4-23 Microphone 2 for 50Hz sound signal in open space

Figures 4-22 and 4-23 display the propagation of a 50 Hz sound frequency in open space, captured at distances of 15 cm and 141.5 cm from the source, respectively. In Figure 4-22, the waveform recorded at 15 cm shows more pronounced oscillations than the one in Figure 4-23, captured at 141.5 cm, where the amplitude significantly decreases, and the waveform flattens. This attenuation

highlights the rapid dispersion of low-frequency sounds in open environments, which leads to a quicker reduction in amplitude compared to propagation in a confined space. The findings indicate that despite the lower frequency's capability to travel longer distances, the open environment allows for broader sound wave dispersion, reducing the sound's intensity and clarity over distance.

4.4.3 Superposition with Secondary Speaker

The analysis of the superposition principle in both closed and open environments will particularly emphasize low-frequency signals, aligning with the study's focus on engine sounds, which predominantly involve low frequencies. This approach will allow for a more detailed examination of how these types of sound waves, characteristic of engine noise, interact and combine under different environmental conditions. By focusing on low frequencies, the experiment will provide insights into the behavior of sound waves that are most relevant to practical scenarios involving engine sounds, thereby enhancing the relevance and applicability of the findings.

4.4.3.1 **Summation of Sound in Closed Environment**

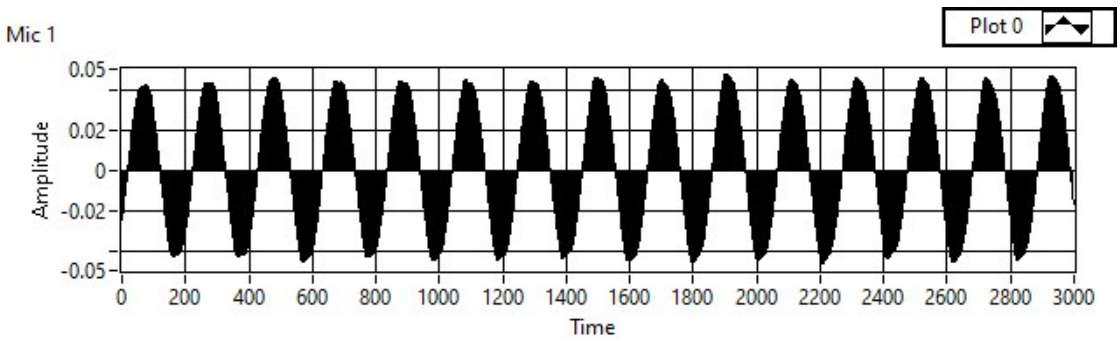

Figure 4-24 Microphone 1 for summation of 50 Hz sound signal in Closed Environment

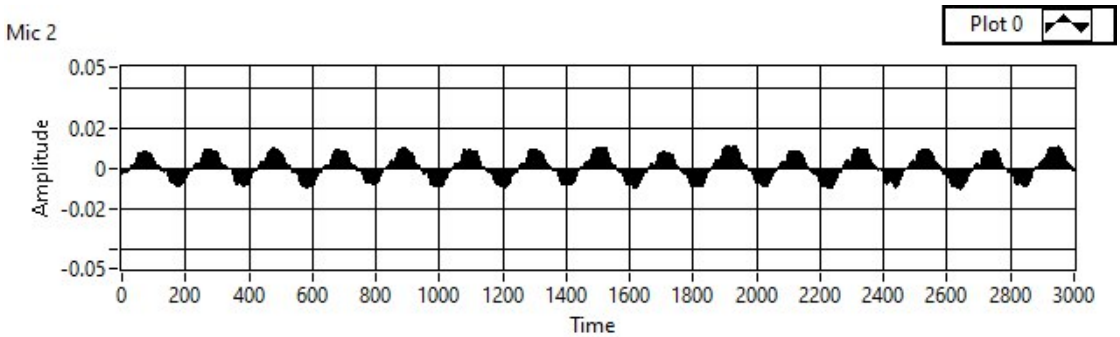

Figure 4-25 Microphone 2 for summation of 50 Hz sound signal in Closed Environment

Figures 4-24 and 4-25 illustrate the summation of a 50 Hz sound signal in a closed environment with the inclusion of a second speaker positioned 120 cm from the first, recorded at distances of 15 cm and 141.5 cm from the primary speaker, respectively. Comparing these results with the previous recordings of single-source propagation (Figures 4-18 and 4-19) in the same environment, noticeable differences emerge in the amplitude and form of the waveforms due to the superposition of sound waves from two sources.

In Figure 4-24, the waveform captured 15 cm from the source displays a higher amplitude compared to Figure 4-18, which only involved a single source. This indicates constructive interference where the sound waves from both speakers are likely in phase, enhancing the overall amplitude. On the other hand, Figure 4-25, captured at 141.5 cm, shows a less pronounced increase in amplitude compared to its counterpart Figure 4-19, suggesting that while superposition still occurs, the effects of constructive interference diminish as the distance from the source increases due to phase differences or attenuation.

These observations underscore the superposition principle's impact in a closed environment, where the addition of a second sound source can significantly alter the sound propagation pattern, particularly near the source. However, as the distance increases, the interaction between the waves becomes less effective at enhancing the sound, reflecting the complex nature of sound wave interaction over distances in confined spaces.

4.4.3.2 **Summation of Sound in Open Environment**

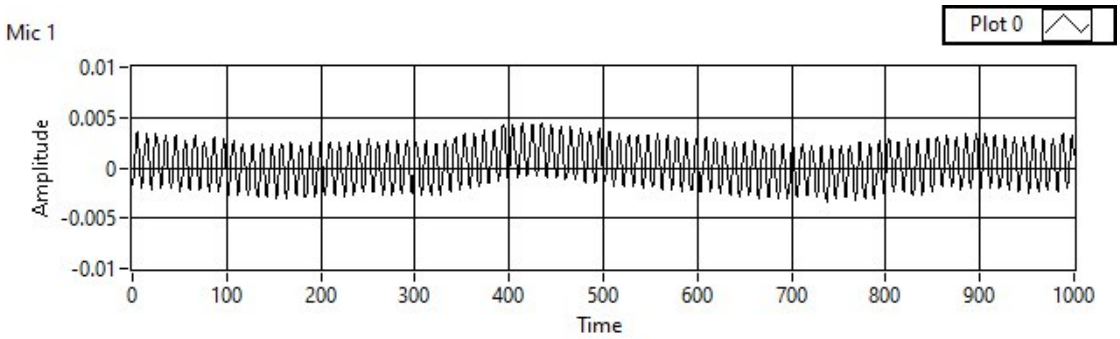

Figure 4-26 Microphone 1 for summation of 50 Hz sound signal in Open Space

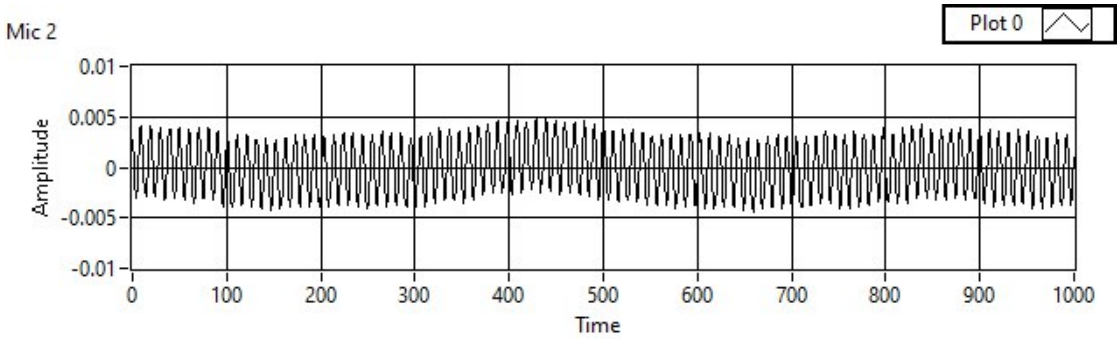

Figure 4-27 Microphone 2 for summation of 50 Hz sound signal in Open Space

Figures 4-26 and 4-27 display the summation of a 50 Hz sound signal in open space, captured by two different microphones. When compared to the earlier data from Figures 4-22 and 4-23, which showed single-source sound propagation in open space, these new figures involve additional complexity due to the interaction of sound waves from two speakers.

In Figure 4-26, the waveform captured by Microphone 1 shows more pronounced fluctuations in amplitude compared to Figure 4-22, suggesting that the inclusion of the second speaker has introduced additional interference and complexity to the sound wave pattern. However, the overall amplitude appears to be slightly subdued, potentially indicating destructive interference at certain points where the phases of the sound waves from the two speakers do not align constructively.

Similarly, Figure 4-27, recorded by Microphone 2 at a further distance, also shows subdued amplitudes compared to Figure 4-23. The waveform here is less distinct and the amplitude fluctuations are more contained, indicating that the effects of superposition are less pronounced as the distance increases. This reduced impact is likely due to phase differences becoming more significant with distance, leading to less effective constructive interference and more prevalent destructive interference.

These observations highlight how the introduction of a second sound source in an open space influences the superposition of sound waves, with varying effects of constructive and destructive interference observed at different distances. This supports the understanding of how sound wave interactions are governed by distance and phase alignment in open environments.

4.4.4 Active Noise Cancellation using Adaptive Filter

4.4.4.1 **Result Analysis on Car Engine Sound Signal**

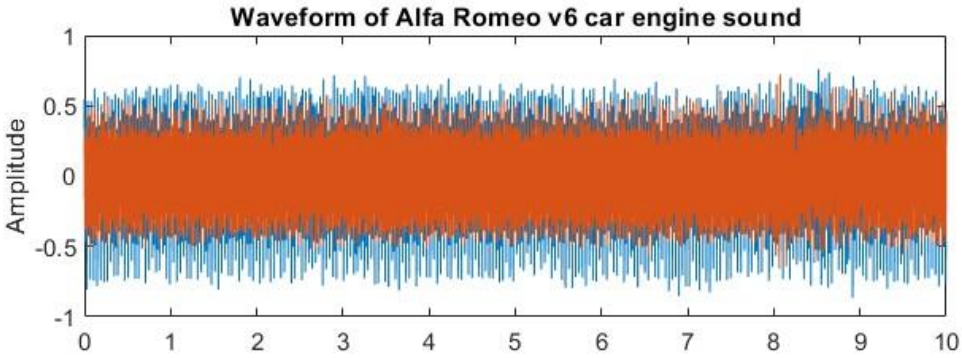

Figure 4-28 Time Domain on Alfa Romeo V6 car engine

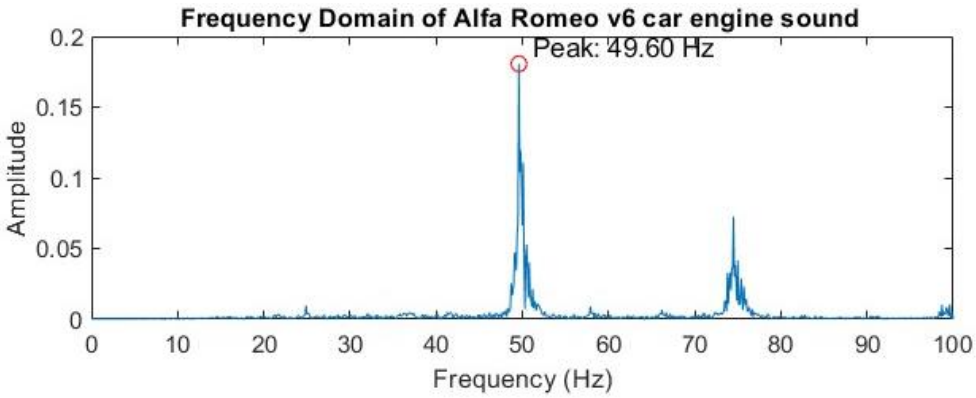

Figure 4-29 Frequency domain on Alfa Romeo V6 car engine

The provided graphs in Figures 4-28 and 4-29 depict the time domain and frequency domain analyses of the Alfa Romeo v6 car engine sound. Figure 4-28 shows the time domain waveform, representing how the amplitude of the engine sound varies over a period of ten seconds. This graph captures the complex pattern of vibrations generated by the engine, characterized by rapid fluctuations in amplitude which are typical in automotive engine outputs.

When dealing with sound signals recorded using a microphone, the amplitude in the time domain graph is typically represented in volts (V). This representation measures the electrical signal produced by the microphone as it converts acoustic pressure waves into an electrical audio signal. The amplitude shown reflects the voltage variations that correspond to the pressure fluctuations of the sound waves captured by the microphone.

Figure 4-29, derived from the time domain data via a Fast Fourier Transform (FFT), showcases the frequency domain of the same engine sound. FFT is employed to decompose the time-varying signal into its constituent frequencies, revealing the most prominent frequencies that compose the engine noise. The sharp peak at 49.60 Hz, indicating that this frequency is the dominant component of the engine's sound. Using the equation 3-32, the RPM of the engine is 2976 RPM.

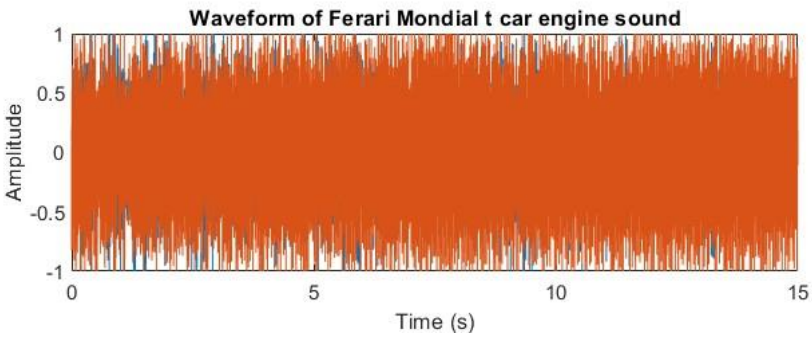

Figure 4-30 Time Domain on Ferrari Mondial t car engine

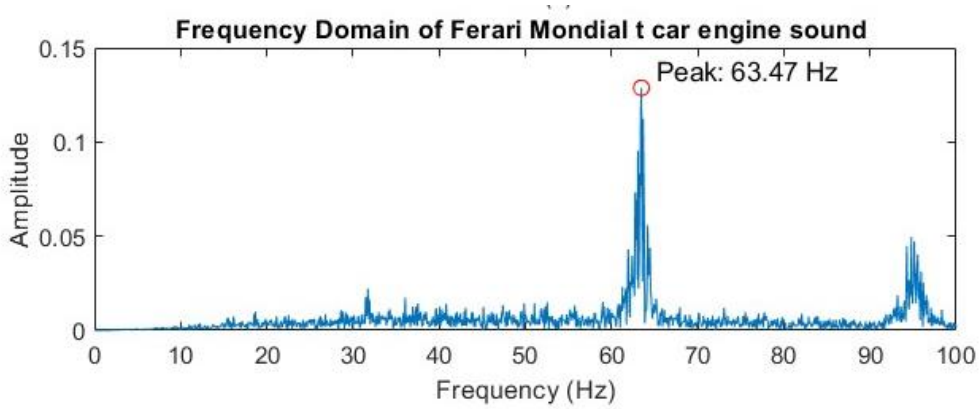

Figure 4-31 Frequency Domain on Ferrari Mondial t car engine

Figure 4-30 shows the time domain graph that analyse directly from recorded sound using MATLAB. By using FFT, the frequency domain graph show in Figure 4-31 also has been obtained. The peak is 63.47 Hz indicating that the frequency for the car engine sound at that time is 63.47 Hz. Using equation (3-32), the RPM for the Ferrari Mondial at that time is 3808.2 RPM.

4.4.4.2 **Reduction of 200 Hz noise**

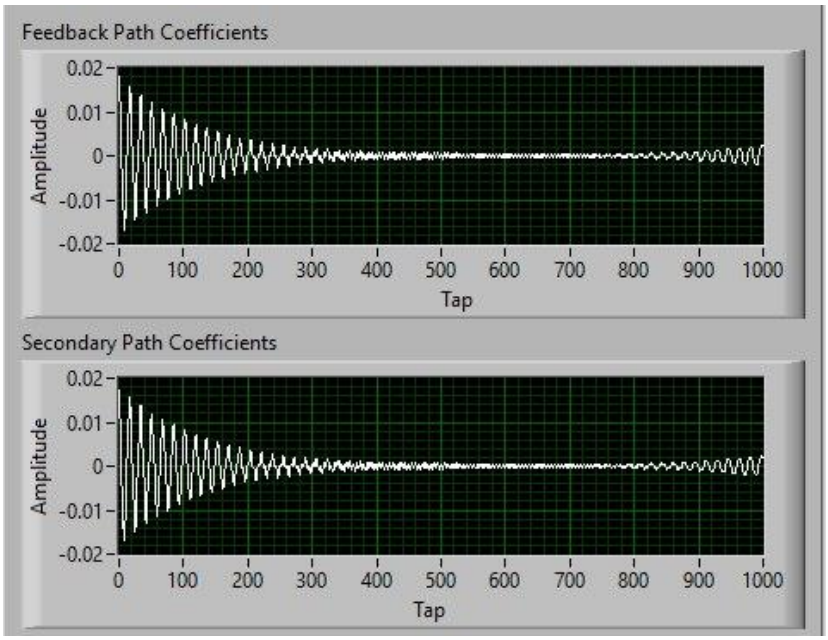

Figure 4-32 Secondary and Feedback Path Coefficient for 200 Hz Sound

Figure 4-32 displays the Secondary and Feedback Path Coefficients for a 200 Hz sound signal. The converge graph illustrating that the program successfully identified both coefficients. The similarity in the appearance of the coefficients can be attributed to the minimal distance between both microphones, situated in a closed environment, which leads to similar acoustic paths. Despite their resemblance, the Feedback Path coefficients are slightly higher compared to the Secondary Path coefficients. This subtle difference likely reflects distance or path differences between the error microphone's position relative to the control speaker and the reference microphone's position relative to the noise source. The coefficient is find using 1000 filter length and 0.002 step size for the LMS filter.

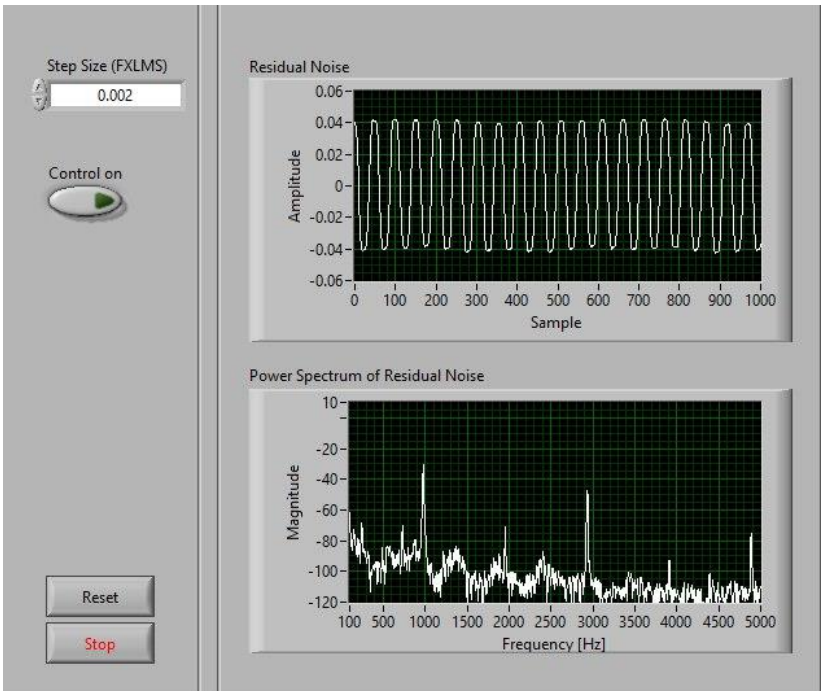

Figure 4-33 Residual Noise for 200 Hz went control off

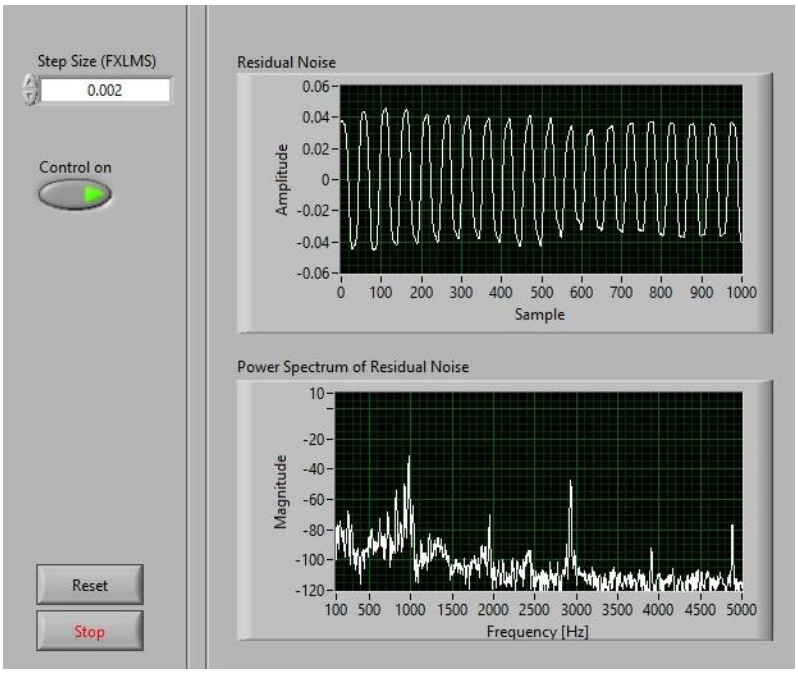

Figure 4-34 Residual Noise for 200 Hz went control on

Figure 4-33 shows the residual noise for signal in 200 Hz frequency when the control speaker is turned off while Figure 4-34 shows the residual noise after the

control speaker has turned on. The step size for the FxLMs filter used is 0.002. From both diagrams, it can be seen there is slightly noise reduction after the control speaker has turned on. The amplitude response for the sample time of 610 before the control is 0.04 V while the amplitude response after the control is 0.03 V. Hence, based on the equation 3.33 the noise reduction is approximately at 6.02 dB.

4.4.4.3 **Reduction of 63.47 Hz, Ferrari Mondial T Engine Car Sound**

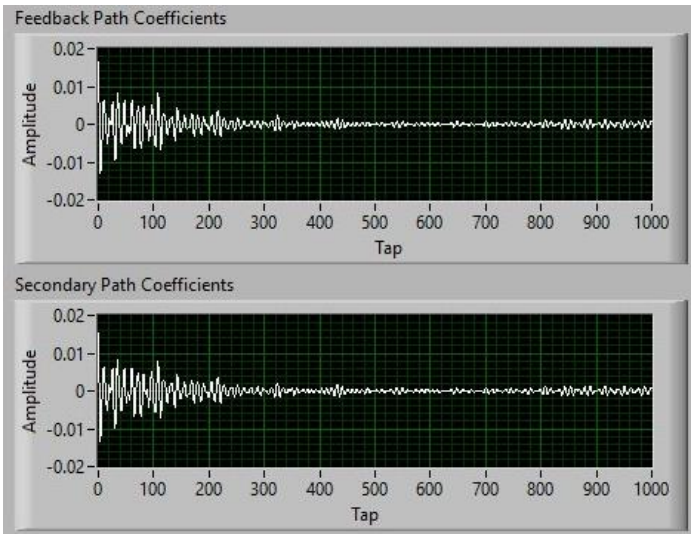

Figure 4-35 Secondary and Feedback Path Coefficient for Ferrari Mondial T Sound

Figure 4-35 shows the Secondary and Feedback Path Coefficients for a Ferrari Mondial T engine sound. The graph indicates that both coefficients were successfully determined by the program. Just like the 200 Hz before, the similar appearance of the coefficients is due to the proximity of the microphones, both located in a confined space, resulting in similar acoustic paths. However, if observe carefully, the Feedback Path coefficients are slightly higher than those of the Secondary Path. This minor variation is probably due to differences in the distances

or paths from the error microphone to the control speaker and from the reference microphone to the noise source. The coefficients were calculated using an LMS filter with a length of 1000 and a step size of 0.002.

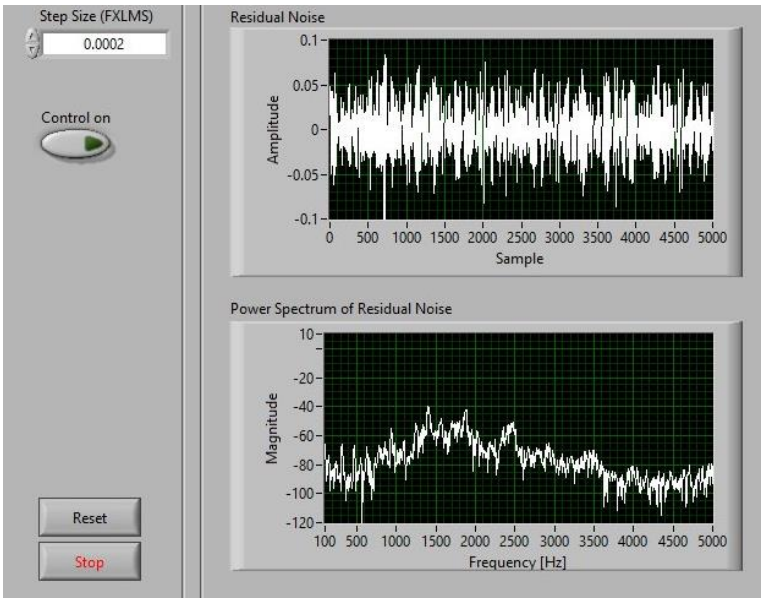

Figure 4-36 Residual Noise for Ferrari Mondial T engine car went control off

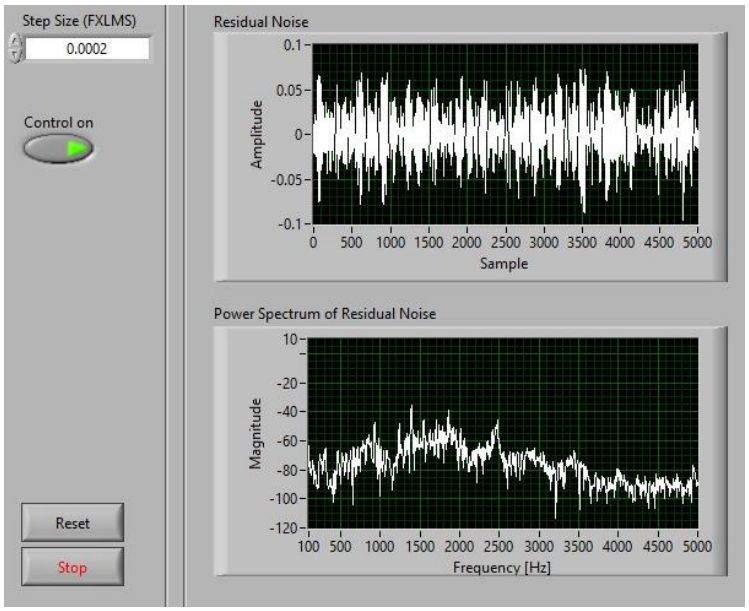

Figure 4-37 Residual Noise for Ferrari Mondial T engine car went control on

Figure 4-36 presents the residual noise from a Ferrari Mondial T engine car with the control speaker off, while Figure 4-37 shows the residual noise with the control speaker on. Referring to Figure 4-31, the engine operates at a frequency of 63.47Hz and 3808.2 RPM. The FxLMS filter, used with a step size of 0.002, demonstrates a modest noise reduction when the control speaker is activated. Specifically, the amplitude response before activating the control measures at 0.075 volts, whereas post-activation, it drops to 0.05 volts. Thus, the noise reduction achieved, as calculated using equation 3.33, is approximately 3.52 dB.

4.5 SUMMARY

This chapter provides an overview and explanation of the results obtained through the methodology. It covers the simulation outcomes from MATLAB Simulink and includes some findings from the COMSOL Multiphysics simulation. Also it contains all the analysis from experiment setup that has done based on described on the chapter 3.

CHAPTER 5

CONCLUSION AND RECOMMENDATION

5.1 CONCLUSION

The objective of this study was to simulate the propagation of sound waves from a sound source to the error sensor location using MATLAB and COMSOL Multiphysics software. Additionally, the study aimed to create a local active noise control system utilizing the feedforward controller method and to assess the system's performance through experimentation.

In conclusion, a mathematical model for the sound pressure equation has been developed for use in this study. Furthermore, the transfer function for the feedforward Active Noise Control (ANC) system was derived from the block diagram, serving as a crucial component in both simulations and experimental setups. Simulation using MATLAB Simulink was also conducted to cancel noise using the feedforward controller, resulting in an exceptionally small error measure of 1.77 e-15. An adaptable active noise control system was developed to reduce noise using LabVIEW 2014 and Compact RIO 9004. The controller was tested to reduce noise at 200 Hz and 63.47 Hz from a car engine, achieving noise attenuation of approximately 6.02 dB and 3.52 dB, respectively.

It can be concluded that the first and second objectives of the study have been successfully completed. Regarding the third objective, although the noise reduction levels were not exceptionally high, the objective to verify the system's performance using an experimental setup was also achieved.

5.2 RECOMMENDATION

For future enhancements of this research project, there are specific areas where the design and application of the active noise control system could be significantly improved. Firstly, the current project only addresses noise reduction at a single, constant engine RPM, which limits its real-world applicability. It would be beneficial for subsequent research to develop a controller capable of adapting to the changes in engine RPM that affect the frequency of sound signals. Consideration could be given to integrating more sophisticated adaptive filter technologies such as recursive least squares (RLS) or multi-reference adaptive filters, which may offer faster convergence and better performance in environments where engine speeds vary.

Furthermore, enhancing the noise attenuation capabilities by upgrading the controller design could lead to more effective noise suppression. Currently employing a feedforward controller with LMS and FxLMS filters, future work could explore the inclusion of feedback ANC strategies or hybrid ANC systems that combine both feedforward and feedback elements to cover a broader range of noise frequencies and disturbances.

Regarding the technological tools utilized, this project uses LabVIEW 2014 and CompactRIO 9004. To harness advancements in software and hardware, upgrading to the latest versions of LabVIEW and CompactRIO would be advisable. Newer versions, such as LabVIEW 2020 and the latest CompactRIO models, offer enhanced processing capabilities, support for more complex algorithms, and improved usability. Additionally, exploring alternative real-time controllers like

Speedgoat real-time solutions or dSPACE systems could provide valuable comparative insights. These platforms are known for their robust performance in real-time simulation and testing environments, potentially offering improved efficiency and adaptability for complex noise control applications.

REFERENCES

Akhtar, M. T., & Mitsuhashi, W. (2011). Improving performance of hybrid active noise control systems for uncorrelated narrowband disturbances. *IEEE Transactions on Audio, Speech and Language Processing*, *19*(7), 2058–2066. https://doi.org/10.1109/TASL.2011.2112349

Cheer, J., & Elliott, S. J. (2015). Multichannel control systems for the attenuation of interior road noise in vehicles. *Mechanical Systems and Signal Processing*, *60*, 753–769. https://doi.org/10.1016/j.ymssp.2015.01.008

Duan, J., Li, M., Lim, T. C., Lee, M. R., Cheng, M. Te, Vanhaaften, W., & Abe, T. (2014). Combined feedforward-feedback active control of road noise inside a vehicle cabin. *Journal of Vibration and Acoustics*, *136*(4), 1–8. https://doi.org/10.1115/1.4027713

Elizabeth González, A. (2023). Overview of Noise Control Techniques and Methods. In *Noise Control*. IntechOpen. https://doi.org/10.5772/intechopen.104608

Foreman, J. E. K. (1990). Sound Analysis and Noise Control. In *Sound Analysis and Noise Control*. Springer US. https://doi.org/10.1007/978-1-4684-6677-5

HELMHOLTZ, H. (1878). The Theory of Sound. *Nature*, *19*(476), 117–118. https://doi.org/10.1038/019117a0

Jiang, T., Liu, J., Peng, C., & Wang, S. (2023). Laboratory Test of a Vehicle Active Noise-Control System Based on an Adaptive Step Size Algorithm. *Applied Sciences (Switzerland)*, *13*(1). https://doi.org/10.3390/app13010225

Kim, S., & Altinsoy, M. E. (2022). Active control of road noise considering the vibro-acoustic transfer path of a passenger car. *Applied Acoustics*, *192*, 108741. https://doi.org/10.1016/j.apacoust.2022.108741

Li, T., He, Y., Wang, N., Feng, J., Gui, W., & Zhao, K. (2021). Active Noise Cancellation of Rail Vehicles Based on a Convolutional Fuzzy Neural Network Prediction Approach. *2021 IEEE Vehicle Power and Propulsion Conference (VPPC)*, *1*, 1–5. https://doi.org/10.1109/VPPC53923.2021.9699325

Moazzam, M., & Rabbani, M. S. (2013). *Performance Evaluation of Different Active Noise Control (ANC) Algorithms for Attenuating Noise in a Duct* [Blekinge Institute of Technology]. www.bth.se/ing

Oh, S., Kim, H., & Park, Y. (2002). Active control of road booming noise in automotive interiors. *The Journal of the Acoustical Society of America*, *111*(1), 180–188. https://doi.org/10.1121/1.1420390

Padhi, T., Chandra, M., Kar, A., & Swamy, M. N. S. (2017). Design and analysis of an improved hybrid active noise control system. *Applied Acoustics*, *127*, 260–269. https://doi.org/10.1016/j.apacoust.2017.06.014

Park, T., Kim, M., Gwak, M., Cho, T., & Park, P. (2020). Active noise control

algorithm robust to noisy inputs and measurement impulsive noises. *International Conference on Control, Automation and Systems*, *2020-Octob*(Iccas), 622–626. https://doi.org/10.23919/ICCAS50221.2020.9268248

Samarasinghe, P. N., Zhang, W., & Abhayapala, T. D. (2016). Recent Advances in Active Noise Control Inside Automobile Cabins: Toward quieter cars. *IEEE Signal Processing Magazine*, *33*(6), 61–73. https://doi.org/10.1109/MSP.2016.2601942

Shi, C., Jia, Z., Xie, R., & Li, H. (2020). An active noise control casing using the multi-channel feedforward control system and the relative path based virtual sensing method. *Mechanical Systems and Signal Processing*, *144*, 106878. https://doi.org/10.1016/j.ymssp.2020.106878

Song, Y. (2022). Active Noise Cancellation and Its Applications. *Journal of Physics: Conference Series*, *2386*(1). https://doi.org/10.1088/1742-6596/2386/1/012042

Sutton, T. J., Elliott, S. J., McDonald, A. M., & Saunders, T. J. (1994). Active control of road noise inside vehicles. *Noise Control Engineering Journal*, *42*(4), 137–147. https://doi.org/10.3397/1.2828351

Wang, W., & Thomas, P. J. (2017). Low-frequency active noise control of an underwater large-scale structure with distributed giant magnetostrictive actuators. *Sensors and Actuators, A: Physical*, *263*, 113–121. https://doi.org/10.1016/j.sna.2017.05.044

Wu, L., Qiu, X., Burnett, I. S., & Guo, Y. (2015). Decoupling feedforward and feedback structures in hybrid active noise control systems for uncorrelated narrowband disturbances. *Journal of Sound and Vibration*, *350*, 1–10. https://doi.org/10.1016/j.jsv.2015.04.018

Wu, L., Wang, L., Sun, S., & Sun, X. (2022). Hybrid active and passive noise control in ventilation duct with internally placed microphones module. *Applied Acoustics*, *188*, 108525. https://doi.org/10.1016/j.apacoust.2021.108525

Yin, L., Zhang, Z., Wu, M., Wang, Z., Ma, C., Zhou, S., & Yang, J. (2023). Adaptive parallel filter method for active cancellation of road noise inside vehicles. *Mechanical Systems and Signal Processing*, *193*(January), 110274. https://doi.org/10.1016/j.ymssp.2023.110274

Zahir, E., Mohajan, S., Barua, A., Hossain, J., & Rabby, M. R. (2019). Investigating an active noise cancellation system for reducing the sound of car horns in an enclosed cavity. *1st International Conference on Robotics, Electrical and Signal Processing Techniques, ICREST 2019*, 652–656. https://doi.org/10.1109/ICREST.2019.8644225

Appendix A

Gantt Chart

	Semester 1														
	2023/2024														
Task	W1	W2	W3	W4	W5	W6	W7	W8	W9	W10	W11	W12	W13	W14	W15
FYP Briefing and title selection															
Do research on topic															
Literature Review															
Perform Simulation															
Analys simulation															
Writing report															
Presentation preparation & presenting															

	Semester 2														
	2023/2024														
Task	Week 1	Week 2	Week 3	Week 4	Week 4	Week 5	Week 6	Week 7	Week 8	Week 9	Week 10	Week 11	Week 12	Week 13	Week 14
Literature Review															
System Design															
Perform and Analyse COMSOL Simulation															
Design Experimental Setup															
Perform Experiment															
Analyse System Performance															
Report Writing															

Appendix B

LabVIEW 2014 Graphic Programming Code for Data Acquisition

FPGA Front Panel

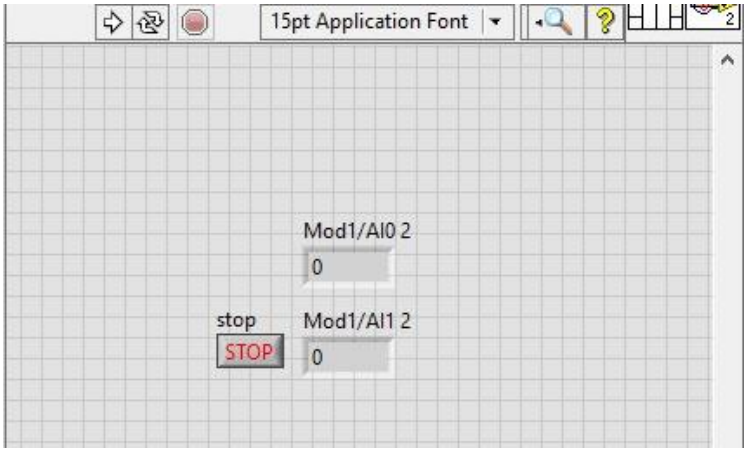

FPGA Block Diagram

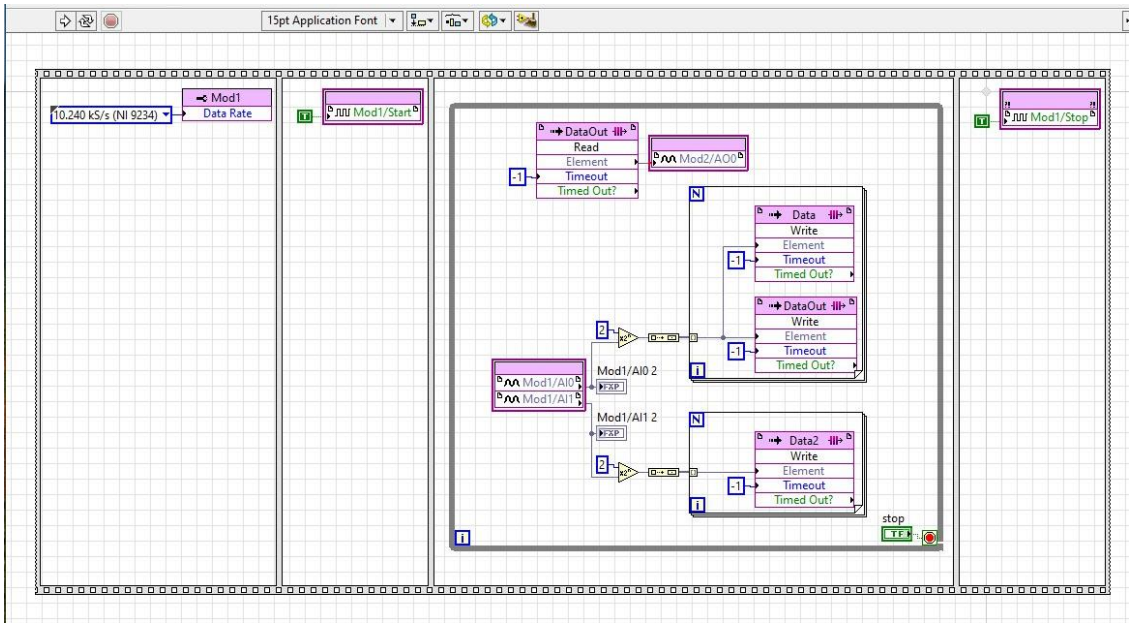

Main RT Front Panel

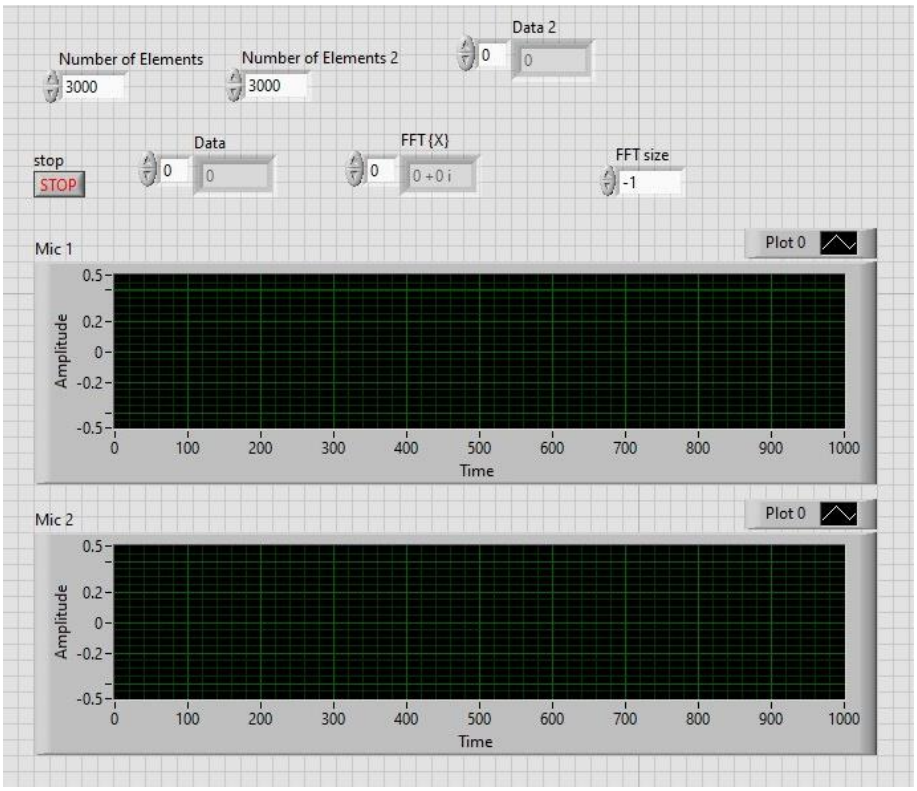

Main RT Block Diagram

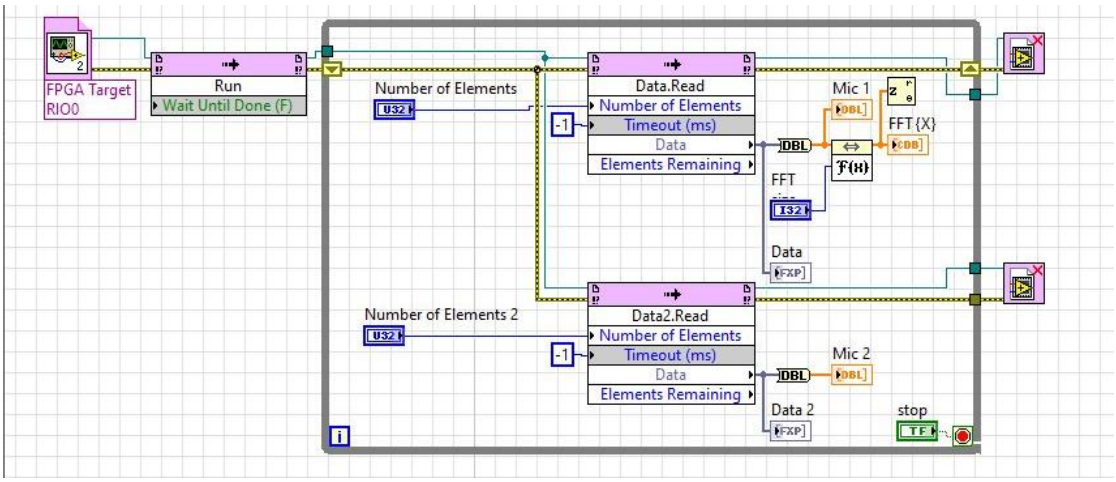

Appendix C

LabVIEW 2014 Graphic Programming Code for ANC Controller

FPGA Front Panel

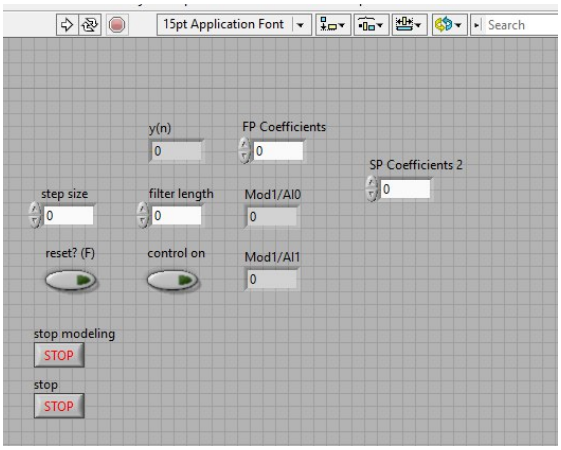

FPGA Block Diagram

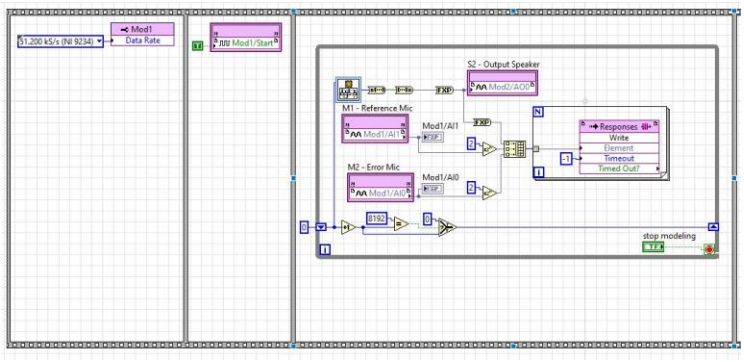

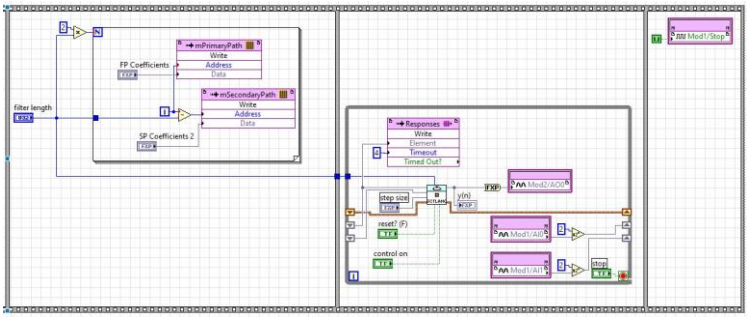

\Main RT Front Panel

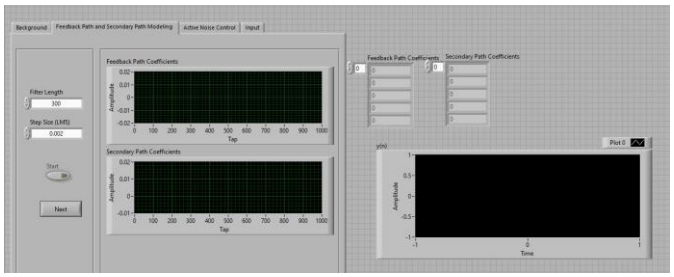

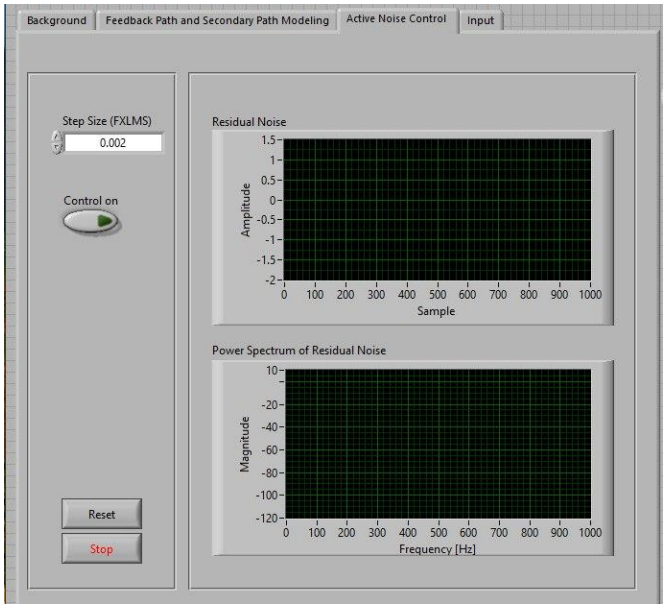

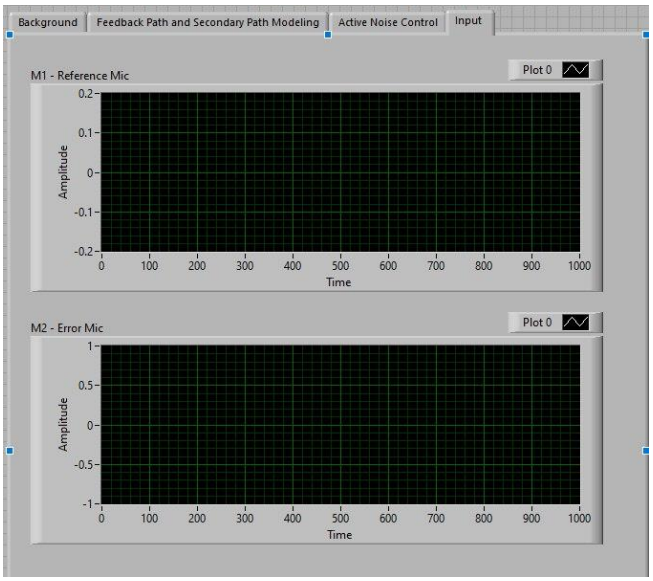
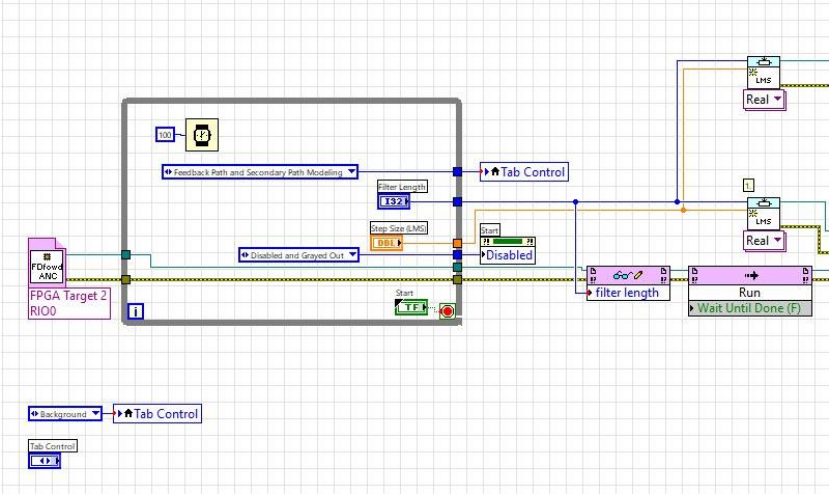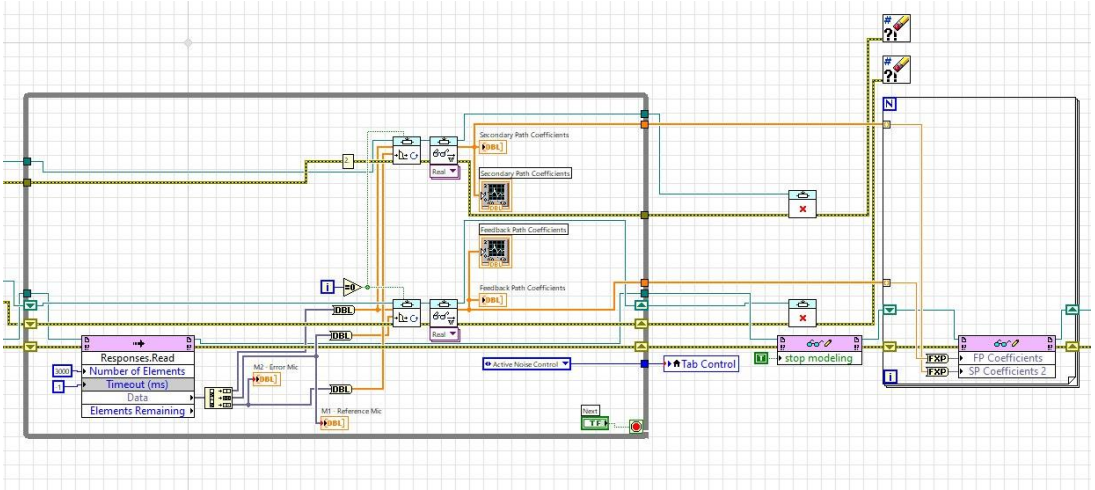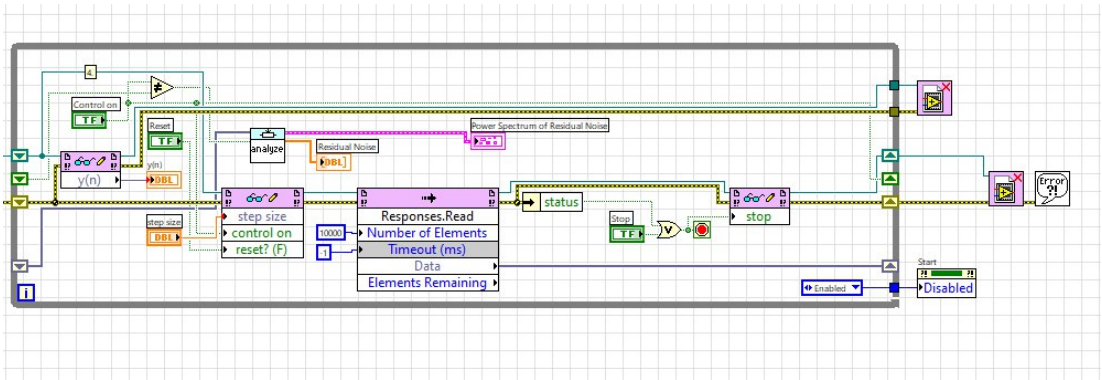
Main RT Block Diagram